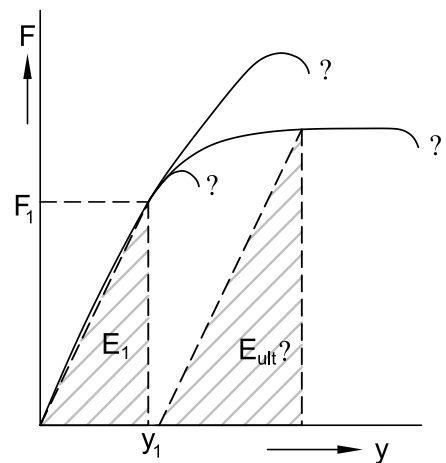
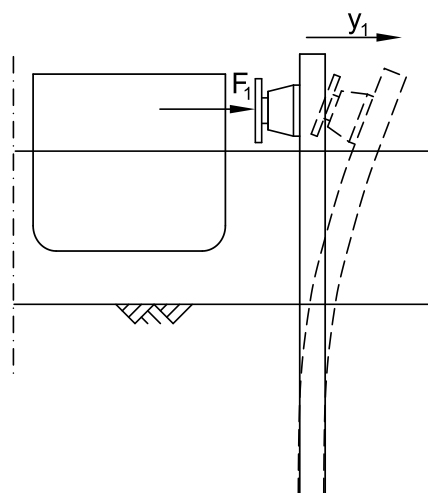


Plastic design of breasting dolphins

Thesis report

16 November 2004
Edward Bruijn



Delft University of Technology

Faculty of Civil Engineering and Geosciences
Department of Hydraulic and Geotechnic Engineering
Section Hydraulic Structures



ROYAL HASKONING

thinking in
all dimensions



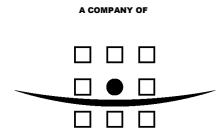
Delft University of Technology

Faculty of Civil Engineering and Geosciences

Department of Hydraulic and Geotechnic Engineering
Section Hydraulic structures

Stevinweg 1
P.O. Box 5048
2600 GA Delft
The Netherlands

Telephone +31 (0)15 278 54 40
Fax +31 (0)15-2787966
E-mail info@citg.tudelft.nl
Internet www.citg.tudelft.nl



ROYAL HASKONING

HASKONING NEDERLAND BV
INFRASTRUCTURE & TRANSPORT

Heer Bokelweg 145
P.O. Box 705
Rotterdam 3000 AS
The Netherlands

+31 (0)10 443 36 66 Telephone
+31 (0)10-4433688 Fax
info@rotterdam.royalhaskoning.com E-mail
www.royalhaskoning.com Internet
Arnhem 09122561 CoC

Document title Plastic design of breasting dolphins
Thesis report

Author Edward Bruijn

Date 16 November 2004

Project name Design of flexible steel breastings: Final
thesis

Project number H32102/36

PREFACE

*“ Safety is a matter of sense;
The challenge is to make it a matter of common sense. “*

This publication is the product of the thesis study which is the final stage of the Masters Civil Engineering at Delft University of Technology, specialisation Structural Hydraulic Engineering.

The thesis study, titled “Plastic design of breasting dolphins”, is executed at Royal Haskoning in Rotterdam under the supervision of Ir. J.D. Terpstra. I would like to express my gratitude to Royal Haskoning for providing the resources and support during my stay in Office Rotterdam2.

The graduation committee for this project consists of the following members:

Prof. drs. ir. J.K. Vrijling	Civil Engineering section Hydraulic Structures
Ir. W.F. Molenaar	Civil Engineering section Hydraulic Structures
Ir. A.M. Gresnigt	Civil Engineering section Steel & Timber Structures
Ir. J.D. Terpstra	Royal Haskoning division Infrastructure & Transport

I would like to thank the graduation committee for the guidance and support which I received during the project.

Rotterdam, 16 November 2004

Edward Bruijn

SUMMARY

Most liquid bulk terminals are equipped with a jetty as berthing facility. The ship mostly berths to dedicated breasting dolphins, which can be single-pile flexible dolphins or multi-pile rigid dolphins.

In design methods for flexible dolphins, the yield limit is approached more and more over the years to employ the load-bearing capacity of the dolphin more optimally. In recent guidelines (EAU 1996 and PIANC 2002) also the plastic yielding capacity is implicitly or explicitly included in the ultimate load-bearing capacity. This movement towards plastic design however is not accompanied by the development of calculation models and design criteria to assess the plastic load-bearing capacity.

Damage cases in recent years seem to support the conclusion that the completeness and safety of those standards and guidelines is questionable.

As a first objective in this thesis report the development of a model for the prediction of the nonlinear structural behaviour of a dolphin is presented. The most important output of the model is a complete load-deflection curve up to failure, including all relevant failure mechanisms, with which the load-bearing capacity in terms of energy absorption can be assessed.

The model, which is called the Bruijn model, is developed for the system of a single steel pile with uniform cross-section and steel grade sufficiently embedded in non-cohesive soil of uniform properties, under influence of a static horizontal load applied at the pile-head. The numerical formulation is based on the theory of subgrade reaction, in which the pile is divided into elements of equal length and the soil is modelled as springs with a bilinear spring characteristic.

The pile behaviour is modelled using the plasticity theory according to Gresnigt, derived for the plastic design of buried steel pipelines. This application shows much resemblance with the case of a dolphin embedded in the soil, as for the 1st order and 2nd order deformation behaviour of the steel tubular section and the influence of soil pressures on the deformation of the pile cross-section.

The soil behaviour is modelled using the theory of Ménard for the soil stiffness and the theory of Brinch Hansen for the full-plastic soil reaction, with which the bilinear spring characteristic for the soil springs is determined.

The Bruijn model is confirmed by a comparison with existing models like FEM application TNO DIANA, although the Bruijn model is assessed to give a conservative estimate of the 2nd order effects (reduction of strength and stiffness under influence of ovalisation) leading to smaller values for the energy absorption capacity than estimated by DIANA.

As the second objective an evaluation of the currently effective design standards and guidelines for dolphins is carried out, in order to assess the safety which can be realised in the plastic range. A representative case is chosen with varying diameter-wall thickness ratio's (D/t ratio of 83, 63 and 42), which is calculated according to all relevant standards and guidelines, and compared to the load-deflection curve generated by the Bruijn model. The case study leads to the conclusion that sufficient plastic yielding capacity is confirmed for a D/t ratio of 42, where an increase in the elastic energy absorption capacity of up to 1,33 times the original elastic energy absorption capacity can be obtained after some plastic yielding. At larger D/t ratio's (60-80) this plastic yielding capacity is significantly smaller due to a much higher buckling sensitivity. At a D/t ratio above 80 buckling in the elastic range can be expected, reducing the ultimate energy absorption capacity to less than the full-elastic energy absorption capacity.

For the standards and guidelines it can be concluded that the employment of the plastic yielding capacity should be accompanied by an assessment of the safety against failure for the failure modes stresses, strains, buckling and ovalisation. This means that the current standards and guidelines should be expanded with limit state criteria for failure modes buckling and ovalisation and should be adjusted for failure mode yielding. By doing this the safety of a design for any value of the D/t ratio will be ensured.

It can also be concluded that the energy absorption capacity according to the current design methods for dolphins with D/t ratio 50-70 is confirmed by the Bruijn model. This means that most of the dolphins currently in use are designed with a correct safety assessment.

It is recommended to execute a probabilistic analysis of the entire system assessing the probabilities of failure according to all relevant failure modes. This can be done by performing a Monte Carlo analysis with a model like the Bruijn model.

It is further recommended to evaluate and further develop the Bruijn model, and release such a model to the design environment. Such a model is easier to work with and more suitable for the specific design requirements than complex FEM analysis packages.

SAMENVATTING

De meeste vloeibare bulk terminals zijn uitgerust met een steiger als afmeerconstructie. Het schip meert meestal af aan losstaande dukdalven, die kunnen bestaan uit flexibele enkelvoudige buispalen of uit een stijve constructie opgebouwd uit meerdere palen. In de ontwerpmethode van flexibele stalen dukdalven wordt de vloeigrens de laatste jaren meer en meer benaderd, om zo het draagvermogen van de dukdalf optimaal te benutten. In recente ontwerpnormen (EAU 1996 en PIANC 2002) wordt ook de plastische vervormingscapaciteit impliciet of expliciet in rekening gebracht bij het bepalen van het draagvermogen in uiterste grenstoestand. Deze beweging in de richting van plastisch ontwerpen gaat echter niet gepaard met de ontwikkeling van rekenmodellen en ontwerpcriteria om de plastische vervormingscapaciteit te kunnen bepalen en in rekening brengen. Recente schadegevallen lijken de conclusie te ondersteunen dat de volledigheid en veiligheid van deze ontwerpnormen in twijfel kan worden getrokken.

De eerste doelstelling in dit afstudeerrapport is de ontwikkeling van een rekenmodel voor het bepalen van het niet-lineaire constructiegedrag van een dukdalf. De belangrijkste output van het model is een compleet belasting-vervormingsdiagram tot aan falen waarbij alle relevante faalmechanismen zijn beschouwd. Met dit belasting-vervormingsdiagram kan het draagvermogen in termen van energieopname worden bepaald.

Het model, wat het Bruijn model is genoemd, is ontwikkeld voor het systeem van een enkele stalen buispaal met een uniforme doorsnede en staalkwaliteit, voldoende ingeklemd in de ondergrond die bestaat uit niet-cohesieve uniforme grond. De belasting bestaat uit een statische horizontale kracht die aangrijpt op de paalkop.

De numerieke formulering is gebaseerd op de theorie van de elastisch ondersteunde ligger, waarin de paal is opgedeeld in elementen van gelijke grootte. De grond wordt gemodelleerd als ongekoppelde veren met een niet-lineaire veer karakteristiek.

Het paalgedrag is gemodelleerd met behulp van de plasticiteitsleer volgens Gresnigt, die is afgeleid voor het plastisch ontwerp van ingegraven stalen pijpleidingen. Deze toepassing vertoont veel overeenkomst met de toepassing van een dukdalf ingeklemd in de grond, voor wat betreft het 1^e orde en 2^e orde vervormingsgedrag van een holle stalen buis en de invloed van de gronddrukken op de vervorming van de paaldoorsnede.

Het grondgedrag is gemodelleerd met behulp van de theorie van Ménard voor de grondstijfheden en de theorie van Brinch Hansen voor de volplastische grondreactie, waarmee de bilineaire veer karakteristiek voor de grondveren is bepaald.

Het Bruijn model is geverifieerd met behulp van bestaande modellen, onder anderen het eindige-elementen pakket TNO DIANA. Hoewel het Bruijn model enigszins conservatieve waarden geeft voor de 2^e orde effecten (de reductie van sterkte en stijfheid als gevolg van ovalisering), waardoor lagere waarden voor de energieopnamecapaciteit worden gevonden dan met een DIANA-berekening, mag worden geconcludeerd dat het Bruijn model correcte resultaten geeft.

De tweede doelstelling is de evaluatie van de huidige ontwerpnormen en ontwerprichtlijnen voor dukdalven, om een uitspraak te kunnen doen over de veiligheid die in het plastische gebied kan worden gerealiseerd. Een representatieve case is gekozen met een variërende wanddikte-diameterverhouding (D/t ratio van 83, 63 en 42), die is doorgerekend volgens de huidige ontwerpnormen en vergeleken met de belasting-vervormingscurve die door het Bruijn model is gegenereerd. Uit deze casestudie kan geconcludeerd worden dat voldoende plastische vervormingscapaciteit is aangetoond voor een D/t ratio van 42, waarbij na enige plastische vervorming een toename in de

elastische energieopnamecapaciteit kan worden waargenomen tot 1,33 maal de oorspronkelijke elastische energieopnamecapaciteit. Bij hogere D/t ratio's (60-80) is deze plastische vervormingscapaciteit aanzienlijk smaller door een veel grotere plooi gevoeligheid. Bij een D/t ratio van boven de 80 kan plooï in het elastische gebied worden verwacht, waardoor de energieopnamecapaciteit in uiterste grenstoestand lager is dan de volestatische energieopnamecapaciteit.

Voor de ontwerpnormen en ontwerprichtlijnen kan de conclusie worden getrokken dat het in rekening brengen van de plastische vervormingscapaciteit gepaard moet gaan met een beschouwing van de veiligheid tegen falen voor faalmechanismen spanningen, rekken, plooi en ovalisering. Dit betekent dat de huidige normen uitgebreid moeten worden met toetsingsregels voor de faalmechanismen plooi en ovalisering en aangepast moeten worden op het gebied van faalmechanisme vloeien. Hierdoor wordt de veiligheid van het ontwerp voor elke waarde van de D/t ratio gewaarborgd.

Ook kan geconcludeerd worden dat de grootte van de energieopnamecapaciteit die volgens de huidige ontwerpnormen is berekend voor dukdalven met een D/t ratio van 50-70 bevestigd is door de uitkomsten van het Bruijn model. Dit betekent dat de meeste momenteel in gebruik zijnde dukdalven zijn ontworpen met een correcte veiligheidsbeschouwing.

Het wordt aanbevolen om een grondige probabilistische analyse van het hele systeem uit te voeren waarbij de faalkansen van alle relevante faalmechanismen worden bepaald. Dit kan worden gedaan door een Monte Carlo analyse uit te voeren met een model als het Bruijn model.

Het wordt ook aanbevolen om het Bruijn model verder te verifiëren en te ontwikkelen, en om een dergelijk model vervolgens ook op de markt te brengen. In de ontwerppraktijk kan dan met een rekenmodel gewerkt worden wat makkelijker is te gebruiken en meer is toegespitst op de specifieke ontwerp situatie dan complexe eindige-elementen pakketten.

CONTENTS

	Page
PREFACE	I
SUMMARY	II
SAMENVATTING	IV
1. INTRODUCTION	1
2. THE MOORING OF A SHIP TO A DOLPHIN	2
2.1. Introduction	2
2.2. Berthing	2
2.3. Breasting dolphins	4
3. PROBLEM ANALYSIS	10
3.1. Introduction	10
3.2. Plastic design in latest generation design standards	10
3.3. Damage to dolphins	13
3.4. Definition of the problem	16
3.5. Research to be performed	17
3.6. Objectives	18
4. DEVELOPMENT OF A CALCULATION MODEL TO PREDICT THE NONLINEAR STRUCTURAL BEHAVIOUR OF A DOLPHIN	19
4.1. Introduction	19
4.2. The system to be considered	19
4.3. Description of the model	20
4.4. Limitations	21
4.5. Theory: plasticity theory according to Gresnigt	22
4.6. Theory: soil behaviour according to Menard and Brinch Hansen	34
4.7. Theory: Limit states for the model	37
4.8. Results of the Bruijn model	43
4.9. Verification of the Bruijn model	47
4.10. Practical application	51
5. EVALUATION OF DESIGN STANDARDS AND GUIDELINES	53
5.1. Introduction	53
5.2. Current standards and guidelines	53
5.3. Comparison of standards and guidelines	54
5.4. What are the consequences of these conclusions for the safety of the system?	61
6. CONCLUSIONS AND RECOMMENDATIONS	65
6.1. Introduction	65
6.2. Conclusions	65
6.3. Recommendations	67

ANNEX I: LITERATURE INVESTIGATION	68
I.1 Introduction	69
I.2 An overview of berthing facilities	69
I.3 What happens when ships berth?	75
I.4 Design philosophy	81
I.5 Calculation models	82
I.6 Standards and guidelines	94
ANNEX II: SETTING UP A CALCULATION MODEL	98
II.1 Introduction	99
II.2 Type of model	99
II.3 Basic formulation model	99
II.4 Modelling of the pile	101
II.5 Modelling of the soil	104
II.6 Actions	111
II.7 Boundary conditions	111
II.8 Solve technique	111
II.9 Input	114
II.10 Output	115
ANNEX III: COMPARISON BRUIJN MODEL WITH LINEAR MODELS	118
ANNEX IV: ASSESSMENT OF THE SAFETY OF THE SYSTEM	122
IV.1 Introduction	123
IV.2 How can I assess the safety of the system in a quantifiable way?	123
IV.3 Qualitative analysis of the safety of the system	125
SYMBOLS	132
REFERENCES	134

1. INTRODUCTION

From the beginning of naval history, ships transporting cargo or people from point A to point B require facilities at both point A and B for safe mooring, loading and unloading purposes. Over time, ship sizes have grown larger and larger and specialised ships, terminals and equipment have been built for handling specific types of cargo like liquid bulk, dry bulk and containers.

For liquid bulk terminals a jetty is the typical berthing facility. The ship mostly berths to dedicated breasting dolphins, which can be single-pile flexible dolphins or multi-pile rigid dolphins with fenders.

In design methods for flexible dolphins, the yield limit is approached more and more over the years to employ the load-bearing capacity of the dolphin more optimally. In recent guidelines (EAU 1996 and PIANC 2002) also the plastic yielding capacity is implicitly or explicitly included in the ultimate load-bearing capacity. This movement towards plastic design however is not accompanied by the development of calculation models to assess the plastic load-bearing capacity.

Damage cases in recent years seem to support the conclusion that the completeness and safety of those standards and guidelines is questionable.

The first objective is to develop a model for the prediction of the nonlinear structural behaviour of a dolphin including all significant failure modes in the elastic and plastic range, resulting in a complete and accurate load-deflection curve up to failure.

The second objective is to compare the current design methods and guidelines with each other and to evaluate them using the developed calculation model, so conclusions can be taken about the safety which can be realised in the plastic range.

The outline of this report is as follows.

In chapter 2 the subject of mooring a ship to a dolphin is introduced. In chapter 3 the problem analysis is presented resulting in a concise problem definition for this thesis project and objectives for the research to resolve the problem.

Chapter 4 is dedicated to the development of a calculation model for the prediction of the nonlinear structural behaviour of a dolphin, which is able to generate a load-deflection curve up to failure. In chapter 5 the current standards and guidelines are compared and evaluated using the calculation model presented in chapter 4.

In the last chapter, chapter 6, the conclusions and gains from this thesis project are presented and recommendations are given how to proceed and resolve the problems stumbled upon in the current research.

2. THE MOORING OF A SHIP TO A DOLPHIN

2.1. Introduction

In this chapter the subject of mooring a ship to a dolphin is introduced. Firstly the berthing process and berthing structures are treated. Secondly the breasting dolphin is analysed in more detail.

Most of the text of this chapter is borrowed from the literature investigation in Annex I, which comprises a more detailed analysis of berthing, berthing structures, calculation models, design and failure.

2.2. Berthing

Berthing process

The berthing process (with large vessels) generally takes place as follows, refer to Figure 2-1:

1. With the assistance of tugs the vessel is positioned parallel to the berthing structure
2. Two tugs push the vessel sideways to the berthing structure and keep pushing during all following steps; two tugs pull the vessel to control the motions of the vessel
3. The vessel makes contact with the fender system (consisting of a breasting dolphin and/or a fender) and the kinetic energy of the vessel is converted into potential energy via deflection or compression of the fender system
4. The fender system springs back, converting the potential energy back into kinetic energy of the vessel, in the form of translation and rotation
5. The vessel rotates around the first point of contact and makes contact with the fender system at a second point
6. At the second point of contact the kinetic energy of the vessel is converted into potential energy of the fender system
7. The fender system springs back, converting the potential energy back into kinetic energy of the vessel
8. The vessel rotates around the second point of contact toward the first point of contact
9. This movement repeats itself until all kinetic energy of the vessel is dissipated and the vessel has stopped moving

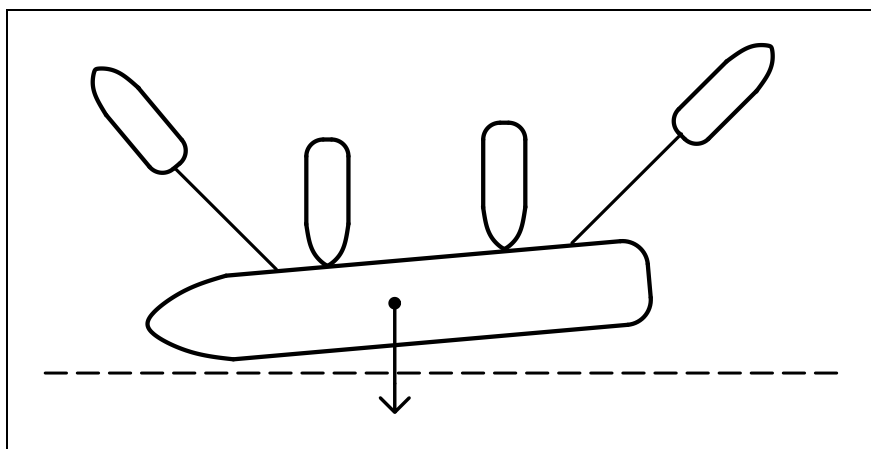


Figure 2-1 Berthing model

Berthing structures

Two basic types of berthing structure are distinguished:

- Quay wall
- Jetty

The quay wall, schematically presented in Figure 2-2, is the traditional berthing facility, consisting of an earth-retaining wall and fenders to ensure soft berthing. Because of the high stiffness of the quay, it is important to design a good fendering system to absorb the energy of the berthing ship without causing damage to the ship or the quay.

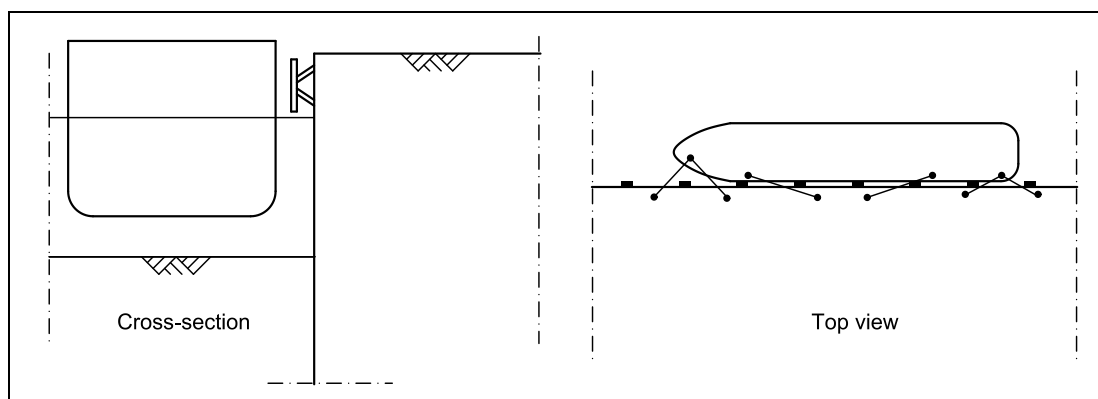


Figure 2-2 Schematic view of a quay wall

The jetty is an open pier structure. Generally less expensive than a quay wall, the jetty is applied in situations where loading- and unloading equipment allows for a lighter berthing structure. Liquid bulk terminals are generally equipped with jetties.

In some cases the ships berth directly to the jetty, refer to Figure 2-3. But in most cases the functions of berthing and loading/unloading are separated by application of a detached berthing structure like a breasting dolphin, refer to Figure 2-4. The advantage of this separation of functions is that the jetty and the dolphins can be designed for the specific requirements of loading/unloading and berthing respectively.

The detached berthing structure consists of breasting dolphins for handling the berthing impact and mooring dolphins for handling mooring lines. Breasting dolphins are discussed in more detail in the next section.

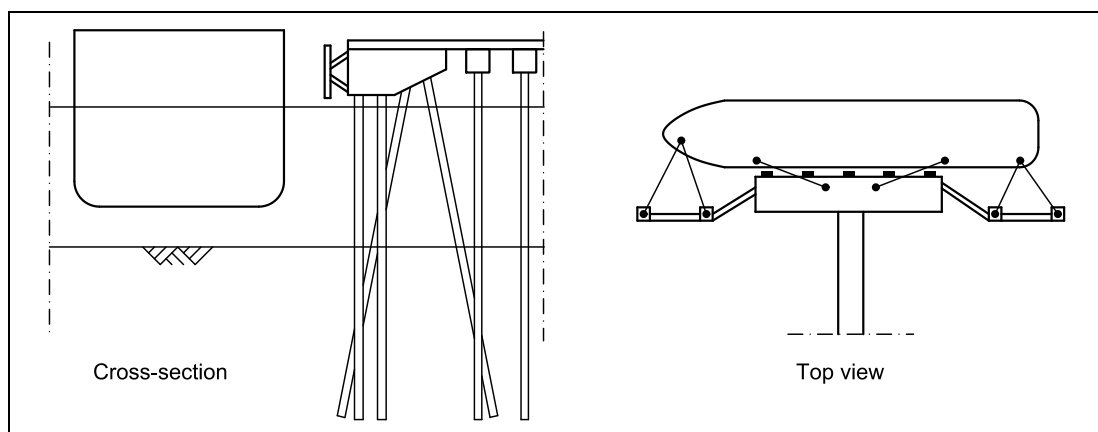


Figure 2-3 Jetty structure

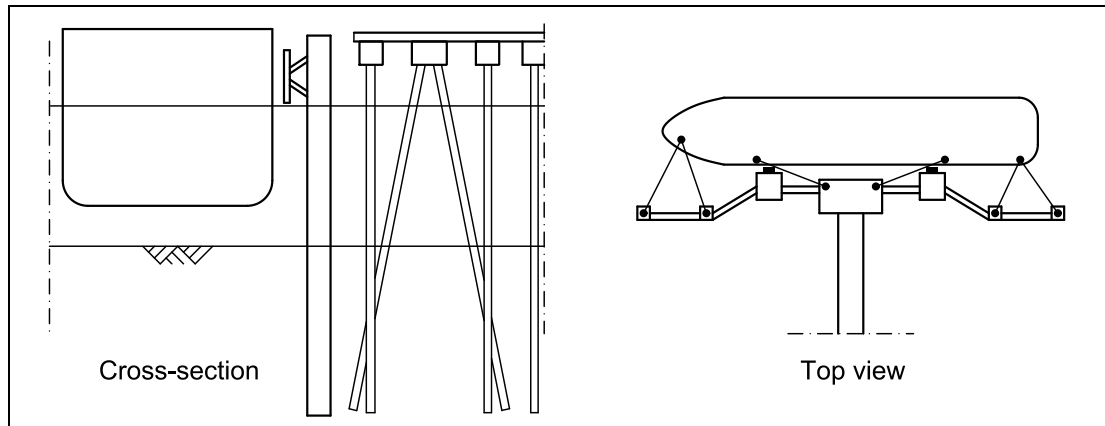


Figure 2-4 Jetty with detached dolphins

2.3. Breasting dolphins

Dolphin types

Breasting dolphins for the berthing of large ships are made of steel tubular piles driven into the subsoil.

Two principal types of breasting dolphin can be distinguished in respect to the way of handling the impact loads (refer to Figure 2-5):

- Rigid dolphin with fender: the impact energy of the ship is absorbed by the fender; the dolphin is designed to be rigid, and consists of a group of piles
- Flexible dolphin: the impact energy of the ship is absorbed by deflection of the pile; often a fender is added to increase the energy absorption capacity

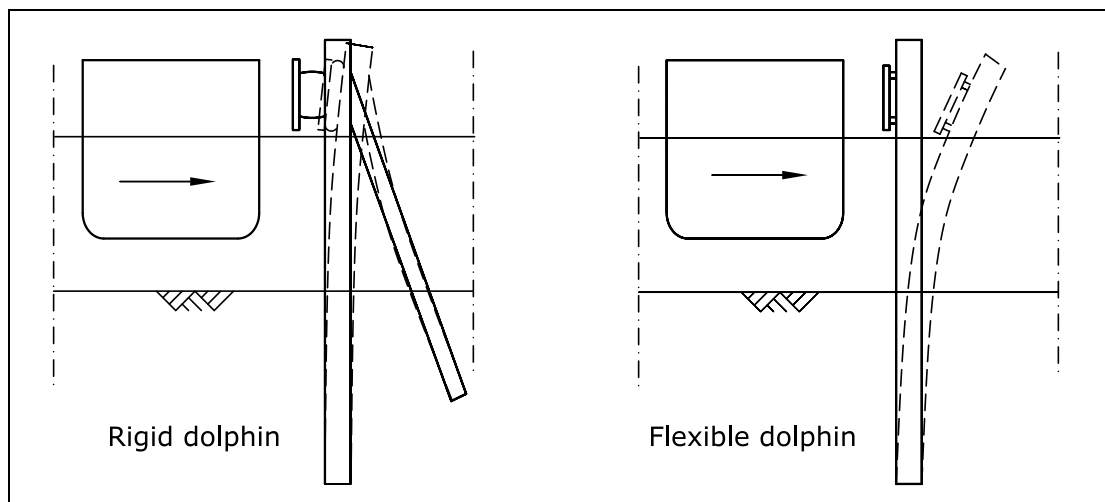


Figure 2-5 Schematic view of rigid and flexible breasting dolphins

Where soil conditions are suitable the flexible dolphin is often attractive because it combines the functions of fender and breasting structure. As the energy absorption capacity of a pile is a function of its length, this type of breasting dolphin is particularly attractive in deep-water applications.

Since the flexible dolphin is designed to absorb the impact energy of the ship by lateral deflection, this means that the capacity of the pile to withstand the loads depends on

both the strength and stiffness of the pile. The pile stiffness should therefore be chosen with care:

- If the stiffness is chosen too low, the deflection of the pile will be too large and failure can occur if the pile touches the jetty or the ship touches the pile under water
- If the stiffness is chosen too high, the reaction force will be high and failure can occur due to yielding of the pile or yielding of the ship's hull

The design of flexible dolphins is therefore different from the design of most other structural applications.

In the case of rigid dolphins the fender is designed to absorb the impact energy of the ship. The group of piles the fender is attached to is designed to transfer the reaction forces from the fender to the subsoil. The strength and stiffness of the group of piles should therefore be high enough to withstand these reaction forces without too large deformations, which means that a rigid dolphin is designed as every other structural application.


In Figure 2-6 a picture is presented of a ship mooring to a flexible dolphin fitted with a fender.



Figure 2-6 Ship mooring to a flexible dolphin fitted with a fender

Fenders

For the rigid dolphin the fender is the main energy absorption element; the flexible dolphin can be equipped by a fender to enlarge the energy absorption. The principal function of fenders is to transform ships' berthing energies into reactions which both the ship and the dolphin can safely sustain.

In Table 2-1 the fender systems most widely used in new installations are presented . The performance is expressed as a curve where the fender reaction R is plotted against fender compression δ . The area under the curve represents the energy absorption.

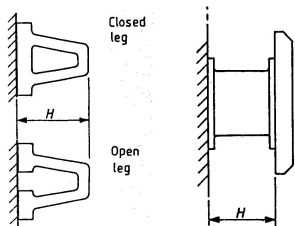
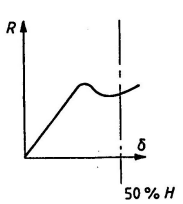
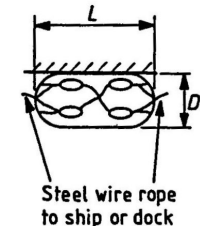
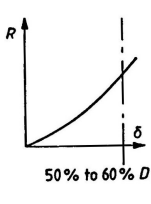
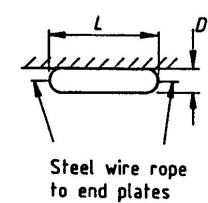
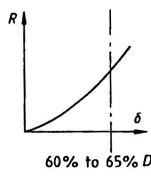
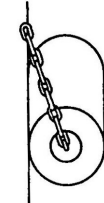
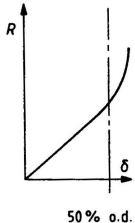

Type	Shape	Performance
Buckling fenders: <ul style="list-style-type: none"> + low reaction & high energy absorption – max reaction occurs almost every berthing – fender panel is required 		
Pneumatic fenders: <ul style="list-style-type: none"> + full tidal range can be covered + low reaction force – large diameter keeps vessel further from wharf requiring larger reach for (un)loading equipment 		
Foam-filled fenders: <ul style="list-style-type: none"> + full tidal range can be covered + low reaction force – large diameter keeps vessel further from wharf requiring larger reach for (un)loading equipment 		
Side-loaded fenders: <ul style="list-style-type: none"> + economical – relatively low energy absorption – susceptible to damage by surging motion ship 		

Table 2-1 Fender types and characteristics

Structural behaviour of the flexible dolphin

The impact energy of the ship is transferred to the dolphin by the berthing ship. This energy is absorbed by lateral deflection of the dolphin. The magnitude of the energy absorption by lateral deflection is determined by the integral :

$$E = \int_{y_0}^{y_2} F \cdot dy$$

<2.1>

with

E = absorbed energy [kJm]

F = lateral pile-head force (contact force between ship and dolphin) [kN]

y = horizontal deflection of the pile-head [m]



BS 6349-4:1994

Chapter 5



Vasco Costa, F., 1964

If the deflection of the pile-head is known for all values of the static pile-head load F this integral can be calculated. This can be made visible by a load-deflection curve, refer to Figure 2-7. The hatched area under the curve is equal to the amount of energy absorbed by the dolphin.

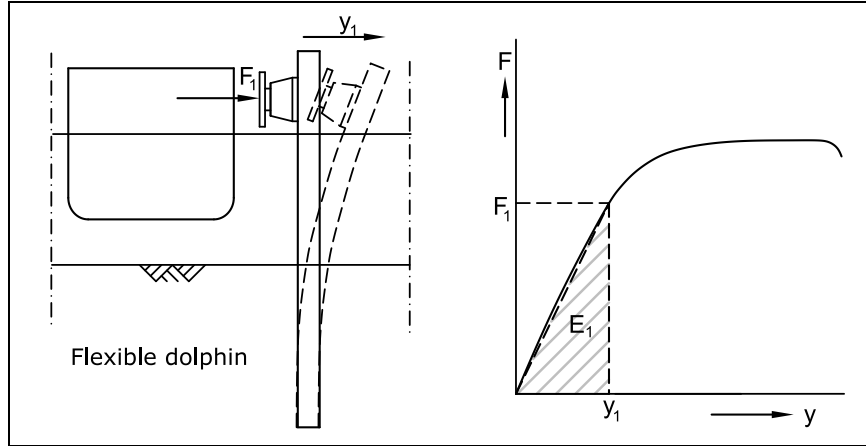


Figure 2-7 Load-deflection curve and energy absorption capacity

In most cases the load-deflection curve is assumed linear, so that the integral reduces to:

$$E_i = \frac{1}{2} \cdot F_i \cdot y_i \quad <2.2>$$

Design method for the flexible dolphin

The design of a flexible dolphin is based on the rule that the loads on the structure must not exceed the strength of the structure. This can be described in general form by the following safety verification:

$$R_d - S_d \geq 0 \quad \text{or} \quad \frac{R_d}{S_d} \geq 1 \quad <2.3>$$

with

R_d = Design value of the resistance (strength), produced as function of the characteristic resistance of structural elements divided by the

corresponding partial safety factor: $R_d = \frac{R_k}{\gamma_R}$

S_d = Design value of actions, produced from the characteristic values of the actions multiplied by the corresponding partial safety factors:

$$S_d = \gamma_S \cdot S_k$$

In the case of a flexible dolphin the safety verification can be written as:

$$\frac{E_u}{E_d} \geq 1 \quad <2.4>$$

with

E_u = The ultimate energy absorption capacity of the dolphin

E_d = The design impact energy of the ship, which is proportional to the kinetic energy of the ship at the time of impact ($E_d \sim \frac{1}{2} \cdot m_{ship} \cdot v_{ship}^2$)

A safety margin is incorporated by applying a safety factor on the impact energy of the ship and/or on the ultimate energy absorption capacity of the dolphin. The result can be seen in Figure 2-8.

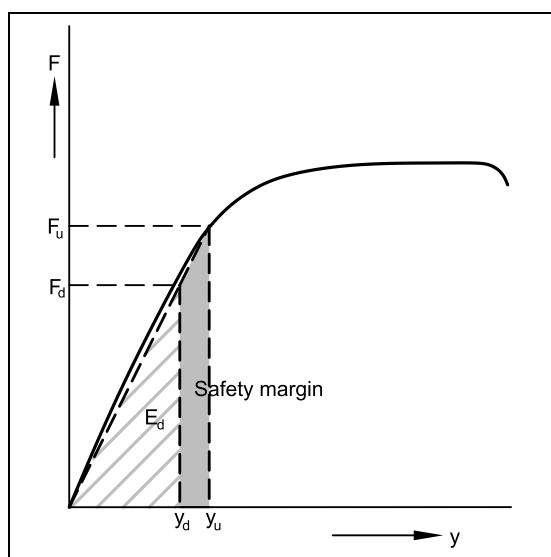


Figure 2-8 Safety margin in energy absorption

The safety verification can also be expressed in terms of bending moments, refer to Figure 2-9:

$$\frac{M_u}{M_d} \geq 1 \quad <2.5>$$

with

M_u = The ultimate bending moment capacity of the dolphin

M_d = The design value of the bending moment as a result of the maximum pile-head load F .

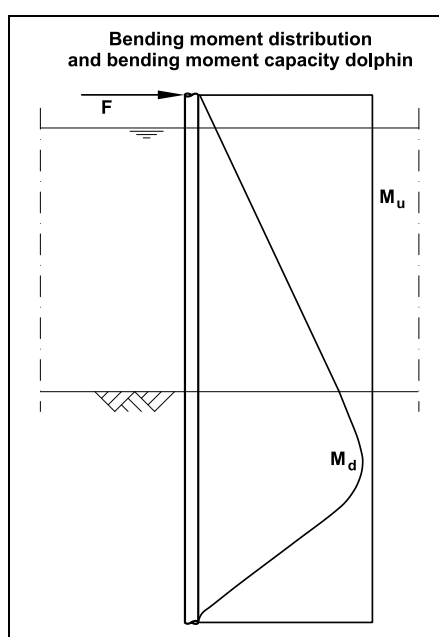


Figure 2-9 Bending moment verification

In order to activate as much deformation capacity as possible, the dolphin is normally assembled of sections with the same outside diameter but with varying wall thickness and steel grade, refer to Figure 2-10.

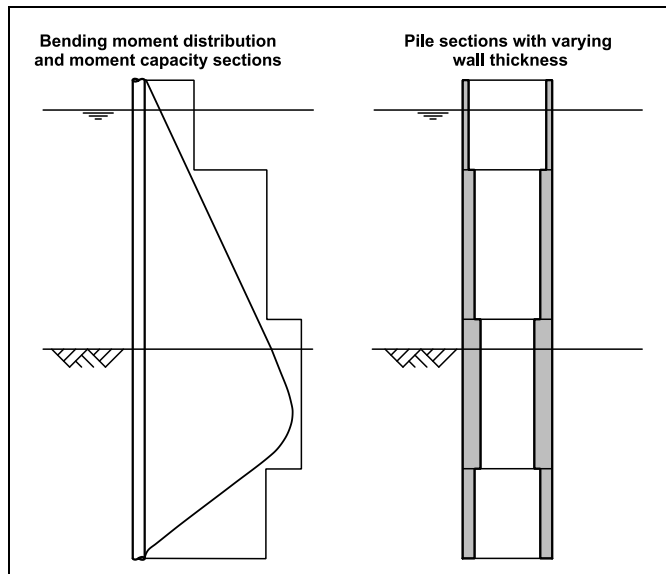


Figure 2-10 Pile sections and bending moments

At the location of the largest bending moments the strongest cross-section is applied, and at positions of smaller bending moments cross-sections with less strength and stiffness are applied. This way the strength and stiffness of every pile section is used more optimally.

Application of high grade steel is usually recommended, due to high strength and energy absorption characteristics.

An often used design parameter for a dolphin is the diameter-wall thickness (D/t) ratio. This ratio is used as a measure for the stiffness of the pile, which depends entirely on the diameter D and wall thickness t of the cross-section. Application of a D/t ratio of 50-70 is common practice in the design environment.

3. PROBLEM ANALYSIS

3.1. Introduction

In this chapter the problems under investigation in this thesis project are first identified and analysed. This analysis results in a concise problem definition. Next possible solutions in terms of further research are identified, and a decision is made for the research to be performed in this thesis project. To conclude the objectives for the thesis research are defined.

3.2. Plastic design in latest generation design standards

In the design standards and guidelines applicable to flexible dolphins a trend towards plastic design can be identified, i.e. allowing some plastic deformation of the dolphin to occur when dealing with abnormal ship impact.

Firstly the concept of design standards is introduced. Secondly currently effective standards and guidelines for dolphins are treated. Thirdly the trend towards plastic design is discussed.

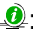
Introduction design standards and guidelines

In general, design standards and guidelines dictate the design method to be followed, the safety factors to be applied and the mechanisms to be checked in the structural design. They provide the framework for a safe and reliable structural design.

Distinction can be made between:

- a. Standards for a specific material
 - b. Standards for a specific structural application
- ad a. Most countries have established standards dealing with the application of a specific construction or foundation material in the design of buildings and civil engineering structures. Of these standards those dealing with steel as construction material and those dealing with soil as foundation material are relevant for dolphin design.
- ad b. In addition to these material-specific standards, standards specifically for the design of breasting dolphins are available in the UK and Germany. The International Navigation Association (PIANC) also provides design guidelines for dolphins.

Currently effective standards and guidelines applicable to dolphins

The following standards and guidelines are effective :

- NEN 6770: Dutch standards for steel structures
- EAU 1996: German guidelines for dolphin design
- BS 6349 Part 2 and Part 4: British standards for Maritime structures including a specific section on dolphin design
- PIANC 1984: Guidelines from the International Navigation Association for fender systems including specific guidelines for dolphin design
- PIANC 2002: Updated guidelines for fender systems



NEN 6770

EAU 1996

BS 6349-2:1988

BS 6349-4:1994

PIANC, 1984

PIANC WG 33, 2002

In Table 3-1 the standards are compared on the subjects of design method, limit states, limit state criteria, partial factors of safety and calculation models.

In the table, the symbol + indicates that the subject is covered in the designated standards, the symbol - indicates that the subject is not covered.

Subject	NEN 6770	PIANC 1984	PIANC 2002	BS 6349	EAU 1996
Parts					
Design method					
Deterministic calculation using $R - S \geq 0$	+	+	+	+	+
Partial factors of safety	+	+	+	+	+
Limit states					
Yield	+	+	+	+	+
Deformation	-	-	+	+	+
Buckling	+	-	-	-	-
Ovalisation	-	-	-	-	-
Limit state criteria					
Yield: f_y (ULS)	+	+	+	+	+
Deformation: $y_{\max} = 1,5$ m (SLS)	-	-	+	+	+
Buckling: classification of sections: M (Class 1 section: $D/t < 50 \alpha_y^2$) ~ 25 ¹⁾ M (Class 2 section: $D/t < 70 \alpha_y^2$) ~ 35 ¹⁾ M (Class 3 section: $D/t < 90 \alpha_y^2$) ~ 45 ¹⁾ M (Class 4 section: $D/t > 90 \alpha_y^2$) ~ 45 ¹⁾	M_{pl} M_{pl} M_{el} M_{el}	-	-	-	-
Partial factors of safety					
E (abnormal impact factor)	-	-	1,25 – 2	2,0	-
F	1,5	-	1,25 ²⁾ 1,0	-	1,0
f_y	-	1,22	-	1,25	1,0
Hydrodynamic calculation models					
KE approach	-	+	+	+	+
IRF / LW approach	-	named	named	-	-
Pile-soil interaction calculation models					
Blum	-	+	+	-	+
P-y curve method	-	+	+	+	-
Subgrade reaction model	-	named	+	-	-
FEM method	-	named	+	-	-

Table 3-1 Contents of standards

¹⁾ Classification of sections according to NEN 6770 section 10.2.4.1

$$\alpha_y = \sqrt{\frac{f_{ref}}{f_{y;d}}} \quad \text{with } f_{ref} = 235 \text{ N/mm}^2$$

Values given (25, 35, 45) are D/t values for $f_{y;d} = 460 \text{ N/mm}^2$

²⁾ Depends on pile capacity to resist overloading by plastic yielding:

- No yielding possible: $\gamma = 1,25$

- Yielding possible until a displacement of at least $2 \cdot y_{el}$: $\gamma = 1,0$

Trend towards plastic design

In the design of steel flexible dolphins the main strength parameter used in the calculation is the yield stress of the steel pile. Apparently the criterion is that no permanent deformation of the steel pile occurs. However, in EAU 1996 a load factor of 1,0 is applied. This can be explained as follows.

The loads on the berthing structure take the form of energy: (part of) the kinetic energy of the moving ship is transferred to the dolphin and temporarily stored as potential energy by a combination of reaction force between ship and dolphin and lateral deflection of the pile:

$$E = \int F \cdot dy \quad <3.1>$$

If the yield stress is exceeded some plastic deformation of the pile occurs. After impact the dolphin swings back to a position with only a small permanent deformation. The dolphin will now have a larger elastic energy absorption capacity due to the incurred plastic deformation, refer to Figure 3-1.

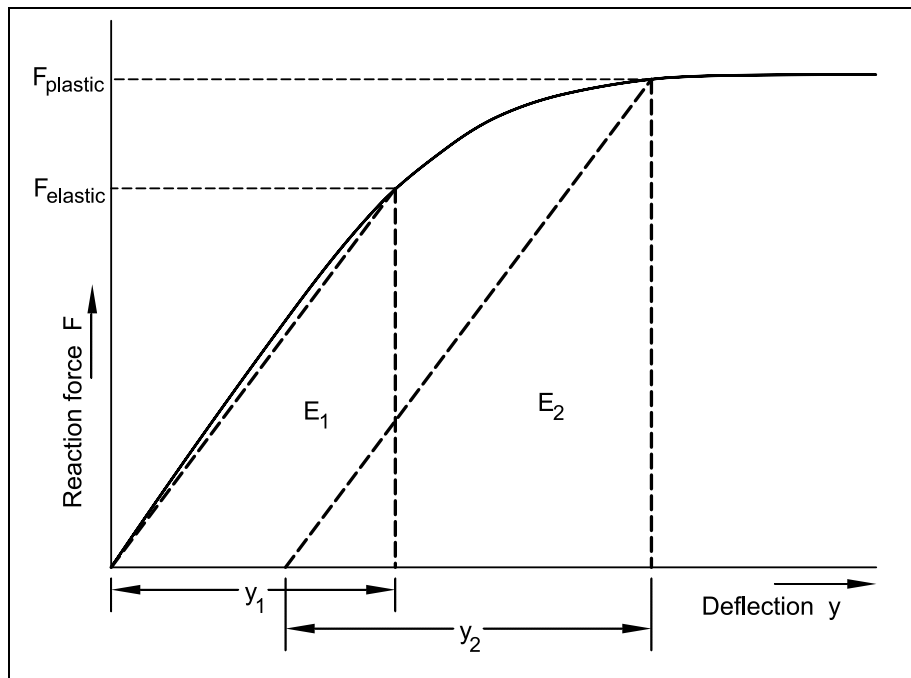


Figure 3-1 Load-deflection curve with increase of elastic energy absorption capacity

This safety can theoretically increase to as much as 1,7, provided that no failure due to buckling, ovalisation or soil failure occurs first:

$$\left. \begin{aligned} F_{plastic} &\approx 1,3 \cdot F_{elastic} \\ y_2 &\approx 1,3 \cdot y_1 \end{aligned} \right\} E_2 \approx (1,3^2) \cdot E_1 \approx 1,7 \cdot E_1 \quad <3.2>$$

PIANC 2002 explicitly mentions this plastic yielding capacity and proposes a load factor of 1,0 (instead of 1,25) if yielding is possible until a displacement of at least two times the maximum elastic displacement.

However, the current design method is not suitable to safely employ this plastic yielding capacity, for the following reasons:

- The precise form of the load-deflection curve is not known, so the magnitude of the safety which can be realised by plastic yielding is not known
- Only yielding and excessive deformation are identified as a failure mode in standards, while it is expected that buckling and ovalisation will be significant failure modes in the plastic range and may even be significant in the elastic range for some designs

In Figure 3-2 this uncertainty about the form of the load-deflection curve and the magnitude of the safety in the plastic range is visualised.

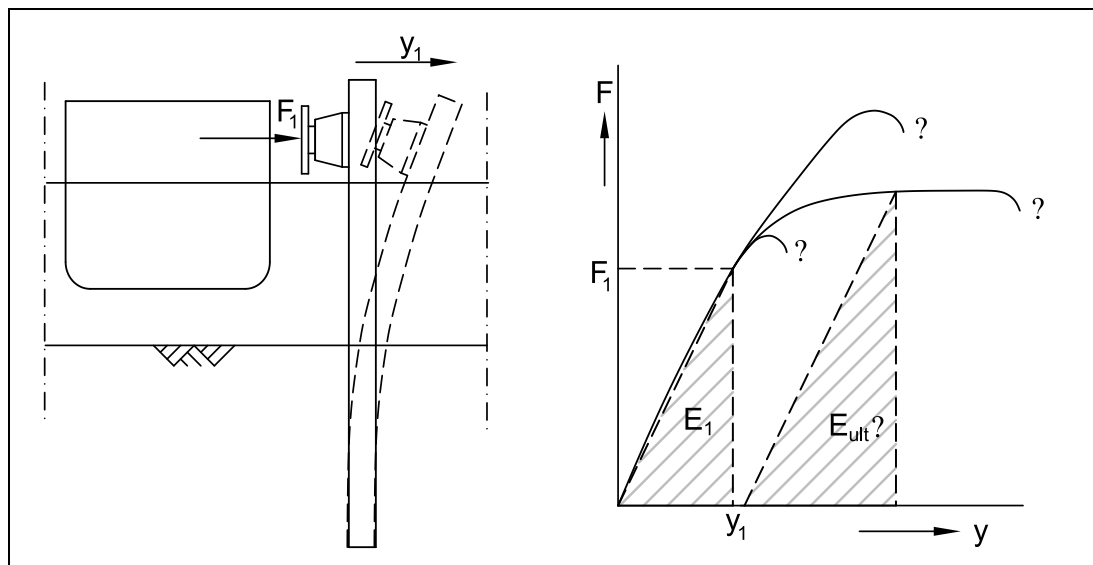


Figure 3-2 Load-deflection curve in the plastic range not known

3.3. Damage to dolphins

Doubt about the employment of plastic deformation capacity in design standards seems to be supported by damage cases in recent years. If some permanent deformation of the pile is observed after a single berthing, questions rise about:

- The nature of the permanent deformation: yield / buckling / soil failure
- The remaining energy absorption capacity
- Course of action: repair / replacement / continued use without action
- The cause of the damage: excessive loading / insufficient strength
- The responsibility for the damage: ship owner / terminal operator / designer

There are even lawsuits running which are based on these type of damage cases, in order to determine which party should be held responsible for the damage and pay for the necessary repairs.

The following questions are discussed subsequently in this section:

1. Which causes for the occurrence of failure can be identified and what are the underlying problems leading to the damage?
2. Which failure modes cause damage to the dolphin in the form of permanent deformation?
3. Why does damage to dolphins in recent years lead to questions about the safety of the design method? Which changes or trends in dolphin design are responsible for this development?

Which causes for the occurrence of failure can be identified?

The possible causes can be categorised as follows:

- Construction errors
- Excessive loading
- Insufficient strength

Construction errors

Construction errors mostly lead to unexpected failure of specific structural parts like brittle fracture of welds at the location of weld faults. This type of failure is different from the type of failure currently under investigation, so it is concluded that construction errors are not the problem in this case.

Excessive loading

If the allowable values for load parameters are exceeded, e.g. the allowed approach velocity is exceeded or a larger than allowed ship uses the berth, the loads exceed the strength leading to failure.

The task of the designer (in deliberation with the terminal operator) is to establish allowable values for these load parameters which are practicable in operational conditions and which provide a safety margin against failure of the berthing structure or ship. These allowable values should be chosen with great care and consideration, based on a thorough assessment of the safety of the system.

The following problems regarding the assessment of allowable values for load parameters can be identified:

- The accuracy of hydrodynamic models (used to predict the loads on the berthing structure caused by the berthing ship) is doubted; the result is that the safety against failure due to excessive loading is difficult to assess
- The establishment of allowable approach velocities is complicated by:
 - The large variance in approach velocities due to the complexity of the berthing manoeuvre and the dependency on human judgement
 - The limited amount of data available from real-time measurements; the establishment of appropriate allowable approach velocities using a statistical approach is therefore difficult

Refer to Annex I.5, pages 82 and further for a more detailed treatment of hydrodynamic models.

Insufficient strength

The following causes for insufficient strength can be distinguished:

- Strength degradation due to time-effects:
 - Corrosion of the steel parts
 - Fatigue due to recurrent loading; this however is assessed to be insignificant because of the very low frequency of loading
- Poor prediction of system behaviour:
 - Load-deflection behaviour predicted by pile-soil interaction models is limited to the elastic range and is based on a poor theoretical representation of the deflection behaviour
- Inadequate safety assessment in design:
 - No or little safety margin within elastic range
 - Plastic yielding capacity is included in safety of design while not verifiably founded on knowledge of the structural behaviour in the plastic range
 - Failure modes buckling and ovalisation are not checked in design

Which failure modes cause permanent deformation?

Out of all possible failure modes for the berthing system (refer to Annex I.3, page 80), only the ones responsible for permanent deformation of the dolphin are important for the current investigation. These are (refer to the marked area in Figure 3-3):

- Failure of the pile: yield, buckling, ovalisation (location e)
- Failure of the soil: wedge-type failure, plastic soil flow (location f and g respectively)

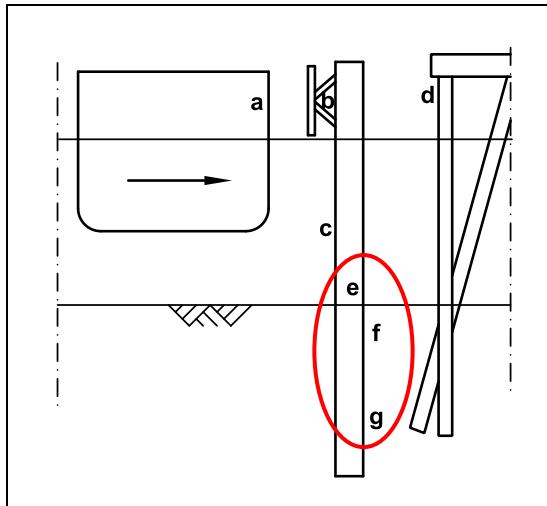


Figure 3-3 Locations of failure modes, red marked is the area under investigation

This means that the problem focuses on the behaviour of the pile in the soil, which is made visible by the hatched area in the fault tree in Figure 3-4.

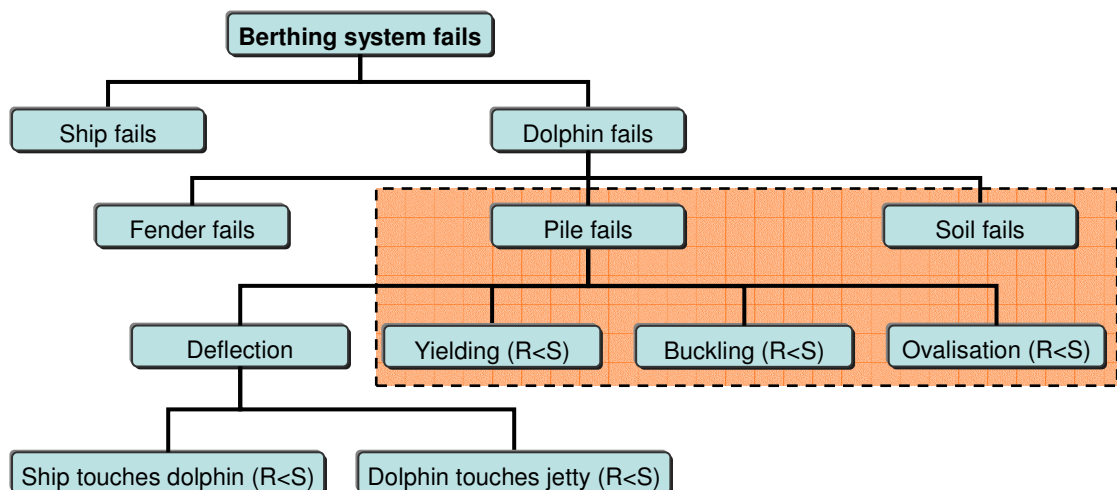


Figure 3-4 Fault tree for a berthing system

Note that the failure modes buckling and ovalisation are not yet proven to be significant for the ultimate strength of the pile, this will have to be investigated.

The occurrence of these failure modes can only be assessed by an appropriate pile-soil interaction model which is able to describe the structural behaviour of the dolphin up to failure. The currently used models (Blum, p-y curve method) are not suitable for this assessment.

Why did damage to dolphins lead to questions about the safety of the design?

Trends that can be identified in dolphin design over the years:

1. Application of high grade steel, resulting in higher strength and consequently higher energy absorption capacity
2. Application of flexible dolphins consisting of single large diameter piles with relatively low wall thickness (D/t ratio up to 70-80), for the following reasons:
 - Single-pile flexible dolphins are cheaper and easier to install than multi-pile rigid dolphins
 - The stiffness is chosen as low as possible (by choosing a low wall thickness) to increase the deflection and (consequently) energy absorption capacity
 - The amount of steel in the pile is minimised by reducing the wall thickness as much as possible to minimise the total cost of the dolphin
3. Assembling the pile from pile sections of varying wall thickness and steel grade, for the following reasons:
 - The strength of each pile section can be set to meet the local requirements
 - The overall stiffness is reduced allowing for larger deflections (= larger energy absorption capacity) while not sacrificing the required strength
 - The overall weight and cost of the pile can be reduced significantly compared to a pile with uniform cross-section
4. Implicit or explicit assumption of plastic yielding capacity in EAU 1996 and PIANC 2002 respectively, for the following reasons:
 - More optimal use of the pile's energy absorption capacity
 - After some plastic yielding the elastic energy absorption capacity has increased, with which theoretically a safety up to 1,7 can be realised

Consequences of these trends:

- The safety margin in the elastic range is reduced more and more over the years
- The incorporation of the plastic yielding capacity in the safety of the system leads to a change in design philosophy, where the criterion of no permanent deformation occurring is left
- The buckling sensitivity has increased compared to earlier designed dolphins, due to the noticed increase in the diameter-wall thickness ratio

3.4. Definition of the problem

The problem is assessed to be twofold:

1. EAU 1996 and PIANC 2002 implicitly or explicitly employ the plastic yielding capacity of the dolphin in the safety against failure. However:
 - No method is available to predict the load-deflection behaviour up to failure in order to assess the magnitude of the safety in the plastic range
 - Guidelines regarding the failure modes to check in elastic and plastic design are assessed to be incomplete: only yielding and excessive deformation are identified as failure modes, while it is expected that buckling and ovalisation will occur in the plastic range and even in the elastic range for some designs
2. Recent cases of damage to dolphins after a berthing lead to questions about the safety of the design, which can be traced back to:
 - The accuracy of hydrodynamic models to predict the loads on the dolphin
 - The difficulty in establishing allowable approach velocities
 - Above mentioned employment of plastic yielding capacity as safety margin, while the magnitude of this safety is unknown
 - Developments in dolphin design leading to less safe and more buckling sensitive designs

3.5. Research to be performed

Research alternatives solving (part of) the problem

Research dealing with the prediction of system behaviour (refer to Figure 3-5):

- a. Hydrodynamic models
 - Evaluation and verification of different models for hydrodynamic coefficients for: (1) sheltered conditions with no significant influence from wind, waves, current; (2) exposed conditions with large influence of wind, waves, current
- b. Approach velocity
 - More real-time measurement data of approach velocities in different (exposed / sheltered) conditions is needed for establishing accurate design criteria based on statistical analysis
- c. Pile-soil interaction models
 - Development of a calculation model to predict the load-deflection behaviour of a dolphin up to failure, including possible failure mechanisms occurring in the elastic and plastic range

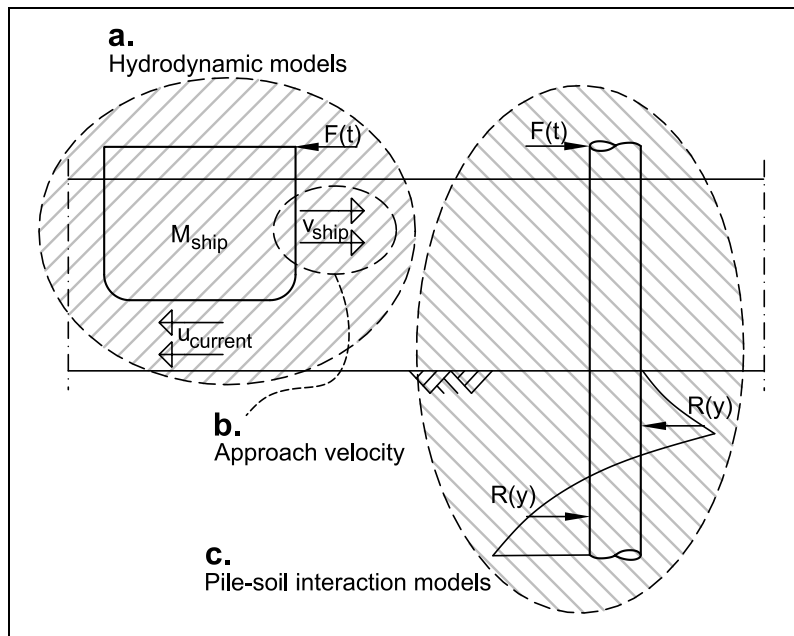


Figure 3-5 Research alternatives for system behaviour

Research dealing with the safety of the entire system:

- d. Damage analysis
 - Analysis of failure mechanism occurred, extent of damage, remaining energy absorption capacity, course of action to be undertaken
- e. Evaluation of standards and guidelines
 - A comparison of standards and guidelines to assess the influence of incorporating the plastic yielding capacity in the design on the safety of the design
- f. Probabilistic analysis
 - Assessment of the safety of the system including all failure modes using probabilistic methods; establishment of partial safety factors for all failure modes which provide the necessary safety in design guidelines

Choice

The choice is made to carry out the following assignments:

- c. Pile-soil interaction models
 - e. Evaluation of standards and guidelines
- ad c. A model for the prediction of the load-deflection behaviour of a dolphin up to failure should be developed to get insight into the nonlinear structural behaviour.
- ad e. The developed model can be used to evaluate current standards and guidelines, in order to assess the magnitude of the safety which can be realised by plastic design

This assignment can be visualised by Figure 3-6: developing a load-deflection curve up to failure in order to assess the safety in the plastic range.

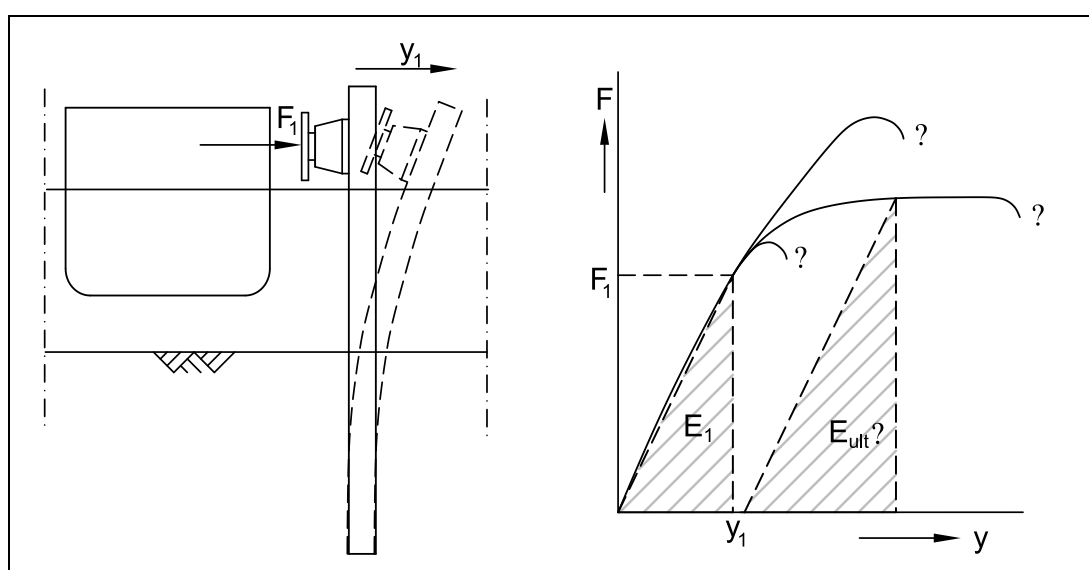


Figure 3-6 Assignment: develop load-deflection curve to assess safety in plastic range

3.6. Objectives

The first objective is to develop a model for the prediction of the nonlinear structural behaviour of a dolphin including all significant failure modes in the elastic and plastic range, resulting in a complete and accurate load-deflection curve up to failure.

This assignment is reported in Chapter 4.

The second objective is to compare the current design methods and guidelines with each other and to evaluate them using the developed calculation model, so conclusions can be taken about the safety which can be realised in the plastic range.

This assignment is reported in Chapter 5.

4. DEVELOPMENT OF A CALCULATION MODEL TO PREDICT THE NONLINEAR STRUCTURAL BEHAVIOUR OF A DOLPHIN

4.1. Introduction

In this chapter the development of a calculation model for the prediction of the nonlinear structural behaviour of a dolphin is presented.

Firstly the system to be considered is defined, followed by a description of the model. The theory of pile behaviour according to the plasticity theory of Gresnigt, soil behaviour according to Ménard and Brinch Hansen and limit states for the model are treated subsequently.

The results of the developed Bruijn model are presented next, followed by the verification of the model by comparison with existing calculation models. To conclude, some examples are given for the practical application of the developed model.

4.2. The system to be considered

The system to be considered is depicted in Figure 4-1, and consists of:

- A steel pile with uniform cross-section and steel grade
- The surrounding subsoil, being uniform, non-cohesive soil
- A static horizontal load at the pile-head, representing the loads induced by the berthing ship

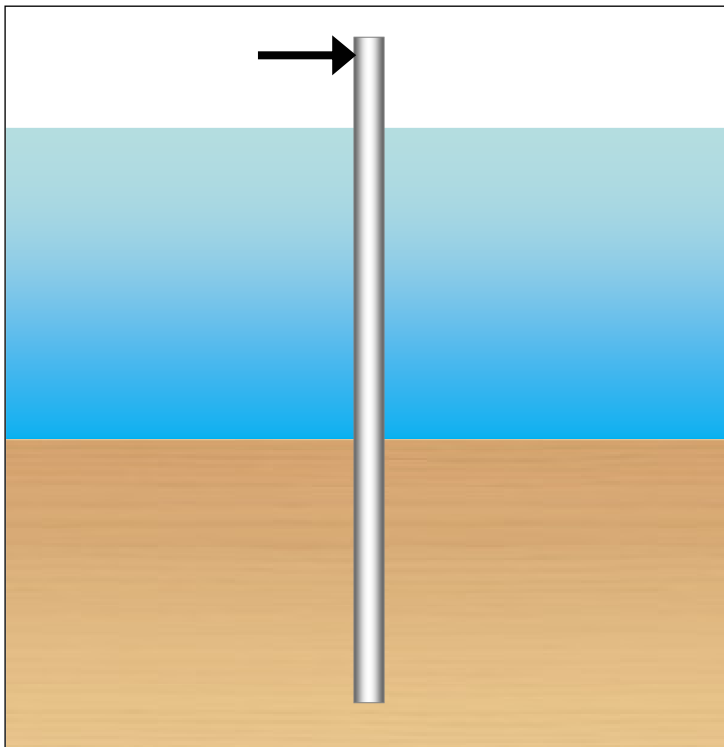


Figure 4-1 The system considered

4.3. Description of the model

In Annex II the complete development of the calculation model including design choices is presented. In this section only the resulting model is presented.

The choice is made to develop a numerical model based on the theory of subgrade reaction. In this model the soil is modelled as springs (Figure 4-2a), which leads to the static scheme presented in Figure 4-2b

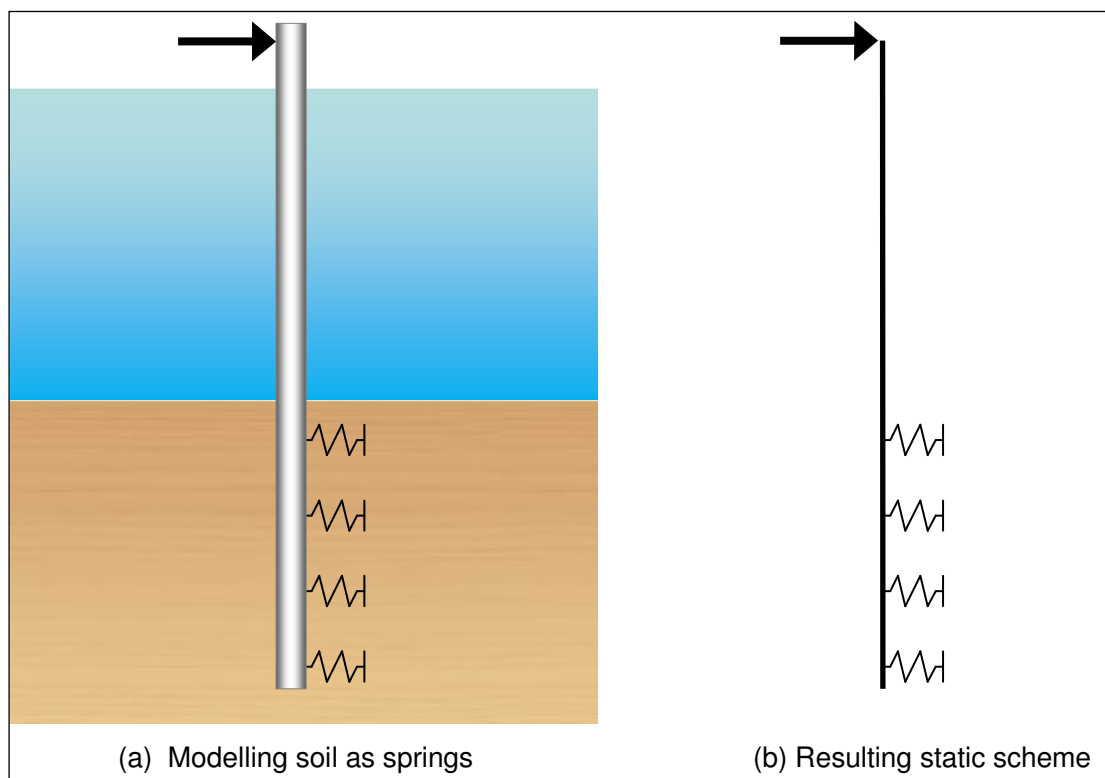


Figure 4-2 The static scheme

The pile is divided into elements for which constitutive relations, equations of equilibrium and kinematical equations can be drawn up, refer to Figure 4-3.

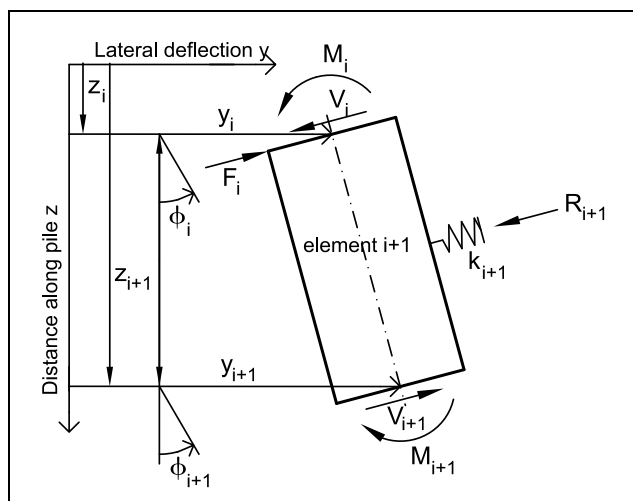


Figure 4-3 Element of pile, numerical representation

The basic formulation of the model is given by the following partial differential equation:

$$\boxed{EI \cdot \frac{d^4 y}{dz^4} + k_h \cdot y = f(z)} \quad <4.1>$$

For the nonlinear behaviour of the pile (the first term in equation <4.1>) the plasticity theory according to Gresnigt is used. This theory is presented in section 4.5 on pages 22 and further.

For the soil behaviour (the second term in equation <4.1>), the bilinear spring characteristic is drawn up by using the theory of Ménard for the soil stiffness and the theory of Brinch Hansen for the plastic limit of the soil. These theories are presented in section 4.6 on pages 28 and further.

The following limit states for the model are taken into account:

- Stresses in the pile
- Strains in the pile
- Deformation of the pile
 - Ovalisation of the pile cross-section
 - Buckling of the pile wall
- Soil failure

These limit states are elaborated in section 4.7 on pages 37 and further.

The model is written and calculated in Microsoft Excel and Visual Basic:

- Input, output and formulas are in an Excel sheet
- The solve technique by calculation of the forces and displacements of all nodes through iteration is performed by the macro functionality in Excel and written in Visual Basic

The output consists of:

- Pile and soil forces and displacements for all nodes due to a single static load F
- A complete load-deflection curve up to failure, representing the pile-head deflection for all values of the static load F

NB. the developed model is called the Bruijn model for future reference.

4.4. Limitations

Assumptions / limitations which are effective for the model:

- Cross-sections remain straight
- Uniform cross-section over the length of the pile (no varying wall thickness or steel grade)
- Bilinear stress-strain diagram
- Moment-curvature relation is approximated by a sixth order polynomial
- No post-buckling behaviour
- No torsional moments incorporated
- Uniform, non-cohesive soil
- Drained deformation
- No influence of soil in pile is taken into account
- Actions on the dolphin are considered as static loads

4.5. Theory: plasticity theory according to Gresnigt



Gresnigt, A.M., 1986
Chapter 2 and 6

The theory described in this section is borrowed from the report “Plastic design of buried steel pipelines in settlement areas” by A.M. Gresnigt.

Moment-curvature relation: linear elastic

Under assumption of the linear stress-strain relationship depicted in Figure 4-4 the following formulas are deduced from the analysis of a straight pipe subjected to bending, refer to Figure 4-5.

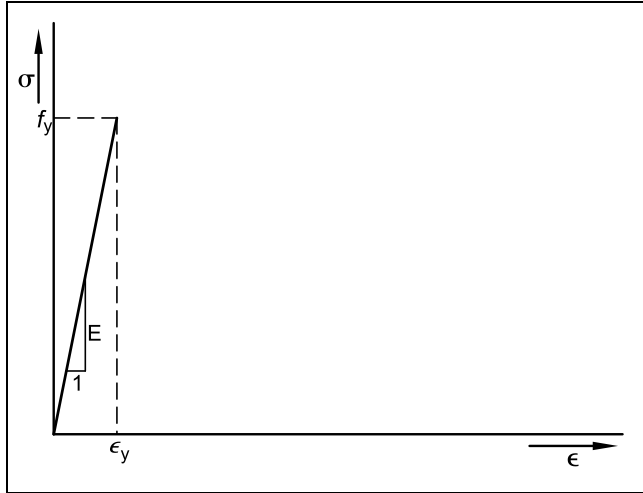


Figure 4-4 Linear stress-strain diagram

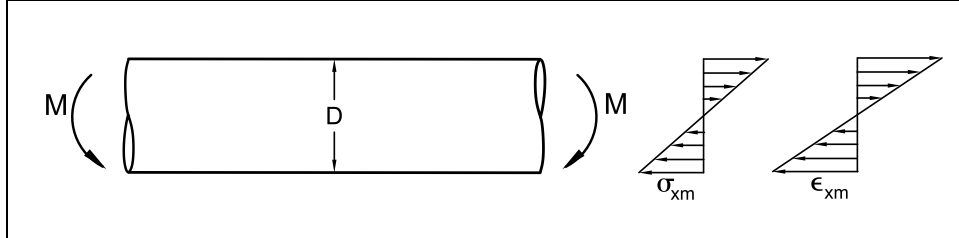


Figure 4-5 Pipe section with stress and strain distribution due to bending

For the stress σ_{xm} we obtain:

$$\sigma_{xm} = \frac{M}{W_e} = \frac{M}{I / (0,5 \cdot D)} = \frac{M}{\pi \cdot r^2 \cdot t} \quad <4.2>$$

For the strain ϵ_{xm} we obtain:

$$\epsilon_{xm} = \frac{\sigma_{xm}}{E} = \frac{M}{E \cdot I / (0,5 \cdot D)} = \frac{M \cdot (0,5 \cdot D)}{EI} \quad <4.3>$$

And for the curvature κ we obtain:

$$\kappa = \frac{\epsilon_{xm}}{0,5 \cdot D} = \frac{M \cdot 0,5 \cdot D / EI}{0,5 \cdot D} = \frac{M}{EI} \quad <4.4>$$

When the yield stress is reached the bending moment will be:

$$M = \pi \cdot r^2 \cdot t \cdot f_y = M_e \quad <4.5>$$

The curvature is then:

$$\kappa = \frac{M_e}{EI} = \kappa_e \quad <4.6>$$

So the relation between the bending moments due to lateral loading and the response of the pile in terms of curvature is linear and limited to the full-elastic moment and corresponding curvature. This moment-curvature relation is depicted in Figure 4-6.

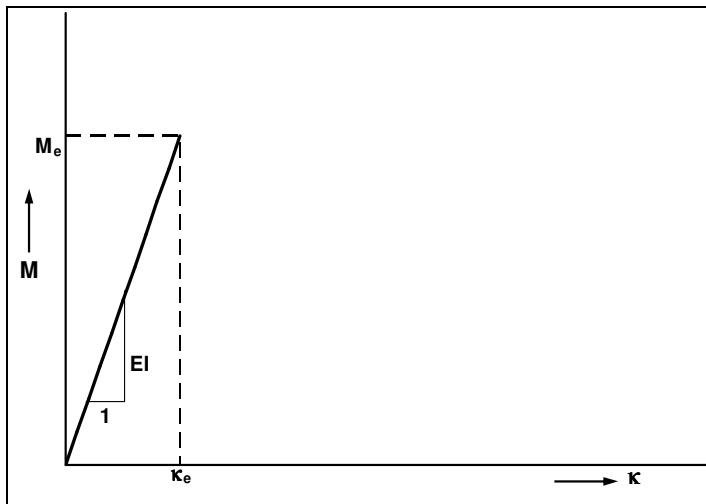


Figure 4-6 Linear moment-curvature diagram

Moment-curvature relation: elastoplastic

When the stresses due to bending reach the yield stress, the plastic branch of the assumed bilinear stress-strain diagram (Figure 4-7) is reached.

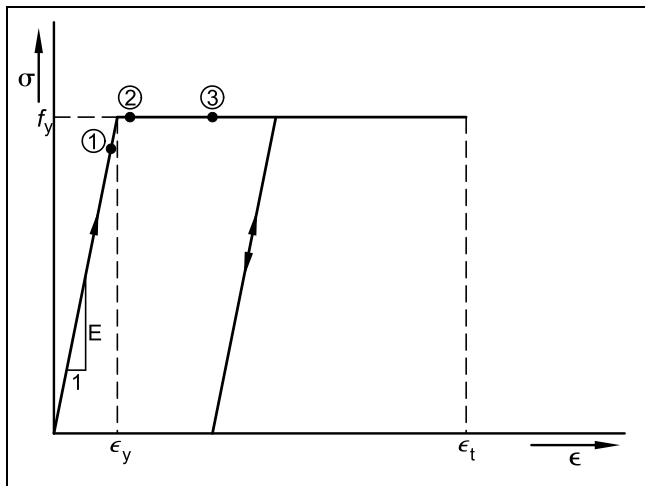


Figure 4-7 Bilinear stress-strain diagram

The three points indicated in the stress-strain diagram (Figure 4-7) correspond with the stress and strain distributions as shown in Figure 4-8.

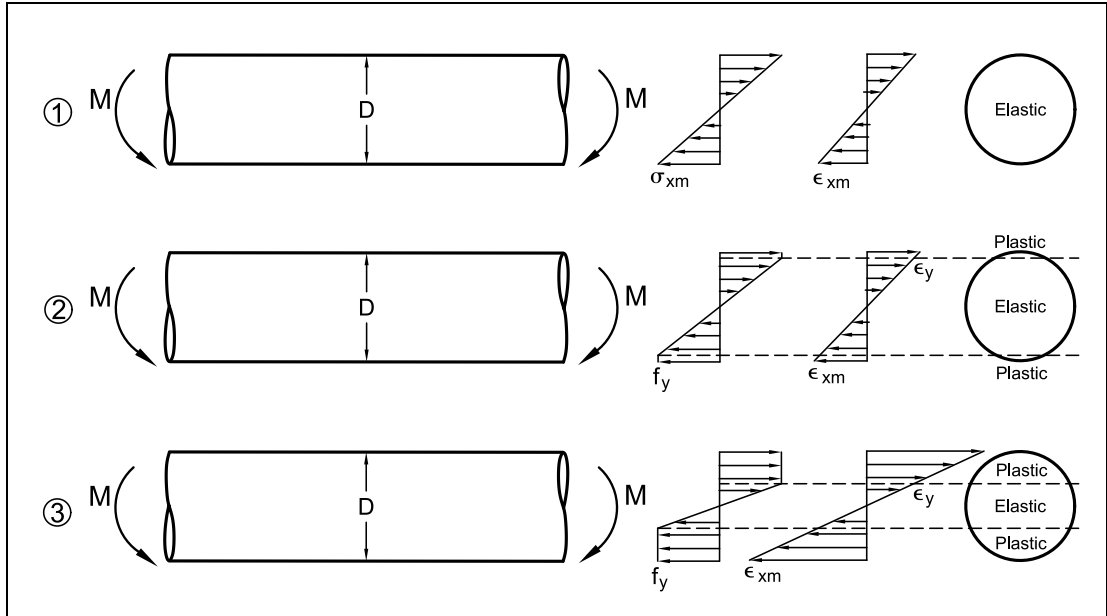


Figure 4-8 Stress and strain distribution for three points in stress-strain diagram

For points 2 and 3 the linear relations: $\sigma_{xm} = \frac{M}{W_e}$ and $\epsilon_{xm} = \frac{\sigma_{xm}}{E}$ are no longer valid for the entire cross-section. So the response of the pipe to bending moments exceeding the full-elastic moment (equation <4.5>) must be calculated differently.

If the cross-section is partly elastic and partly plastic, a variable λ can be defined which is a measure for the part of the cross-section in which yielding occurs, see Figure 4-9.

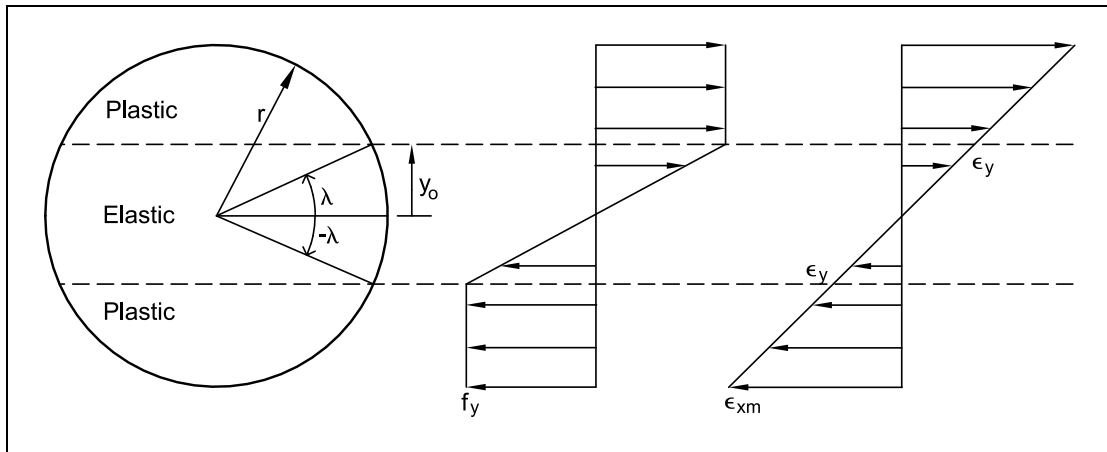


Figure 4-9 Definition sketch λ parameter

The curvature of the partly plastified section can be calculated by considering the transition between the elastic and plastic part, where the following is true:

$$\kappa = \frac{\epsilon_y}{y_0} = \frac{f_y/E}{r \cdot \sin \lambda} = \frac{f_y}{E \cdot r \cdot \sin \lambda} \quad <4.7>$$

This way the curvature is expressed as a function of λ .

The bending moment can be calculated with the integral:

$$M = \int_A \sigma \cdot y \cdot dA \quad <4.8>$$

For the given stress distribution this yields:

$$\begin{aligned} M &= 4 \cdot \int_0^{\lambda_0} r \cdot t \cdot f_y \cdot \frac{\sin^2 \lambda}{\sin \lambda_0} \cdot r \cdot \sin \lambda \cdot d\lambda + 4 \cdot \int_{\lambda_0}^{\pi/2} r \cdot t \cdot f_y \cdot r \cdot \sin \lambda \cdot d\lambda \\ &= 2 \cdot r^2 \cdot t \cdot f_y \cdot \left(\int_0^{\lambda_0} \frac{2 \cdot \sin^2 \lambda}{\sin \lambda_0} \cdot d\lambda + \int_{\lambda_0}^{\pi/2} 2 \cdot \sin \lambda \cdot d\lambda \right) \\ &= 2 \cdot r^2 \cdot t \cdot f_y \cdot \left(\left[\frac{\lambda_0}{\sin \lambda_0} - \frac{1/2 \cdot \sin(2 \cdot \lambda_0)}{\sin \lambda_0} \right] + [2 \cdot \cos \lambda_0] \right) \\ &= 2 \cdot r^2 \cdot t \cdot f_y \cdot \left(\frac{\lambda_0}{\sin \lambda_0} + \cos \lambda_0 \right) \end{aligned} \quad <4.9>$$

In general form, after replacement of λ_0 by λ :

$$\left. \begin{aligned} M &= 2 \cdot r^2 \cdot t \cdot f_y \cdot \left(\frac{\lambda}{\sin \lambda} + \cos \lambda \right) \\ \kappa &= \frac{f_y}{E \cdot r \cdot \sin \lambda} \end{aligned} \right\} \text{ for } 0 < \lambda < \pi/2 \quad <4.10>$$

For $\lambda = \pi/2$, yielding is just attained. In that case the expressions for M and κ reduce to:

$$M = \pi \cdot r^2 \cdot t \cdot f_y = W_e \cdot f_y = M_e \quad <4.11>$$

$$\kappa = \frac{f_y}{E \cdot r} = \frac{W_e \cdot f_y}{EI} = \frac{M_e}{EI} = \kappa_e \quad <4.12>$$

Notice that these expressions for the full-elastic moment and curvature (<4.11> and <4.12>) match the ones derived in the preceding section (<4.5> and <4.6>).

For $\lambda \rightarrow 0$, the whole cross-section will be plastified and the maximum moment is reached:

$$M = 4 \cdot r^2 \cdot t \cdot f_y = W_p \cdot f_y = M_p \quad <4.13>$$

$$\kappa \rightarrow \infty \quad <4.14>$$

With the expressions in <4.10> the complete theoretical moment-curvature diagram can be drawn, refer to Figure 4-10.

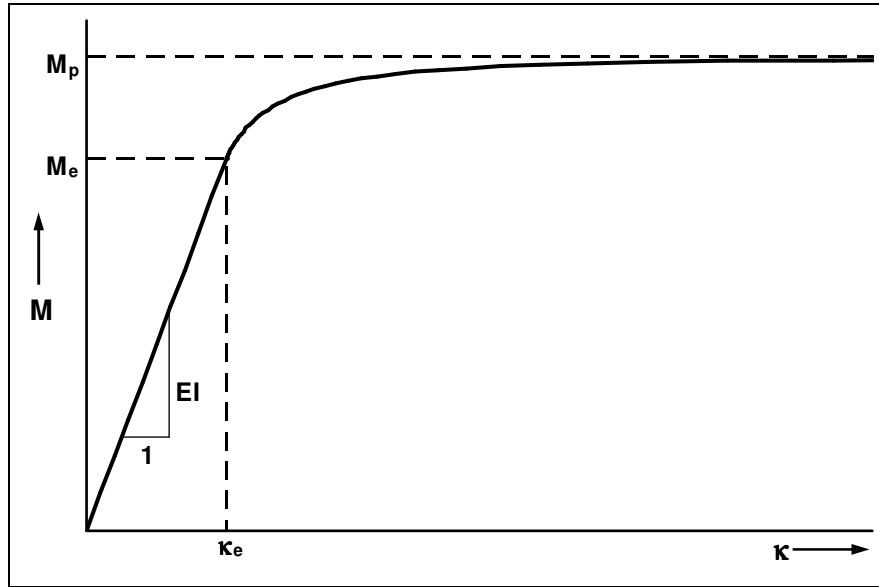


Figure 4-10 Nonlinear moment-curvature diagram

How can the curvatures be calculated from the bending moments?

The calculation sequence in the model requires that the curvature is calculated from the bending moments. This means that the derived formula for $M(\lambda)$ in equation <4.10> must be adapted so that λ is expressed as a function of M , i.e. $\lambda(M)$.

Because as yet it is found impossible to acquire a mathematical expression for $\lambda(M)$, this function is fitted with a sixth order polynomial function.

The formula for $M(\lambda)$ is:

$$M = 2 \cdot r^2 \cdot t \cdot \left(\frac{\lambda}{\sin \lambda} + \cos \lambda \right) \cdot f_y \quad <4.15>$$

Isolating the terms with λ , thus making the right-hand side non-dimensional, yields:

$$\frac{M}{2 \cdot r^2 \cdot t \cdot f_y} = \frac{\lambda}{\sin \lambda} + \cos \lambda \quad <4.16>$$

We define a variable β containing all case-dependent parameters, so that

$$\beta = \frac{M}{2 \cdot r^2 \cdot t \cdot f_y} = \frac{M}{0,5 \cdot M_p} \quad <4.17>$$

Then

$$\lambda(\beta) = f\left(\frac{\lambda}{\sin \lambda} + \cos \lambda\right) \quad \text{for } 0 < \lambda < \frac{\pi}{2} \quad <4.18>$$

When λ is plotted against $(\frac{\lambda}{\sin \lambda} + \cos \lambda)$ the graph in Figure 4-11 is obtained.

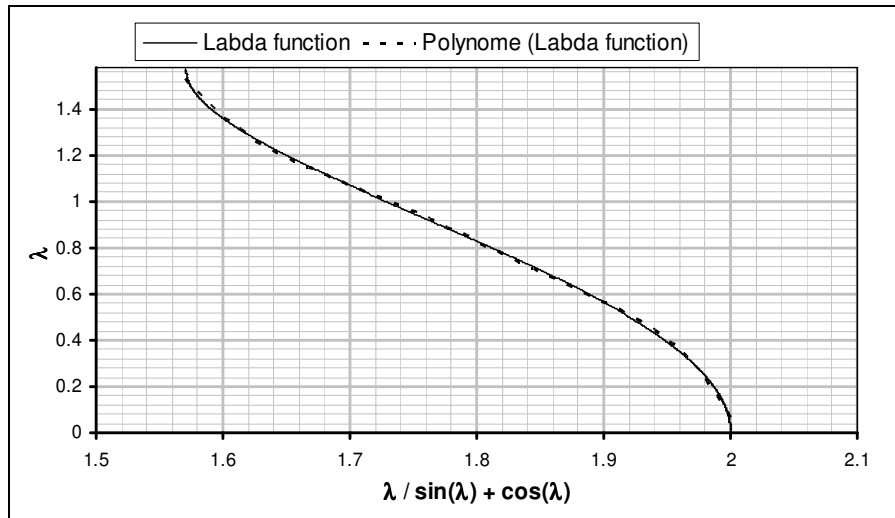


Figure 4-11 Lambda function and fit curve

In Microsoft Excel, this graph can be fitted with a sixth order polynomial function, also shown in Figure 4-11:

$$\begin{aligned} \lambda(\beta) = & -1506,601 \cdot \beta^6 + 15304,715 \cdot \beta^5 - 64514,38 \cdot \beta^4 \\ & + 144383,76 \cdot \beta^3 - 180849,1 \cdot \beta^2 + 120130,99 \cdot \beta - 33034 \end{aligned} \quad <4.19>$$

Using this expression, λ can be calculated from the bending moments. Subsequently, the curvature can be calculated using equation <4.10>

The accuracy of this approximation can be checked by plotting the approximated moment-curvature relation against the original moment-curvature relation, as shown in Figure 4-12. From this plot it can be concluded that the approximation is accurate.

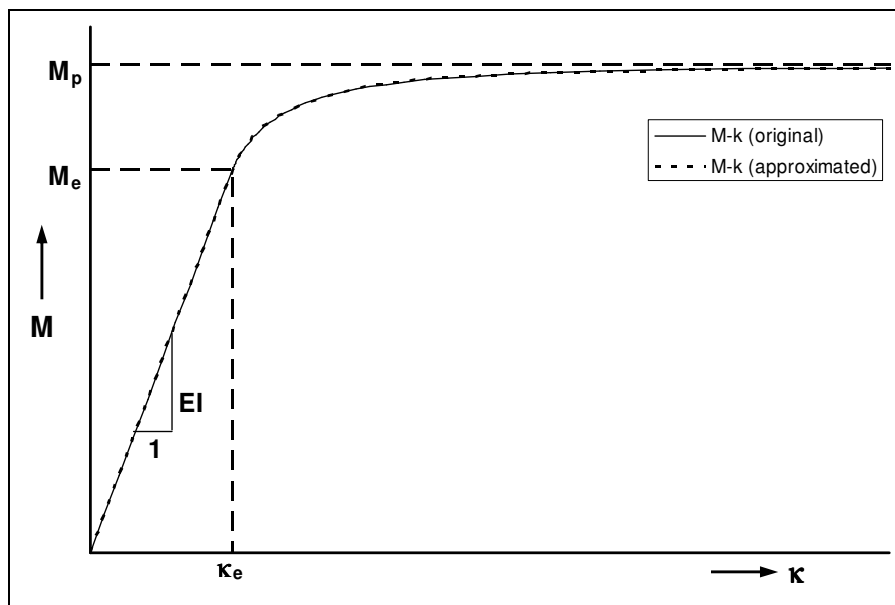


Figure 4-12 Moment-curvature diagram and approximation using $\lambda(M)$

There is however a remark to be made about this moment-curvature relation: the original moment-curvature diagram presented in Figure 4-12 is influenced by e.g. residual stresses from rolling and welding, which are not taken into account. So the moment-curvature relation used in this analysis is an approximation of the moment-curvature relation in reality.

The function $\lambda(\beta)$ is non-dimensional and parameter-independent. This means that the sixth order polynomial with derived coefficients can be used in any case where the plastic curvatures are to be calculated from the bending moments for a tubular hollow section with a given yield strength.

Effect of earth pressure, curvature and ovalisation on the moment-curvature relation

Under influence of earth pressure, curvature and ovalisation the cross-section is deformed. These effects are called 2nd order effects. Due to these 2nd order effects the strength and stiffness of the cross-section is reduced. By analysis of the influences of earth pressure, curvature and ovalisation these effects can be quantified and included in the moment-curvature relation.

The following steps are taken to come to the 2nd order moment-curvature relation:

1. Calculation of plate forces due to earth pressure, curvature and ovalisation
2. Calculation of the resulting maximum moment by integration of these plate forces
3. Formulas to calculate the magnitude of the ovalisation
4. Establishment of the reduced moment-curvature relation by applying adapted parameters

Plate forces due to earth pressure, curvature and ovalisation

When considering a small element of the pile wall the plate forces acting on that element are: bending moments m_x and m_y , normal forces n_x and n_y , where the x-direction is the longitudinal direction of the pile, and the y-direction is the circumferential direction, refer to Figure 4-13.

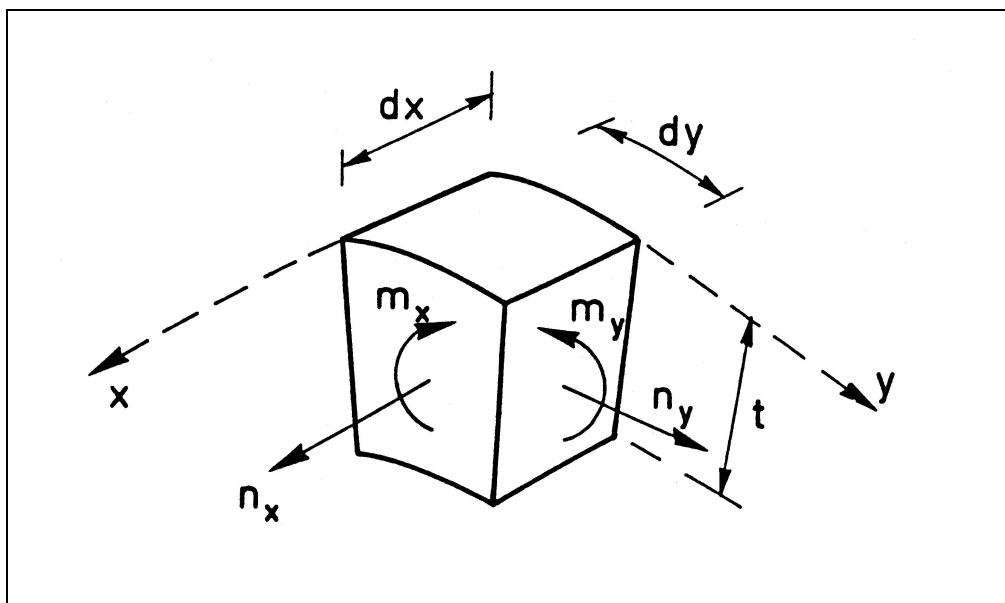


Figure 4-13 Plate forces on a pile wall element

These plate forces are influenced by the earth pressure, curvature and ovalisation. The contributions of the separate phenomena can be superposed using:

$$m_y = m_{yq} + m_{yk} + m_{yp} \quad <4.20>$$

$$m_x = m_{xq} + m_{xk} + m_{xp} \quad <4.21>$$

$$n_y = n_{yq} + n_{yk} + n_{yp} \quad <4.22>$$

$$n_x = n_{xk} + n_{xp} \quad <4.23>$$

In these equations the subscripts stand for:

q = earth pressure
 k = curvature
 p = internal pressure

Influence of earth pressure Q :

The plate moments produced by earth pressure Q are indicated in Figure 4-14, where the subscripts t , s and b are referring to top, sides and bottom of the cross-section.

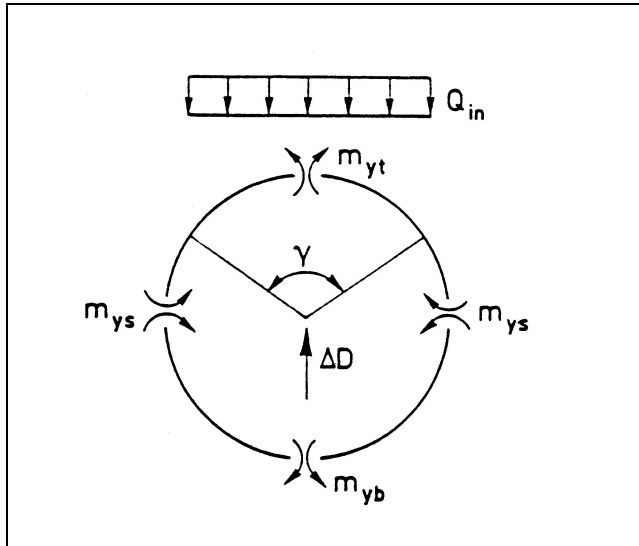


Figure 4-14 Plate moments due to earth pressure Q

From the conditions of equilibrium it follows:

$$|m_{yt}| + 2 \cdot |m_{ys}| + |m_{yb}| = Q \cdot r \cdot \left(\frac{1}{2} - \frac{1}{4} \cdot \sin \frac{\gamma}{2} \right) \quad <4.24>$$

with

γ = Loading angle for earth pressure Q [degrees]

A value of 180 degrees for γ is applied consistently in the Bruijn model.

For the average moment at the top, the side and the bottom:

$$m_{yq} = \frac{1}{4} \cdot Q \cdot r \cdot \left(\frac{1}{2} - \frac{1}{4} \cdot \sin \frac{\gamma}{2} \right) \quad <4.25>$$

The average plate force n_{yq} can be approximated by:

$$n_{yq} = 0,125 \cdot Q \quad <4.26>$$

Influence of curvature κ :

Due to curvature κ caused by a bending moment M on a section of the pile, some ovalisation of the cross-section occurs, refer to Figure 4-15.

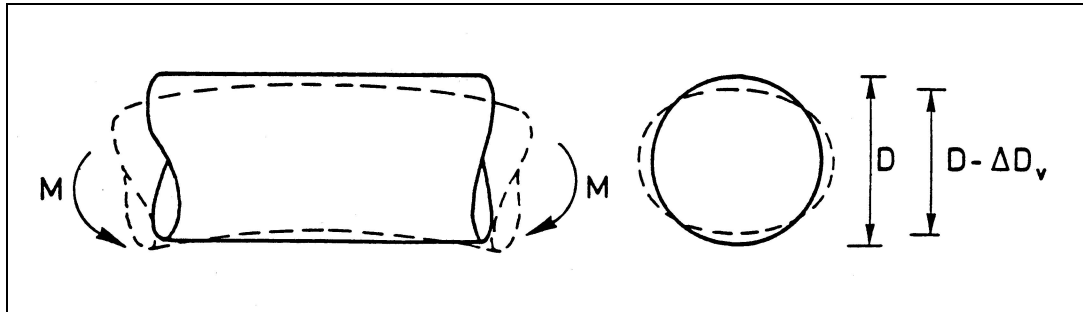


Figure 4-15 Ovalisation due to bending

Similar to the influence of earth pressure Q above, the plate moments due to the curvature κ can be obtained, resulting in expressions for m_{yk} and n_{yk} .

Influence of internal pressure P :

In a pile of circular cross-section an internal pressure P (e.g. in the case of a pipeline due to oil pressures) produces normal forces n_{yp} and n_{xp} in the pile wall. In an oval-section pile the moments m_{yp} will additionally occur, refer to Figure 4-16.

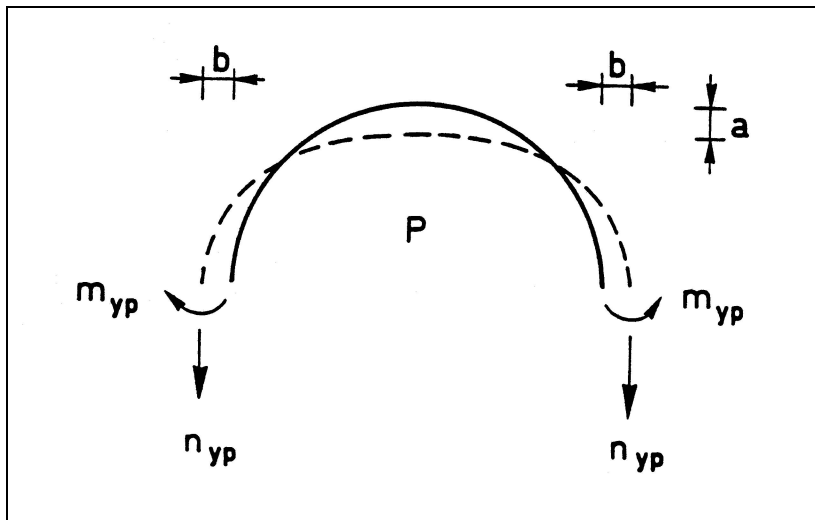


Figure 4-16 Plate forces in circumferential direction due to internal pressure P

Note: the influence of internal pressure is not included in the developed Bruijn Model. However, the theory of internal pressure could possibly be used when evaluating the influence of the soil in the pile on the moment-curvature relation.

Applying plastic theory for obtaining m_x and n_{xk}

The plate forces m_x and n_{xk} must be obtained by applying plastic theory.

According to plastic theory the stresses associated with the plate forces are allowed to be so chosen that the largest possible values for Q and M are obtained, on the following conditions:

- The yield point must not be exceeded
- Equilibrium must be satisfied
- Stresses must be in reasonably good agreement with the strains that occur

By choosing a stress distribution and applying the Von Mises yield criterion, evaluation of the equilibrium leads to expressions for m_x and n_{xk} .

Maximum moment M'_m that can be resisted

The resulting expressions for the plate forces must be integrated over the entire cross-section, leading to the following expression for the reduced full-plastic moment M'_m :

$$M'_m = \left(\frac{c_1}{6} + \frac{c_2}{3} \right) \cdot \left(1 - \frac{2}{3} \cdot \frac{a}{r} \right) \cdot M_p \quad <4.27>$$

with

$$c_1 = \sqrt{4 - 3 \cdot \left(\frac{n_y}{n_p} \right)^2}$$

$$c_2 = \sqrt{4 - 3 \cdot \left(\frac{n_y}{n_p} \right)^2 - 2 \cdot \sqrt{3} \cdot \left| \frac{m_y}{m_p} \right|}$$

$$n_y = -0,125 \cdot Q - 0,2 \cdot \frac{M'_m \cdot \kappa}{r}$$

$$n_p = t \cdot f_y$$

$$m_y = \left(\frac{1}{16} \cdot Q \cdot r + 0,071 \cdot M'_m \cdot \kappa \right) \cdot \left(1 + \frac{a}{r} \right)$$

$$m_p = 0,25 \cdot t^2 \cdot f_y$$

Calculation of ovalisation

In Figure 4-17 the ovalisation and bending of the pile wall due to a local load Q is depicted. The load is taken up by bending of a larger area of the pile wall, leading to ovalisations in this entire area.

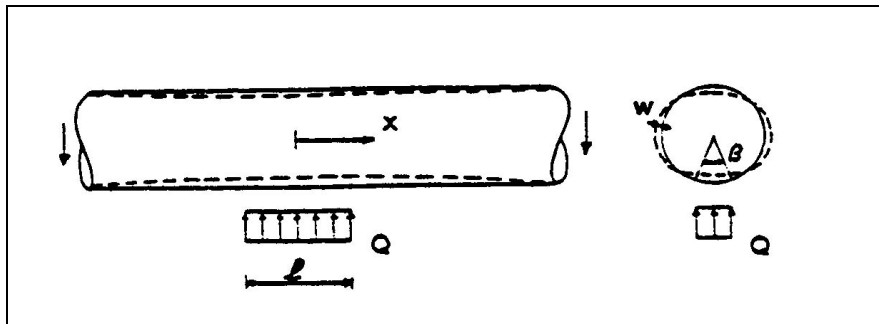


Figure 4-17 Local load Q causing ovalisation and bending of the pile wall

Two analysis methods are available for the calculation of the ovalisation:

- Shell analysis: the effect of a local load on the ovalisation of the pile wall in the entire area of influence is evaluated; this is a simulation of the real behaviour
- Ring analysis: the effect of a local load on the local cross-section is evaluated; this is a simplification of the real behaviour, making it possible to calculate every cross-section independently

For the shell analysis no explicit ovalisation formulas are known. It is also difficult to incorporate the formulase according to the shell analysis into a numerical model because the deformations of each pile element in the numerical model must be related only to the loads on that pile element.

The ring analysis is therefore applied in the Bruijn Model. It is expected that larger values for the ovalisation will be calculated, because the load Q is beared only by the local cross-section, while in the shell analysis the load is distributed over a larger area of the pile wall.

Below are the formulas for calculation of the ovalisation, resulting from the ring analysis. Ovalisation due to curvature:

$$a = \kappa^2 \cdot \frac{r^5}{t^2} \quad <4.28>$$

Ovalisation due to earth pressure:

$$a = 0,5 \cdot k_{yi} \cdot \frac{Q \cdot r^3}{EI_w} \quad <4.29>$$

with

k_{yi} = deformation coefficient, depending on the loading angle γ

$$EI_w = \frac{E \cdot t^3}{12(1-\nu^2)}$$

Effect of geometrical nonlinearity:

$$1 + \frac{3 \cdot a}{r} \quad <4.30>$$

Total ovalisation:

$$a = (a_k + a_q) \cdot \left(1 + \frac{3 \cdot a}{r}\right) = \left(0,5 \cdot k_{yi} \cdot \frac{Q \cdot r^3}{EI_w} + \kappa^2 \cdot \frac{r^5}{t^2}\right) \cdot \left(1 + \frac{3 \cdot a}{r}\right) \quad <4.31>$$

Resulting moment-curvature diagram

The influences of earth pressure, curvature and ovalisation are now expressed in formulas. With the following approximation the reduced moment-curvature relation can easily be simulated:

$$f_y' = \frac{M_m'}{M_p} \cdot f_y \quad <4.32>$$

$$E' = E \cdot \left(1 - 1,5 \cdot \frac{a'}{r}\right) \quad <4.33>$$

with

M'_m according to equation <4.27>

$$a' = \left(0,5 \cdot k_{yi} \cdot \frac{Q \cdot r^3}{EI_w} + \kappa_e'^2 \cdot \frac{r^5}{t^2} \right) \cdot \left(1 + \frac{3 \cdot a'}{r} \right) \quad <4.34>$$

$$\kappa_e' = \frac{f_y'}{E' \cdot r} \quad <4.35>$$

The resulting moment-curvature diagram is depicted in Figure 4-18.

Explanation of the lines in Figure 4-18 :

- The upper line is the theoretical (1st order) M-κ relation for bending only as presented in equation <4.10>
- The lower line is the reduced (2nd order) M-κ relation under influence of bending, curvature and ovalisation. The failure of the cross-section by progressive ovalisation (collapse of the cross-section) can be clearly seen by the snap in the curve.
- The middle line is the approximation as presented in equations <4.32> through <4.35>. This line is used in the Bruijn Model.

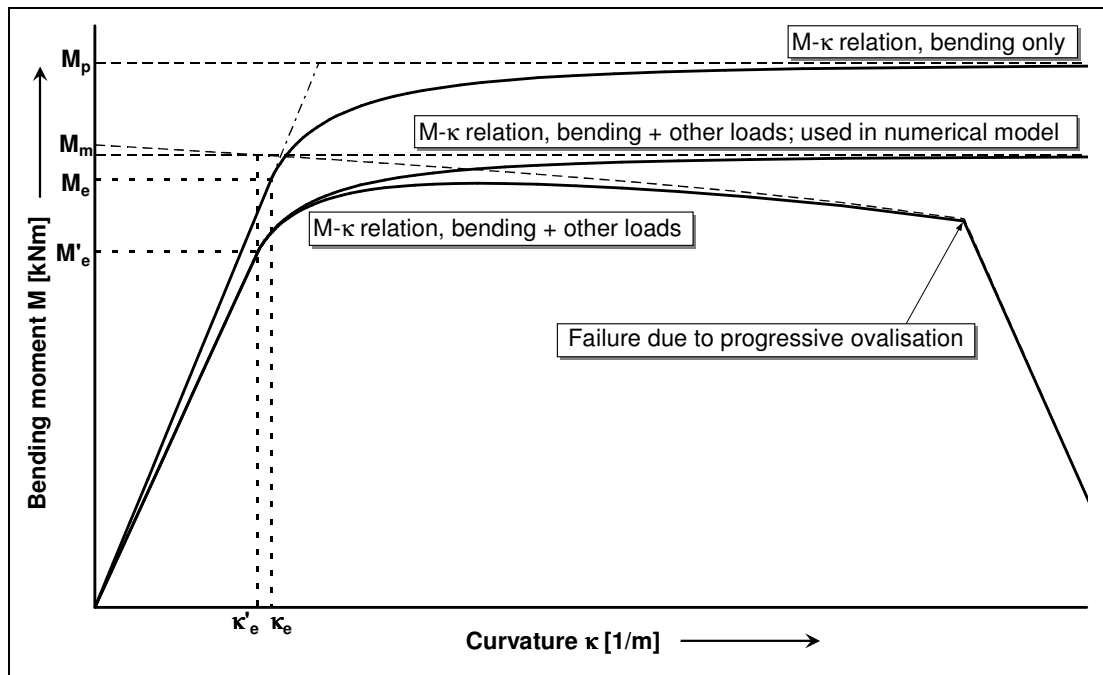


Figure 4-18 Reduced M-κ relation (2nd order) and theoretical M-κ relation (1st order)

4.6. Theory: soil behaviour according to Menard and Brinch Hansen

The subgrade reaction model simulates the soil behaviour using uncoupled springs. The spring characteristic for these springs is given in Figure 4-19. In this figure the elastic deflection is determined by the modulus of subgrade reaction (k_h) and the plastic limit by the limit soil reaction (R_{pl}).

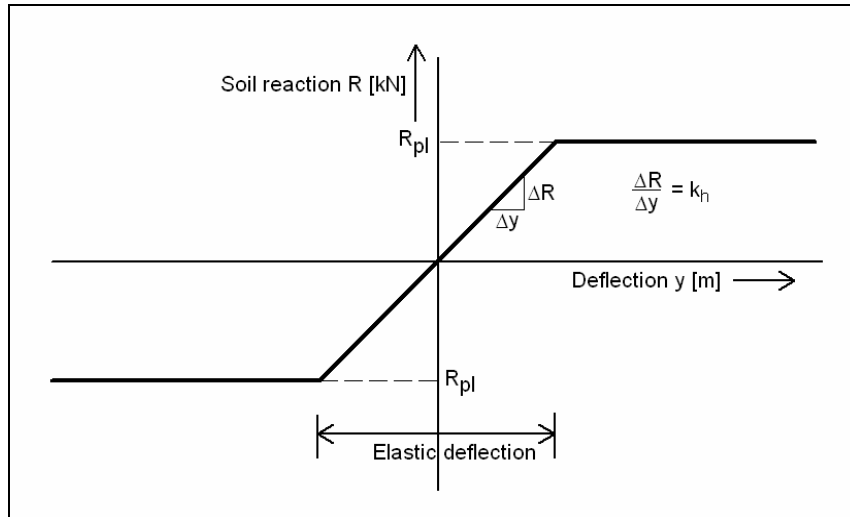



Figure 4-19 Nonlinear spring characteristic for soil reaction

For the modulus of subgrade reaction the theory of Ménard is used, for the plastic limit the theory of Brinch Hansen is applied. These theories are suitable for Dutch soil conditions, and are also used in MHorpile, a commercial program from GeoDelft for the calculation of laterally loaded piles.

Ménard

The Ménard theory  establishes a relation between the modulus of subgrade reaction, the stiffness of the soil, and the pressiometric modulus (E_p), which can be measured in a soil investigation. The relation has an empirical nature and is based on field tests.



Ménard, L. et al, 1971

The Ménard formula is:

$$\frac{1}{k_h} = \frac{1}{3 \cdot E_p} \cdot \left(1,3 \cdot r_0 \cdot \left(2,65 \cdot \frac{r}{r_0} \right)^\alpha + \alpha \cdot r \right) \quad <4.36>$$

with

E_p = pressiometric modulus $\approx \beta \cdot q_c$ [kN/m²]

r_0 = 0,3 m (reference radius)

r = radius = $D/2$ [m]

α = soil-dependent coefficient [-]

β = soil-dependent coefficient [-]

q_c = cone resistance [kN/m²]

For the soil-dependent coefficients α and β the following values are used:

Soil type	α	β
Peat	1	3,0
Clay	$\frac{2}{3}$	2,0
Loam	$\frac{1}{2}$	1,0
Sand	$\frac{1}{3}$	0,7
Gravel	$\frac{1}{4}$	0,5

Table 4-1 Soil-dependent coefficients α and β used in Ménard theory

If the pressiometric modulus is not known from the soil investigation, the cone resistance can also be used, as shown in the formula.

Brinch Hansen

The Brinch Hansen theory ⁽ⁱ⁾ is based upon a further development of the theory of Blum.



Brinch Hansen, J. and
Christensen, N.H.,
1961

Blum developed his theory for the full-plastic soil reaction in non-cohesive soils for sheet piling applications. Brinch Hansen further developed this theory for laterally loaded piles and for cohesive soils.

Brinch Hansen provided graphs for the soil pressure coefficient as a function of depth, pile diameter and soil friction angle, refer to Figure 4-20.

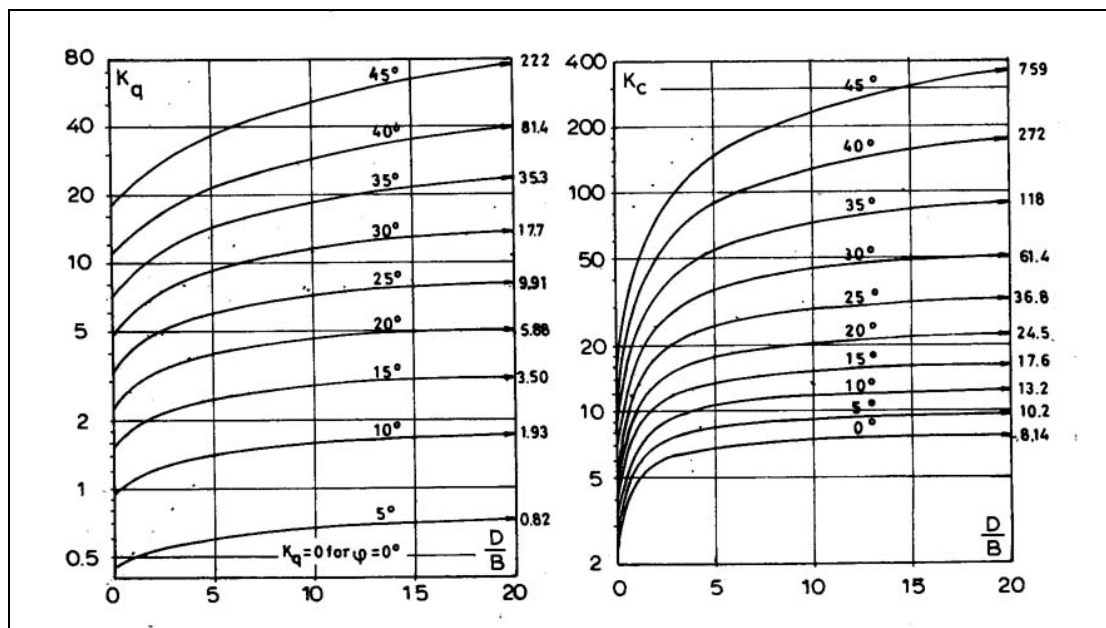


Figure 4-20 Brinch Hansen graphs for earth pressure coefficients

The full-plastic soil reaction as a function of depth according to Brinch Hansen is shown in Figure 4-21.

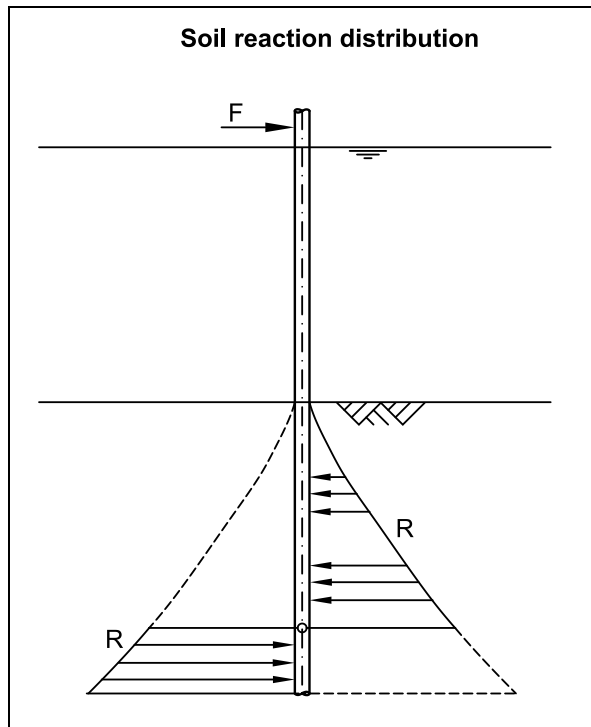


Figure 4-21 Plastic limit according to Brinch Hansen

Brinch Hansen uses the following formula to calculate the horizontal stress:

$$\sigma_p = K_q^{\frac{z}{D}} \cdot \sigma_v' + K_c^{\frac{z}{D}} \cdot C \quad <4.37>$$

with

$K_q^{\frac{z}{D}}$ = lateral earth pressure coefficient [-]

σ_v' = vertical effective stress = $\gamma' \cdot z$ [kN/m²]

$K_c^{\frac{z}{D}}$ = cohesion coefficient [-]

C = cohesion [kN/m²]

γ' = effective unit weight soil [kN/m³]

z = depth below bed level [m]

In this analysis only non-cohesive soils are considered, so the cohesion term is further neglected.

The soil reaction (R_{pl}) for one spring can then be calculated with:

$$R_{pl} = \sigma_p \cdot D \cdot dz = K_q^{\frac{z}{D}} \cdot \gamma' \cdot z \cdot D \cdot dz \quad <4.38>$$

The following procedure is followed for the calculation of $K_q^{z/D}$:

$$K_q^{z/D} = \frac{K_q^0 + K_q^\infty \cdot a_q \cdot (z/D)}{1 + a_q \cdot (z/D)} \quad <4.39>$$

with

$$K_q^0 = e^{(0.5 \cdot \pi + (\pi/180) \cdot \phi) \cdot \tan \phi} \cdot \cos \phi \cdot \tan \left(45^\circ + \frac{\phi}{2} \right) - e^{-(0.5 \cdot \pi - (\pi/180) \cdot \phi) \cdot \tan \phi} \cdot \cos \phi \cdot \tan \left(45^\circ - \frac{\phi}{2} \right)$$

$$K_q^\infty = (1.58 + 4.09 \cdot \tan^4 \phi) \cdot \left(e^{\pi \cdot \tan \phi} \cdot \tan^2 \left(45^\circ + \frac{\phi}{2} \right) - 1 \right) \cdot \cot \phi \cdot K_0 \cdot \tan \phi$$

$$a_q = \frac{K_q^0}{K_q^\infty - K_q^0} \cdot \frac{K_0 \cdot \sin \phi}{\sin \left(45^\circ + \frac{\phi}{2} \right)}$$

$$K_0 = 1 - \sin \phi$$

ϕ = angle of internal friction [degrees]

4.7. Theory: Limit states for the model

The following limit states are distinguished:

- Stresses in the pile
- Strains in the pile
- Deformations of the pile
- Soil failure

Remark regarding stresses and strains: The stresses and strains are directly related to each other, so the question might rise why both stresses and strains are established as limit states. After all, if the limit value for the strains is established the limit value for the stresses is also established via the stress-strain relation.

However, in calculations according to elastic theory a limit value for the stresses is more commonly used than a limit value for the strains. For the plastic range, limit values can only be expressed in terms of strain, since the assumed bilinear stress-strain relation yields only one value for the stress in the plastic range: the yield stress. The yield stress as upper limit of the elastic range marks the transition from the elastic range to the plastic range.

Stresses in the pile

Failure of the pile by arithmetical exceedance of the yield stress f_y :

$$\sigma < f_y \quad <4.40>$$

In case of biaxial stresses yielding is to be checked by using the Von Mises yield criterion:

$$\sigma = \sqrt{\sigma_y^2 + \sigma_z^2 - \sigma_y \cdot \sigma_z - 3 \cdot \tau^2} \quad <4.41>$$

with

σ_y = stresses in circumferential direction [N/mm²]

σ_z = stresses in longitudinal direction [N/mm²]


τ = shear stress [N/mm²]

Strains in the pile

The pile must be able to deflect due to design loading without rupturing or cracking. Sufficient strain capacity should therefore be available in the pile material.

The strain capacity is influenced by:

- Ductility of the plate / weld material
- Degree of 'overmatching' welds: yield stress weld material > yield stress plate material
- Notches in plate / weld material
- Stress concentrations due to weld faults


Sufficient strain capacity is available in any case where the strains do not exceed the following value, according to NEN 3650 :

$$\epsilon_{\max} = 0,5 \% \quad <4.42>$$



NEN 3650-2: 2003

If more strain capacity is needed it must be demonstrated that this strain capacity is available by the application of adequate methods.

An example of such a method is the Crack Tip Opening Displacement (CTOD) theory mentioned by Gresnigt , which provides a method of testing the strain capacity of a wall segment with irregularities due to e.g. welding imperfections.



Gresnigt, A.M., 1986
page 30

It is important to consider the strain capacity when applying the plasticity theory, because by making use of the plastic properties of steel the strains will generally be significantly larger compared to those obtained using the elasticity theory. Reference is made to NEN 3650 for more on strain capacity and welding.

Deformations of the pile

There are two possible mechanisms leading to inadmissibly large deformations:

- Ovalisation of the pile cross-section
- Buckling of the pile wall

Ovalisation of the pile cross-section

Limit state for the change in pile diameter under influence of bending and external soil pressure (source: NEN 3650):

$$a_{\max} = 0,05 \cdot D_e \quad <4.43>$$

with

$$a = \frac{D_{\max} - D_{\min}}{4} \leq a_{\max}$$

The ovalisation a is defined in Figure 4-22 on the next page.

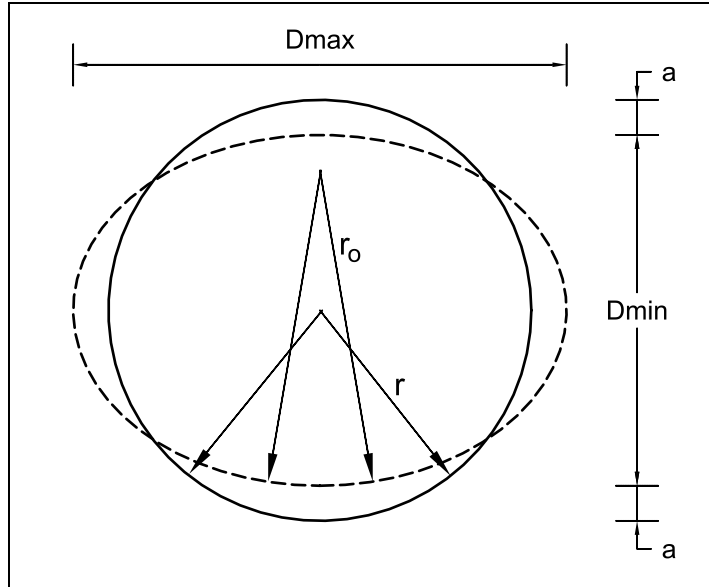


Figure 4-22 Definition sketch ovalisation a and local radius r0

Buckling of the pile wall

Several types of buckling can be distinguished:

- Overall buckling under influence of normal force
- Local buckling under influence of bending

Overall buckling is not likely to occur in the dolphin, because no significant normal force is applied to the pile; only the dead load of the pile itself causes a normal force. So no limit state criteria are employed for overall buckling.

Local buckling however is a mechanism to be thoroughly investigated, since all conditions are present for local buckling to occur: a thin-walled pile designed to be as flexible as possible, leading to large deflections and bending moments.

In NEN 3650 the critical value of the compressive strain ϵ_{cr} is obtained from Gresnigt:

$$\begin{aligned}\epsilon_{cr} &= 0,25 \cdot \frac{t}{r'} - 0,0025 + 3000 \cdot \left(\frac{p \cdot r'}{E \cdot t} \right)^2 \cdot \frac{|p|}{p} \quad \text{for } \frac{r'}{t} \leq 60 \\ &= 0,10 \cdot \frac{t}{r'} + 3000 \cdot \left(\frac{p \cdot r'}{E \cdot t} \right)^2 \cdot \frac{|p|}{p} \quad \text{for } \frac{r'}{t} > 60\end{aligned} \quad <4.44>$$

with

$r' =$ plate curvature of an ovalised cross-section, refer to Figure 4-22
 $p =$ difference in pressure between inside and outside of the pile

If the internal pressure is assumed zero, a D/t ratio lower than 120 is expected and the radius is replaced by the diameter equation <4.44> reduces to:

$$\epsilon_{cr} = 0,5 \cdot \left(\frac{t}{D-t} \right) - 0,0025 \quad \text{for } \frac{D}{t} \leq 120 \quad <4.45>$$



Foeken, R.J. van,
A.M. Gresnigt, 1998



Gresnigt, A.M., 1985

Two reports comparing these and other expressions for the critical strain with test results are:

- TNO Report 96-CON-R0500: Buckling and collapse of UOE manufactured steel pipes
- IBBC-TNO Report OPL 85-343: Kritieke stuik en kritieke rotatie in verband met plooiën van stalen transportleidingen

TNO Report 96-CON-R0500

In this report design formulations for collapse and buckling of UOE manufactured steel pipes are calibrated against experimental and numerical models. Recommendations are given for the design formulas to be used in pipeline design.

The results are applicable to: $15 < D/t < 50$. Since current dolphin designs include D/t ratio's up to 80, this means that the applicability of the results to dolphin design is not confirmed for the entire range of D/t ratio's.

Critical strain formulas according to several sources which are evaluated in the report are summed up in Table 4-2.

Source	Critical strain formula	Value for $D/t = 83$	Value $D/t = 42$
BS8010	$\epsilon_{cr} = 15 \cdot \left(\frac{t}{D}\right)^2$	0,0022	0,0086
Gresnigt	$\epsilon_{cr} = 0,5 \cdot \left(\frac{t}{D-t}\right) - 0,0025$	0,0036	0,0098
Murphey & Langner	$\epsilon_{cr} = 0,5 \cdot \left(\frac{t}{D-t}\right)$	0,0061	0,0123
Igland	$\epsilon_{cr} = 0,005 + 13 \cdot \left(\frac{t}{D}\right)^2$	0,0069	0,0125
PRCI	$\epsilon_{cr} = \frac{t}{D} - 0,01$	0,0020	0,0140

Table 4-2 Critical strain formulas in TNO Report 96-CON-R0500

In Figure 4-23 these strains are presented as function of D/t and compared with test results.

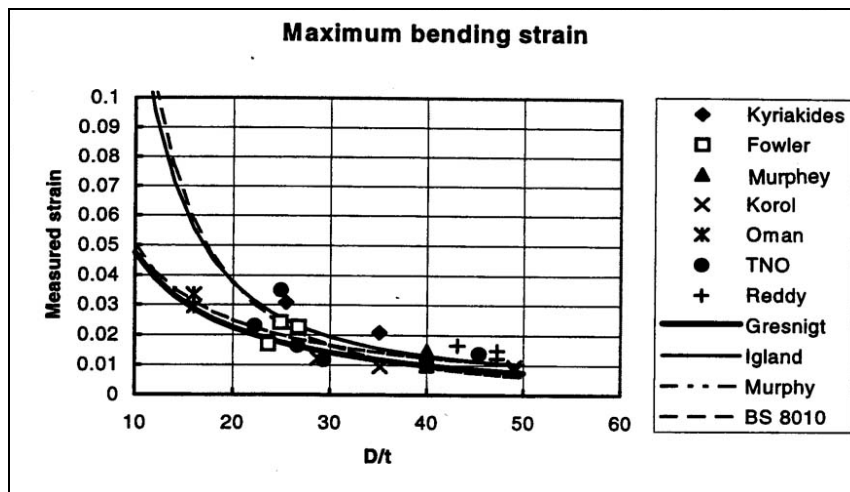


Figure 4-23 Experimental strain versus D/t ; TNO Report 96-CON-R0500

The report recommends the use of the Murphey-Langner formula, but the differences with the Gresnigt formula are very small, the Gresnigt formula being on the conservative side compared to the Murphey-Langner formula.

IBBC-TNO Report OPL 85-343

This report presents a summary of the considerations and tests leading to the proposed limit state criteria recorded in the TGSL (Technische Grondslagen Stalen Leidingen).

The considered critical strain formulas are given in Table 4-3.

Source	Critical strain formula	Value for D/t=83	Value for D/t=42
Timoshenko & Gere	$\epsilon_{cr} = 1,21 \cdot \frac{t}{D}$	0,0145	0,0290
Batterman	$\epsilon_{cr} = \frac{4}{9} \cdot \left(\frac{t}{0,5 \cdot D} \right)^2 \cdot \frac{E_t}{f_y}$	0,0029*	0,0117*
Gresnigt	$\epsilon_{cr} = 0,5 \cdot \left(\frac{t}{D-t} \right) - 0,0025$	0,0036	0,0098

Table 4-3 Critical strain formulas in IBBC-TNO Report OPL 85-343 * $E_t = E/40$, $f_y = 460 \text{ N/mm}^2$

In the report, Gresnigt criteria are also compared with test results published by Sherman, Kato, Murphey, Reddy, Korol, Kimura, and Bouwkamp. It is concluded that Gresnigt criteria are on the safe side. Decision is made to incorporate the Gresnigt criteria in the TGSL.

Only the comparison with the Reddy, Batterman and Bouwkamp test data is graphically presented, refer to Figure 4-24 for that graph. Note that in this graph a double-logarithmic scale is used.

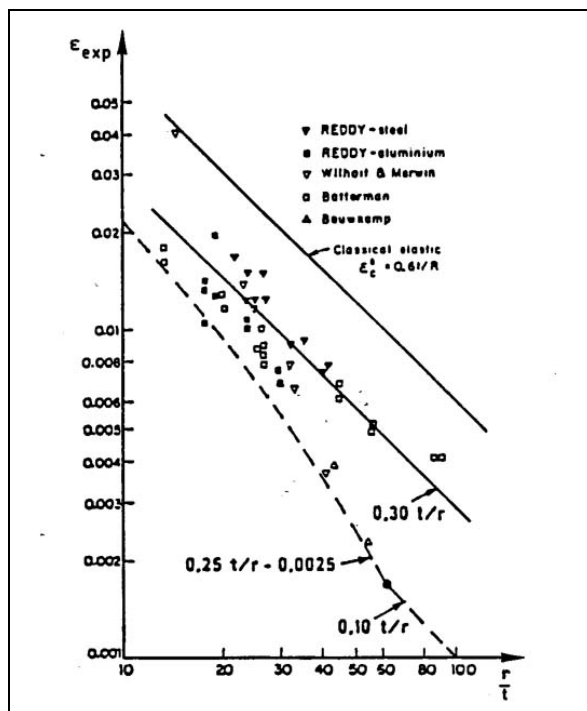


Figure 4-24 Experimental strain versus r/t; IBBC-TNO Report BI-86-111

All formulas in Table 4-2 and Table 4-3 are graphically presented in Figure 4-25. In this graph also a double-logarithmic scale is used, like in Figure 4-24.

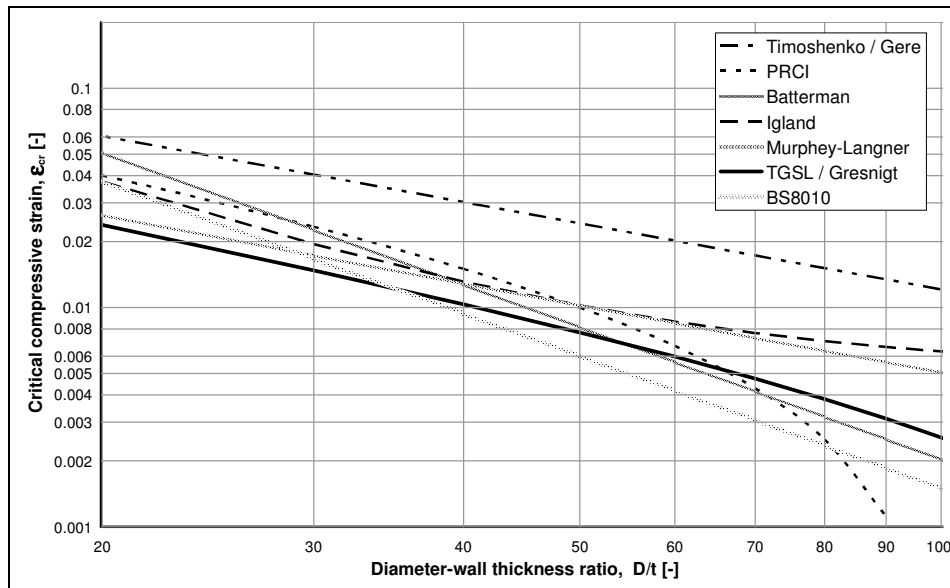


Figure 4-25 Graphical representation of all mentioned critical strain formulas

It can be concluded that the Gresnigt formula gives a lower limit for the critical strain and is confirmed for the entire range of D/t ratio's applied in dolphin design. Therefore the Gresnigt formula will be used in the present analysis.

Soil failure

Two types of soil failure are distinguished, refer to Figure 4-26:

- Wedge-type failure due to foundation instability (depends on embedment)
- Full-plastic soil failure due to excessive loading

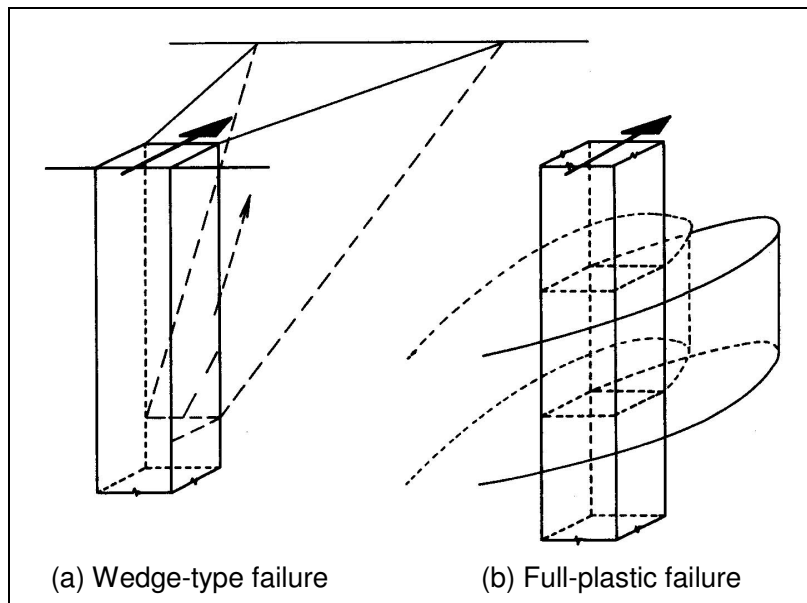


Figure 4-26 Two types of soil failure

Both types of soil failure are incorporated in the theory of Brinch Hansen and can be identified in the model due to extreme deflections in the elastic range.

4.8. Results of the Bruijn model

Case

Consider a case with layout and properties as depicted in Figure 4-27, labelled case 1A.

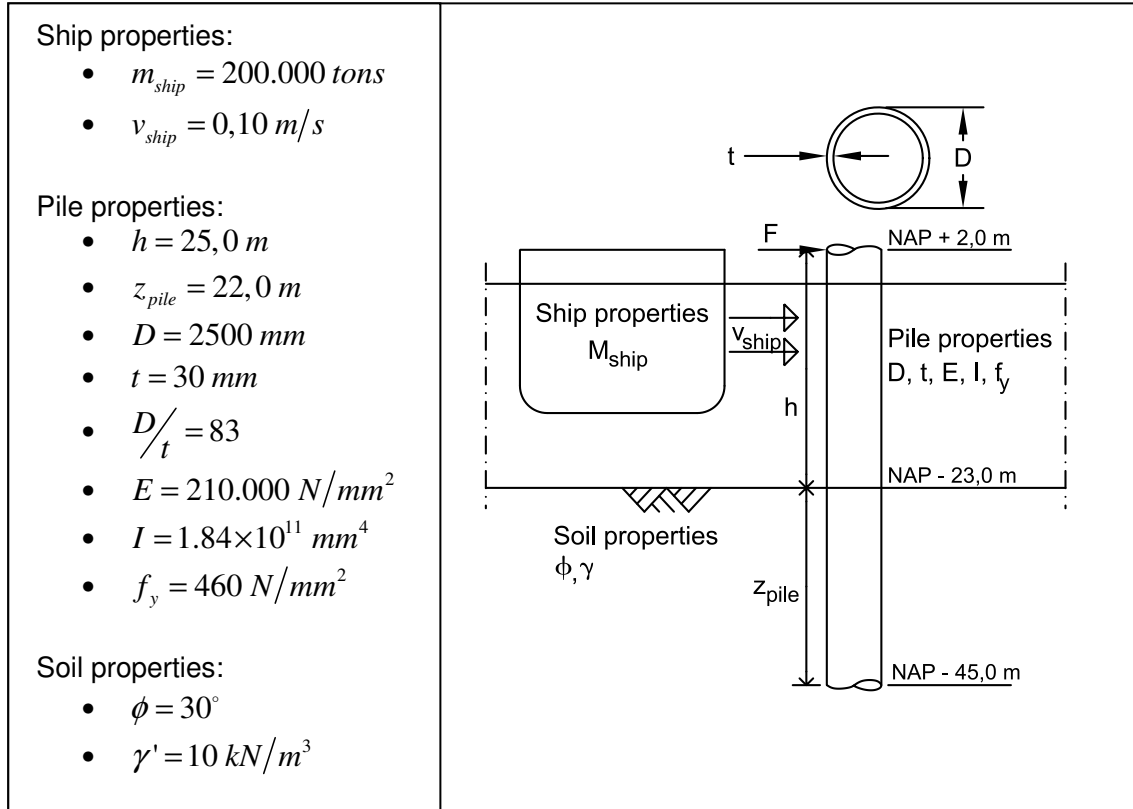


Figure 4-27 Layout and properties case 1A

Next the D/t ratio is varied from 83 (Case 1A) to 63 (Case 1B) and 42 (Case 1C). The parameters for these cases are given in Table 4-4, insofar as the properties differ from Case 1A.

Property	Symbol	Unit	Case 1A	Case 1B	Case 1C
Diameter-wall thickness ratio	D/t	-	83	63	42
Diameter	D	mm	2,500	2,500	2,500
Wall thickness	t	mm	30	40	60
Flexural stiffness	EI	kNm^2	$3.73\text{E}+07$	$4.91\text{E}+07$	$7.19\text{E}+07$
Full-elastic moment	M_{el}	kNm	66,125	87,454	129,056
Full-plastic moment	M_{pl}	kNm	84,192	111,349	164,319

Table 4-4 Properties for cases 1A, 1B and 1C

Load-deflection curve

For each case the load-deflection curve is calculated in a 1st order nonlinear analysis (using the theoretical $M-\kappa$ relation) and a 2nd order nonlinear analysis (using the reduced $M-\kappa$ relation). Also a reference calculation according to Blum is shown. Refer to Figure 4-28 to Figure 4-30 for these graphs.

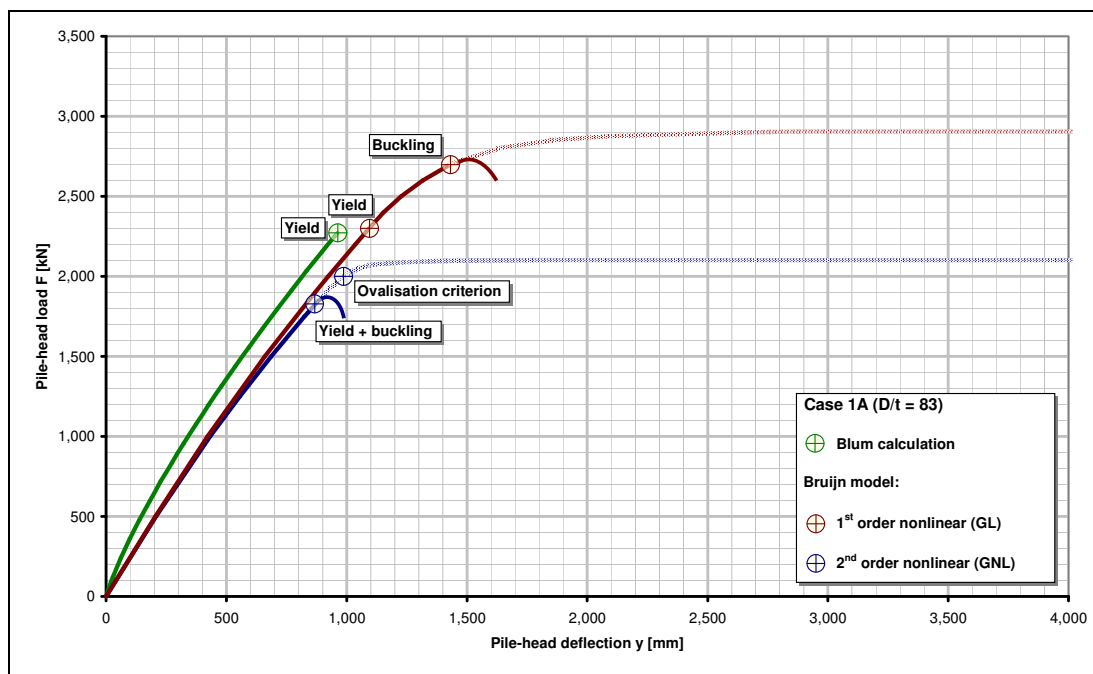


Figure 4-28 Load-deflection curve Case 1A

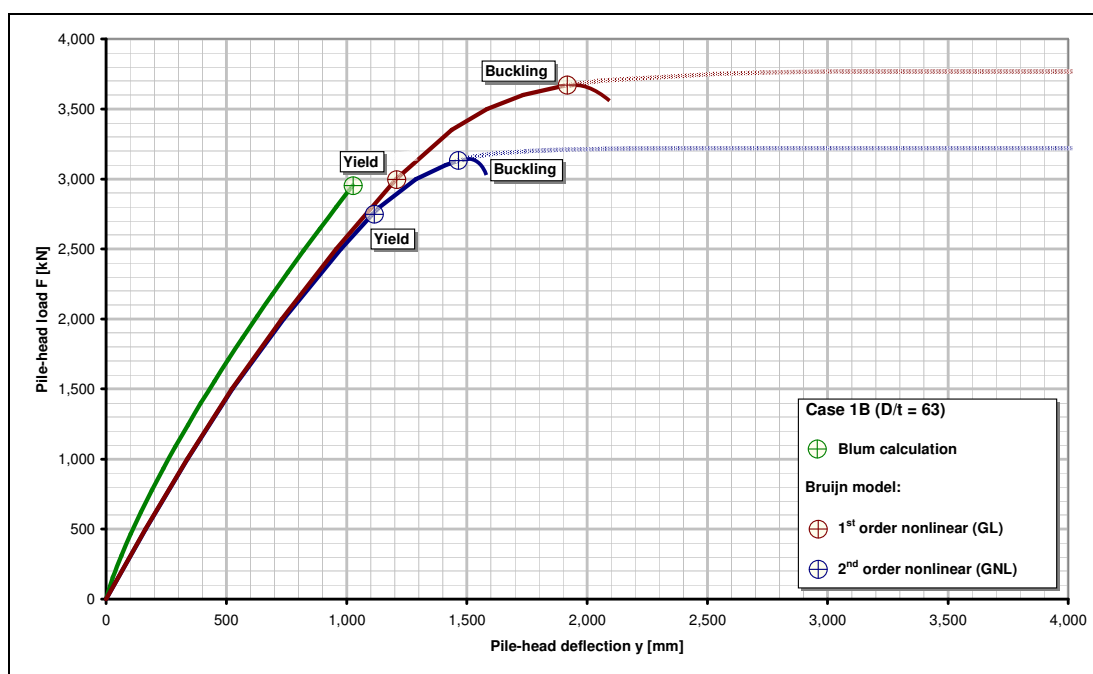


Figure 4-29 Load-deflection curve Case 1B

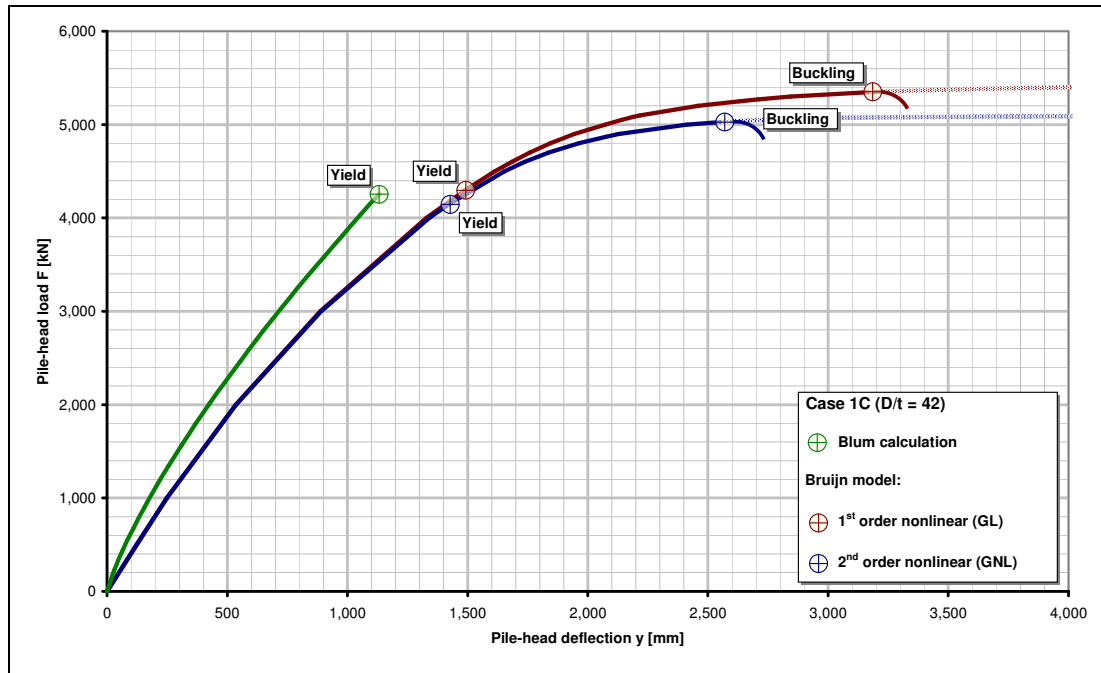


Figure 4-30 Load-deflection curve Case 1C

Comments regarding Figure 4-28 to Figure 4-30:

- The difference between the 1st order and 2nd order calculations becomes larger for larger D/t ratio. Differences are very large for D/t ratio 83. Explanation:
 - For $D/t=83$ plate moments are large while the plastic plate moment is small because of the small wall thickness → the maximum moment is significantly reduced
 - Large plate moments also occur because of the model for ovalisation due to soil reaction → the conservative model leads to conservative results, so it is expected that the 1st order and 2nd order behaviour will in reality be more closer together
- Buckling is influenced by 2nd order effects because it is based on the local curvature of the ovalised cross-section
- Blum yields smaller deflections than the Bruijn Model, which was already concluded when analysing the method of Blum

In Figure 4-31 all three 2nd order nonlinear curves for Case 1 are shown. From this graph the following conclusions can be drawn:

- The graph shows clearly that with increasing D/t ratio, the strength and stiffness of the pile increase substantially.
- Buckling and some ovalisation occurs already in the elastic range for Case 1A, with a D/t ratio of 83
- For lower D/t ratio's, ovalisation is not significant and buckling occurs after significant plastic yielding

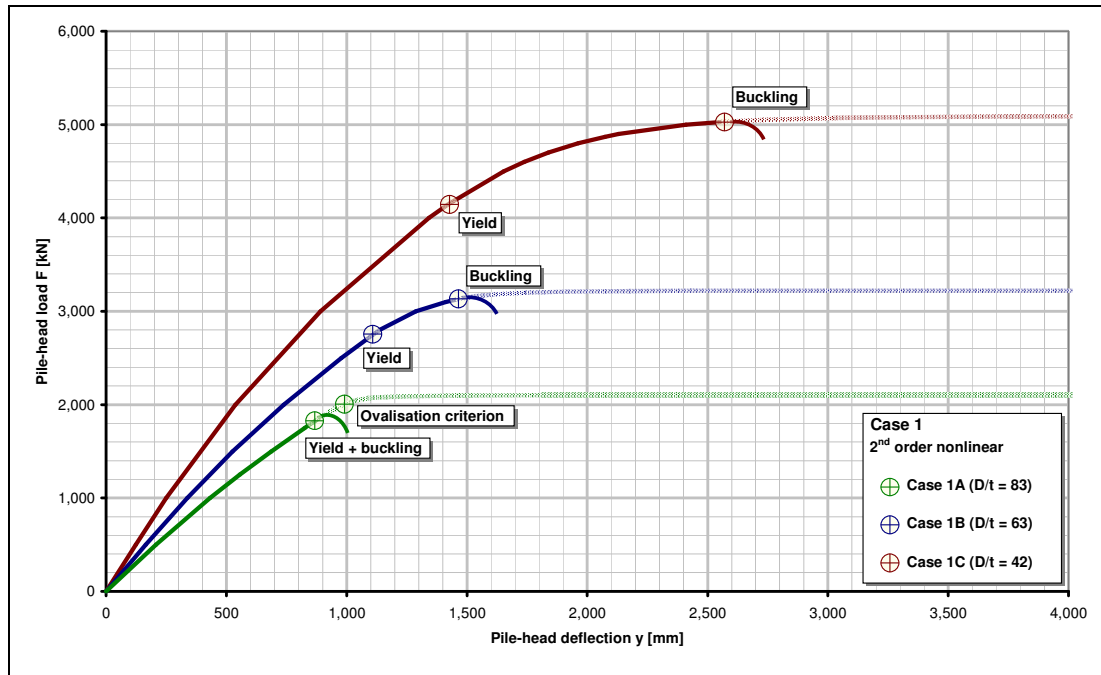


Figure 4-31 Second order nonlinear load-deflection curve Case 1

Plastic hinge

In Figure 4-32 the development of the curvature with increasing load is shown. The development of a plastic hinge a few meters below bed level can be clearly seen.

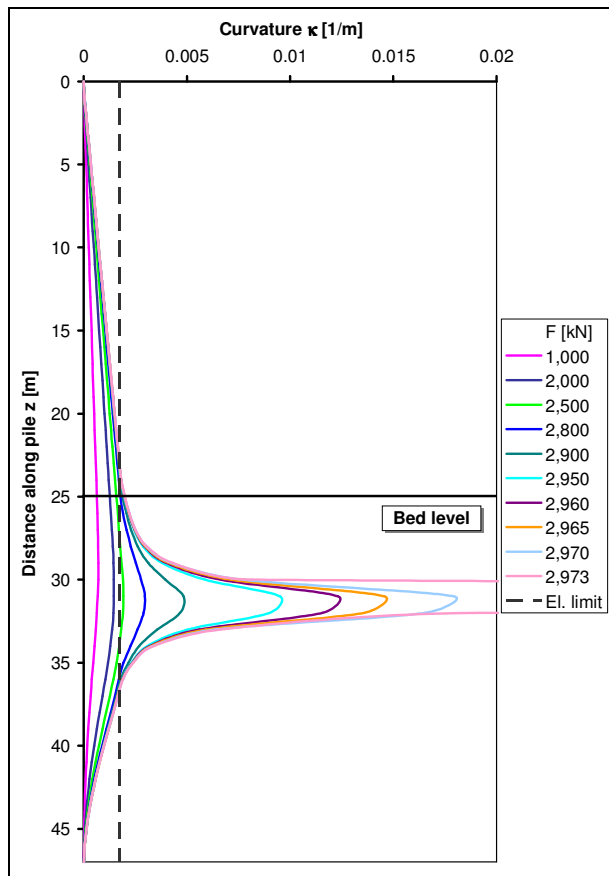


Figure 4-32 Development of curvature with increasing load

Limit states

It can be concluded that :

- Limit state deformations becomes more important for higher diameter-wall thickness ratio's. For $D/t = 83$ buckling happens around yield stress and strain.
- Limit strain criteria → the 0,5% criterion is easily reached, so prove of sufficient strain capacity in welds and plate material is necessary
- Collapse of the cross-section due to progressive ovalisation is not likely to be a significant failure mechanism; however the ovalisation has some influence on the occurrence of other failure mechanisms, especially buckling

4.9. Verification of the Bruijn model

In this section the model results are compared to the results of commercial models for the same cases. For this the distinction is made between linear and nonlinear verification, because some commercial models are only capable of performing linear analysis, others are capable of performing nonlinear analysis.

Another method of verification is the comparison of the model results to field tests. Since reliable data for this purpose has not been found this verification method is not feasible. It is however still advisable to perform verification with field tests.

Linear analysis

In order to assess the reliability of the calculation results in the elastic range, the Bruijn model is compared to three other pile calculation models:

- Blum model
- MHorpile
- ESA Prima-Win

In Annex III the displacement graphs for 2 different cases are plotted for all four mentioned models. The following conclusions can be made:

- The Blum model leads to lower values for the deflections due to a fundamentally different approach, employing the Euler formulas for calculation of the displacements, based on an estimated point of restraint.
- The 1st order calculation with the Bruijn model yields practically the same result as MHorpile and ESA Prima-Win, differences are negligible
- The 2nd order calculation with the Bruijn model results in slightly larger deflections, which can be expected because of the reduced moment-curvature relation

Based on this comparison it can be concluded that the Bruijn model yields accurate results in the linear analysis.

Nonlinear analysis

For the nonlinear verification the FEM package DIANA is used. DIANA is on the market for a wide range of applications, including nonlinear analysis of steel structures and soil.

A model has been generated in DIANA with the properties of Case 1, existing of a pile mesh and an interface around the pile mesh representing the surrounding soil.

The pile mesh and the deformed mesh are shown in Figure 4-33.

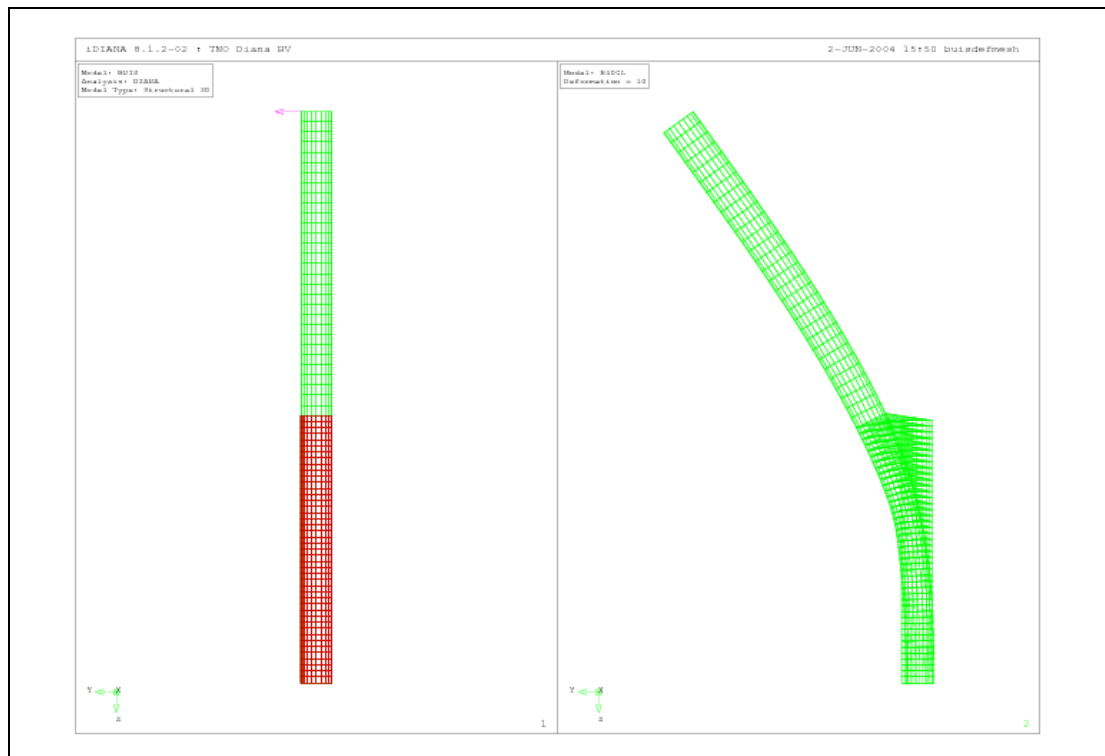


Figure 4-33 DIANA pile mesh and deformed mesh

Comments to Figure 4-33:

- The red part of the pile in the left figure is the embedded part of the pile.
- The soil is modelled as springs at the location of the mesh points, in the right figure the resulting behaviour can be seen.

In Figure 4-34 a pile segment is shown. The segment is divided into square elements which are connected to the other elements at the corners. For every connection point the stresses, strain and deformations are calculated.

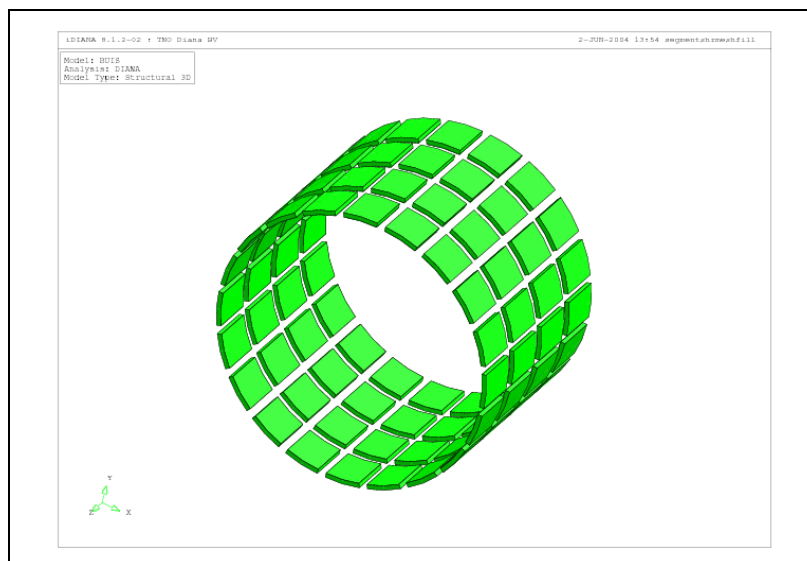


Figure 4-34 DIANA segment mesh hidden shade

The calculation is performed using two methods of analysis:

- 1st order nonlinear analysis: geometrical linear behaviour, the influence of the deformed state is not taken into account for the forces and deformations
- 2nd order nonlinear analysis: geometrical nonlinear behaviour, the deformed state is taken into account

These two methods of analysis are comparable to the Bruijn model calculation which is performed for the theoretical moment-curvature relation (1st order) and the reduced moment-curvature relation (2nd order).

In Figure 4-35 to Figure 4-37 the resulting load-deflection curves for Case 1A, 1B and 1C respectively are shown for:

- The Blum calculation (as reference calculation)
- DIANA 1st order: geometrical linear
- Bruijn 1st order: geometrical linear, using the theoretical moment-curvature relation
- DIANA 2nd order: geometrical nonlinear
- Bruijn 2nd order: geometrical nonlinear, using the reduced moment-curvature relation

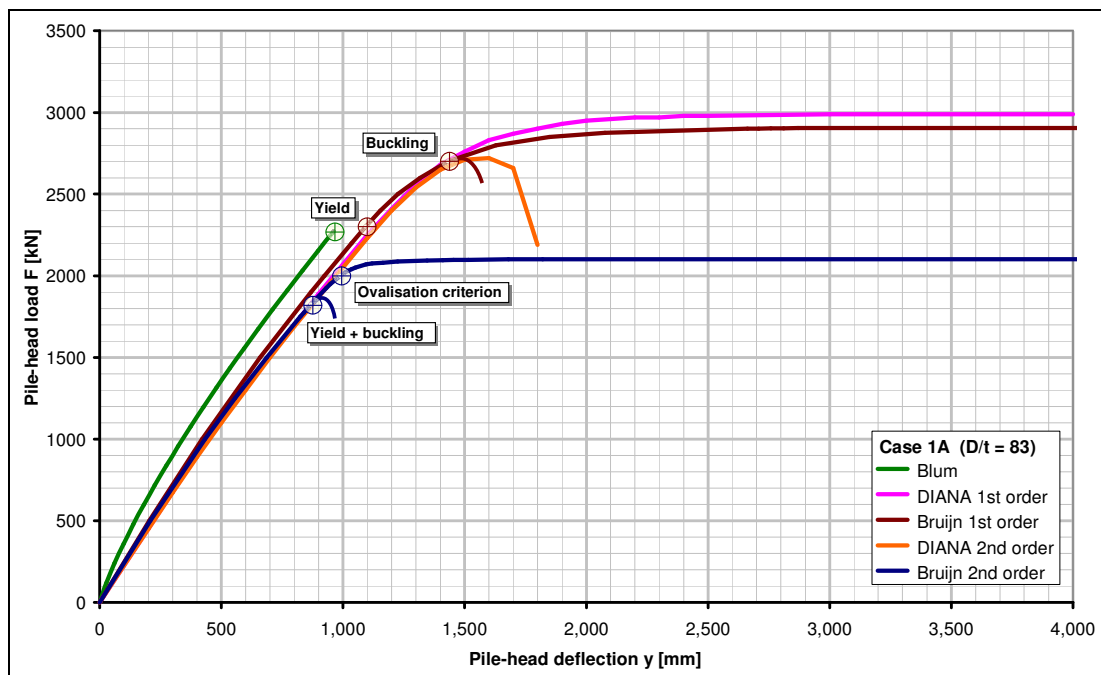


Figure 4-35 Nonlinear verification Case 1A

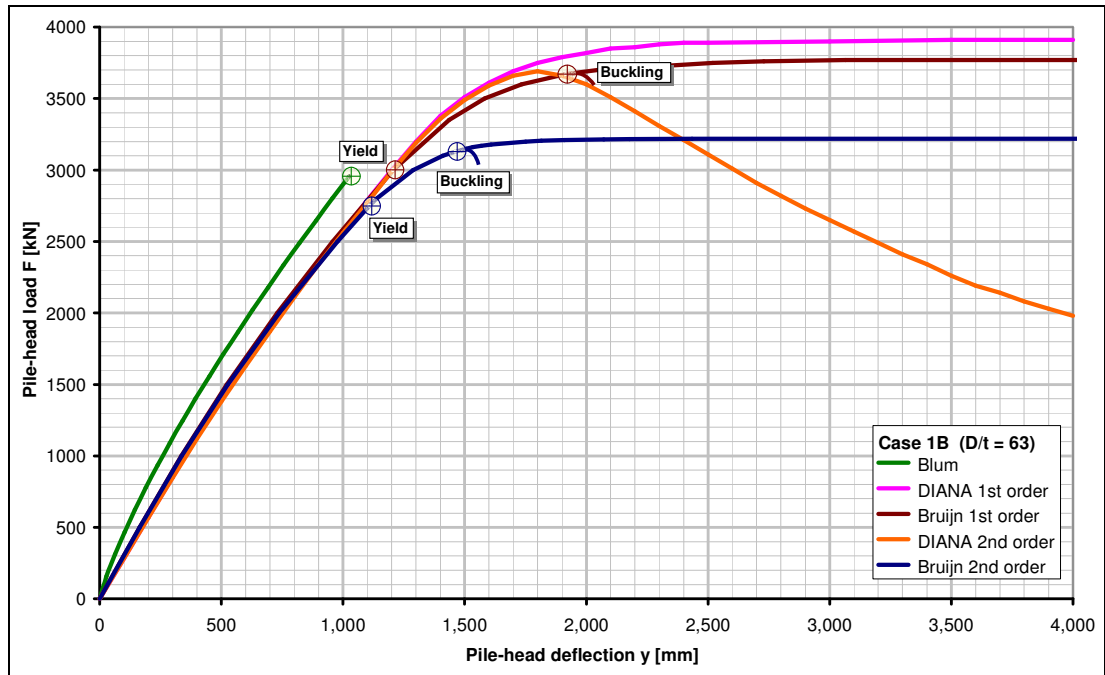


Figure 4-36 Nonlinear verification Case 1B

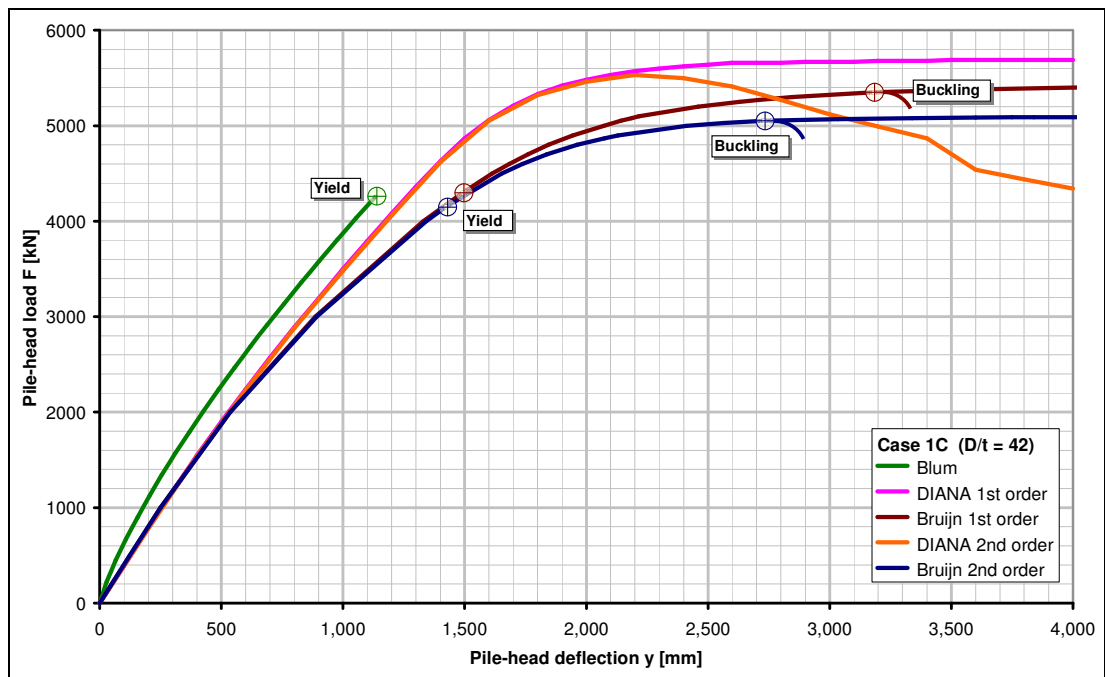


Figure 4-37 Nonlinear verification Case 1C

Conclusions:

- In general it can be concluded that DIANA and the Bruijn model yield comparable results
- 1st order calculations are confirmed by the DIANA calculation
- Bruijn model 2nd order calculations give a conservative estimate of the strength and stiffness compared to DIANA 2nd order calculations, especially for higher D/t ratio (83)

The differences between DIANA and the Bruijn model in 2nd order effects can be attributed to:

- Stress redistribution which is taken into account in DIANA, not in the Bruijn model
- The soil reaction as modelled in the Bruijn model gives large plate moments in the cross-section and consequently larger ovalisation and 2nd order effects, while DIANA models the soil distributed around the cross-section thus reducing the ovalisation and hence the 2nd order effects

4.10. Practical application

The developed Bruijn model or a similar model based on the presented theories for nonlinear structural behaviour can be used for several applications:

- Dolphin design
- Damage analysis
- Advanced modelling

Dolphin design

Steps to follow:

1. Make first assessment of dimensions, embedment and material of pile to be used by performing a Blum calculation
2. Calculate the load-deflection curve of the chosen pile using the Bruijn model
3. Assess the energy absorption capacity (Figure 4-38)
4. Assess the safety of the designed structure with the expected loading conditions
5. Change dimensions, embedment, material parameters in order to optimise the design within a desired safety level

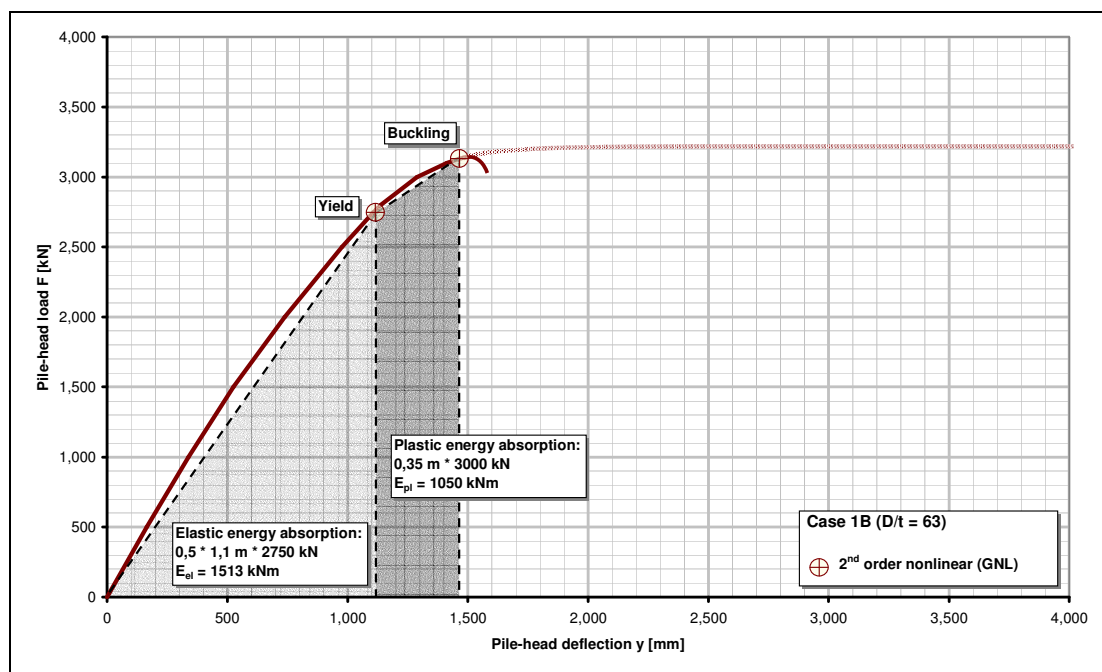


Figure 4-38 Assessment of energy absorption capacity

Damage analysis

Procedure:

1. Gather data of the structural design:
 - Design actions
 - Design strength and stiffness
 - Design calculations
2. Gather data of the damaged state:
 - Pile-head deflection
 - Pile-head rotation
 - Ovalisation
 - Gather data of the loading history:
 - Ship properties of the last berthed ship
 - Approach velocity
 - Climate conditions: waves, currents, wind
3. Generate a load-deflection curve using the Bruijn model, based on the design parameters
4. Calculate the response of the structure under the assumed loading conditions when sustaining damage
5. Perform cross-section analysis of the most heavily loaded sections
6. Assess failure mechanism, based on pile-head deflection – pile-head rotation ratio and cross-section analysis
7. Assess severity of damage and the remaining strength, stiffness, energy absorption
8. Make recommendations for the course of action to be followed: continued normal operation, repair, replacement

Use in advanced modelling: hydrodynamic / probabilistic / dynamic models

In the literature investigation (Annex I, page 82 and further) the models used in dolphin design are divided into hydrodynamic and pile-soil interaction models, because no integrated model is known which can handle both the hydrodynamic behaviour of a berthing ship and the nonlinear behaviour of the pile-soil system.

Using the load-deflection curves from the Bruijn model, the nonlinear behaviour of the pile-soil system can be incorporated into advanced hydrodynamic models, thus enhancing the integration between accurate hydrodynamic behaviour and accurate pile-soil behaviour.

Also in a probabilistic model or in a dynamic model of a ship berthing to more than one dolphin, the generated load-deflection curve can be used to represent the nonlinear pile-soil behaviour due to lateral loading.

5. EVALUATION OF DESIGN STANDARDS AND GUIDELINES

5.1. Introduction

In this chapter firstly the currently effective design standards and guidelines for dolphin design are presented, compared with each other and evaluated with the aid of the structural analysis presented in the preceding chapter.

Secondly the consequences of these conclusions on the safety of the system are treated.

5.2. Current standards and guidelines

The following standards and guidelines are evaluated:

- NEN 6770: Dutch standards for steel structures
- EAU 1996: German guidelines for dolphin design
- BS 6349 Part 2 and Part 4: British standards for Maritime structures including specific guidelines for dolphin design
- PIANC 1984: Guidelines from the International Navigation Association for fender systems including specific guidelines for dolphin design
- PIANC 2002: Updated guidelines for fender systems

Also the current design practice at the Maritime Division of Royal Haskoning, which is based on the EAU guidelines, is included in the evaluation.

In Table 5-1 the standards are compared on the subjects of design method, limit states, limit state criteria, partial factors of safety and calculation models.

Subject	NEN 6770	PIANC 1984	PIANC 2002	BS 6349	EAU 1996	Design practice
Parts						
Design method						
Deterministic calculation using $R - S \geq 0$	+	+	+	+	+	+
Partial factors of safety	+	+	+	+	+	+
Limit states						
Yield	+	+	+	+	+	+
Deformation	-	-	+	+	+	+
Buckling	+	-	-	-	-	+
Ovalisation	-	-	-	-	-	-
Limit state criteria						
Yield: f_y (ULS)	+	+	+	+	+	+
Deformation: $y_{\max} = 1,5$ m (SLS)	-	-	+	+	+	+
Buckling: $\epsilon_{cr} = 0,25 \cdot t/r^4 - 0,0025$ (ULS)	-	-	-	-	-	+
Buckling: classification of sections: M (Class 1 section: $D/t < 50 \alpha_y^2$) $\sim 25^{1)}$ M (Class 2 section: $D/t < 70 \alpha_y^2$) $\sim 35^{1)}$ M (Class 3 section: $D/t < 90 \alpha_y^2$) $\sim 45^{1)}$ M (Class 4 section: $D/t > 90 \alpha_y^2$) $\sim 45^{1)}$	M_{pl} M_{pl} M_{el} M_{ef}	-	-	-	-	-
Partial factors of safety						
E (abnormal impact factor)	-	-	1,25 – 2	2,0	-	1,5
F	1,5	-	1,25 ²⁾ 1,0	-	1,0	-
f_y	-	1,22	-	1,25	1,0	1,0
$\epsilon_{cr, buckling}$	-	-	-	-	-	2,0

Hydrodynamic calculation models						
KE approach	-	+	+	+	+	+
IRF / LW approach	-	named	named	-	-	-
Pile-soil interaction calculation models						
Blum	-	+	+	-	+	+
P-y curve method	-	+	+	+	-	-
Subgrade reaction model	-	named	+	-	-	-
FEM method	-	named	+	-	-	-

Table 5-1 Content standards

¹⁾ Classification of sections according to NEN 6770 section 10.2.4.1

$$\alpha_y = \sqrt{\frac{f_{ref}}{f_{y;d}}} \quad \text{with } f_{ref} = 235 \frac{N}{mm^2}$$

Values given (25, 35, 45) are D/t values for $f_{y;d} = 460 \text{ N/mm}^2$

²⁾ Depends on pile capacity to resist overloading by plastic yielding:

- No yielding possible: $\gamma = 1,25$
- Yielding possible until a displacement of at least $2 \cdot y_{el}$: $\gamma = 1,0$

5.3. Comparison of standards and guidelines

The same case as in the preceding chapter is used for the comparison. The case consists of three parts with varying diameter-wall thickness ratio's (83, 63 and 42). The case is calculated according to mentioned standards and guidelines and compared with a Bruijn model calculation.

Firstly the case is described. Secondly the results of a calculation of the energy absorption capacity and the maximum allowed impact energy according to the standards and guidelines are presented. Thirdly the case is evaluated using the Bruijn model.

The section is concluded with some conclusions which can be drawn from the comparison

Case

The case has a representative set of values for material and geometrical properties, but is calculated for different D/t ratio's (D/t of 83, 63 and 42 respectively). Refer to Figure 5-1 for a schematic view and to Table 5-2 for the parameter values.

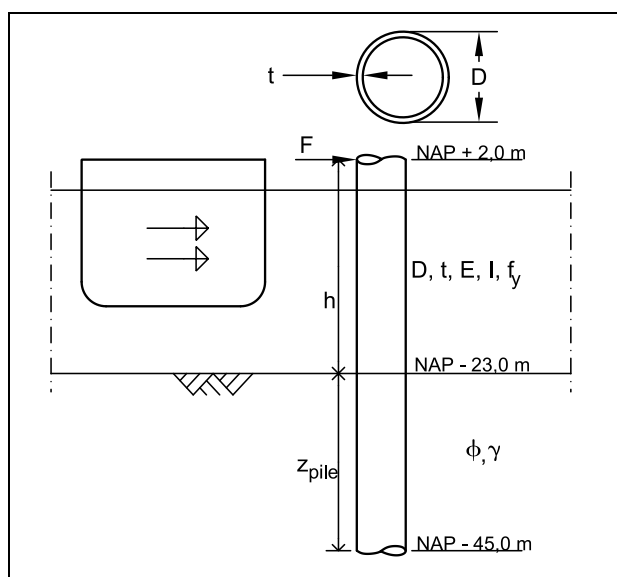


Figure 5-1 Schematic view Case 1

Parameter	Unit	Case 1A	Case 1B	Case 1C
D/t	-	83	63	42
D	mm	2.500	2.500	2.500
t	mm	30	40	60
EI	kNm ²	3,73E+07	4,91E+07	7,19E+07
f _v	N/mm ²	460	460	460
M _{el}	kNm	66.125	87.454	129.056
M _{pl}	kNm	84.192	111.349	164.319
h	bed + ... m	25,00	25,00	25,00
Z _{pile}	bed - ... m	22,00	22,00	22,00
φ	°	30,0	30,0	30,0
γ'	kN/m ³	10,0	10,0	10,0

Table 5-2 Material and geometrical properties for case 1A, B and C

Comparison

Firstly the following calculations are performed using the Blum model:

- Limit values of the bending moment M_u , reaction force F_u , lateral pile-head deflection y_u , and energy absorption E_u in Ultimate Limit State
- The normative ULS mechanism for the limit values is mentioned
- From the limit values the design values are deduced according to the limit state criteria and safety factors applicable according to the different guidelines.
- The normative ULS mechanism for the design values is mentioned

Secondly the energy absorption capacity and the allowed impact energy for normal and abnormal impact are represented graphically.

Thirdly the results of a calculation with the Bruijn model are added for comparison, using the obtained load-deflection curve to assess the energy absorption capacity of the pile.

Case 1A

In Table 5-3 the results of the calculation for Case 1A are presented. The resulting values for the energy absorption capacity and the allowed impact energy are presented in a column graph in Figure 5-2.

Case 1A								
Parameter	Unit	NEN 6770	PIANC 1984	PIANC 2002	BS 6349	EAU 1996	Design practice	Bruijn model
<i>Limit values</i>								
M _u	kNm	20,125	66,125	66,125	66,125	66,125	66,125	51,578
F _u	kN	731	2,272	2,272	2,272	2,272	2,272	1,825
y _u	mm	232	961	961	961	961	961	869
E _u	kNm	85	1,092	1,092	1,092	1,092	1,092	794
Mechanism		Buckling	Yield	Yield	Yield	Yield	Yield	Buckling
<i>Design values</i>								
M _d	kNm	20,125	54,200	66,125	52,900	66,125	52,000	
F _d	kN	487	1,883	1,818	1,840	2,272	1,810	
y _d	mm	142	755	723	734	961	721	
E _{d,abnormal}	kNm	34	711	657	675	1,092	653	
E _{d,normal}	kNm	34	711	526	338	1,092	435	
Mechanism		Buckling	Yield	Yield	Yield	Yield	Buckling	

Table 5-3 Case 1A comparison of standards and guidelines

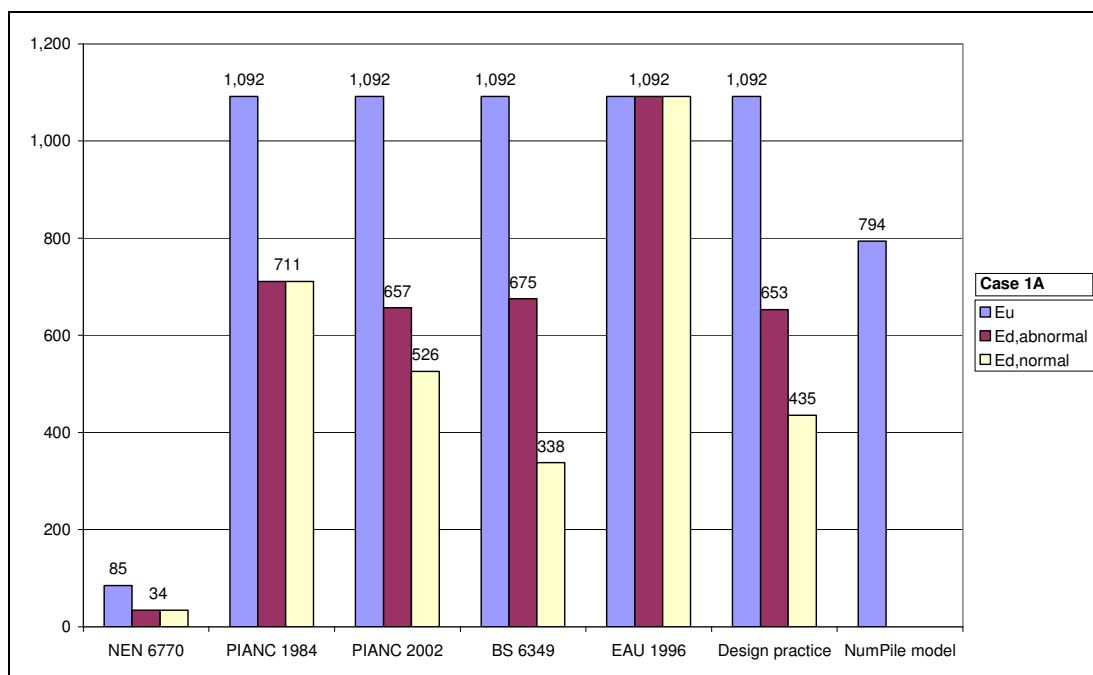


Figure 5-2 Graph of energy absorption capacity and allowed impact energy, Case 1A

Calculation of case 1A with the Bruijn model leads to the load-deflection curves displayed in Figure 5-3, with failure mode limits as indicated. Also the load-deflection curve according to the Blum model is plotted.

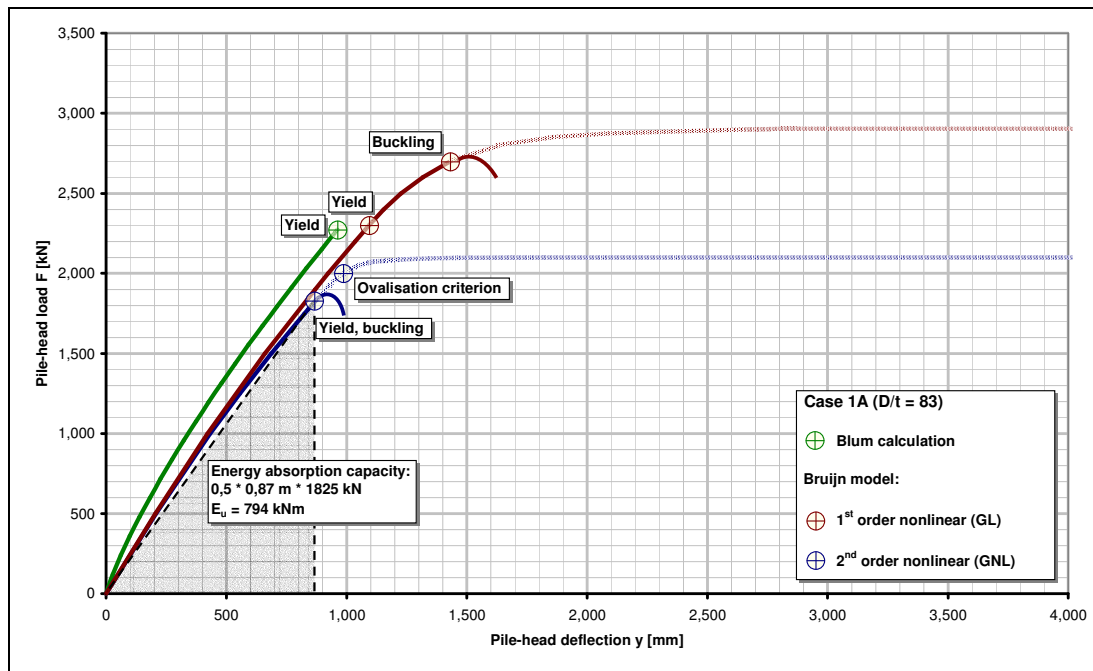


Figure 5-3 Load-deflection curves for Case 1A (Blum and Bruijn model)

Comments on Case 1A comparison:

- According to the Bruijn model buckling occurs in the elastic range (around yield stress); other standards and guidelines except for NEN 6770 does not recognise that

- According to NEN 6770 classification the cross-section is a Class 4 section (D/t ratio $\gg 45$), so the limit value for the bending moment is limited to a value well below the yield moment due to buckling sensitivity
- The current design practice, which employs the buckling criterion also used in the Bruijn model, gives results for the occurrence of buckling and the safety against buckling which are different from the Bruijn model results. This is due to the difference between the 1st order calculation with Blum and the 2nd order calculation with the Bruijn model
- The design values according to EAU 1996 are higher than the limit values according to the elastoplastic model, indicating that according to the Bruijn model buckling is likely to occur during normal operation conditions for structures designed strictly according to EAU 1996 guidelines.
- Other guidelines employ more safety resulting in lower design values for berthing energy, but safety against failure is smaller than expected if compared with Bruijn model results

Case 1B

In Table 5-4 the results of the calculation for Case 1B are presented. The resulting values for the energy absorption capacity and the allowed impact energy are presented in a column graph in Figure 5-4.

Case 1B									
Parameter	Unit	NEN 6770	PIANC 1984	PIANC 2002	BS 6349	EAU 1996	Design practice	Bruijn model	
<i>Limit values</i>									
M_u	kNm	39,843	87,454	87,454	87,454	87,454	87,454	91,388	
F_u	kN	1,406	2,956	2,956	2,956	2,956	2,956	3,130	
y_u	mm	396	1,027	1,027	1,027	1,027	1,027	1,463	
E_u	kNm	278	1,517	1,517	1,517	1,517	1,517	1,565	
Mechanism		Buckling	Yield	Yield	Yield	Yield	Yield	Buckling	
<i>Design values</i>									
M_d	kNm	39,843	71,684	68,997	69,963	87,454	87,454		
F_d	kN	937	2,452	2,365	2,396	2,956	2,956		
y_d	mm	239	805	769	782	1,027	1,027		
$E_{d,abnormal}$	kNm	112	987	909	937	1,517	1,517		
$E_{d,normal}$	kNm	112	987	727	469	1,517	1,011		
Mechanism		Buckling	Yield	Yield	Yield	Yield	Yield		

Table 5-4 Case 1B comparison of standards and guidelines

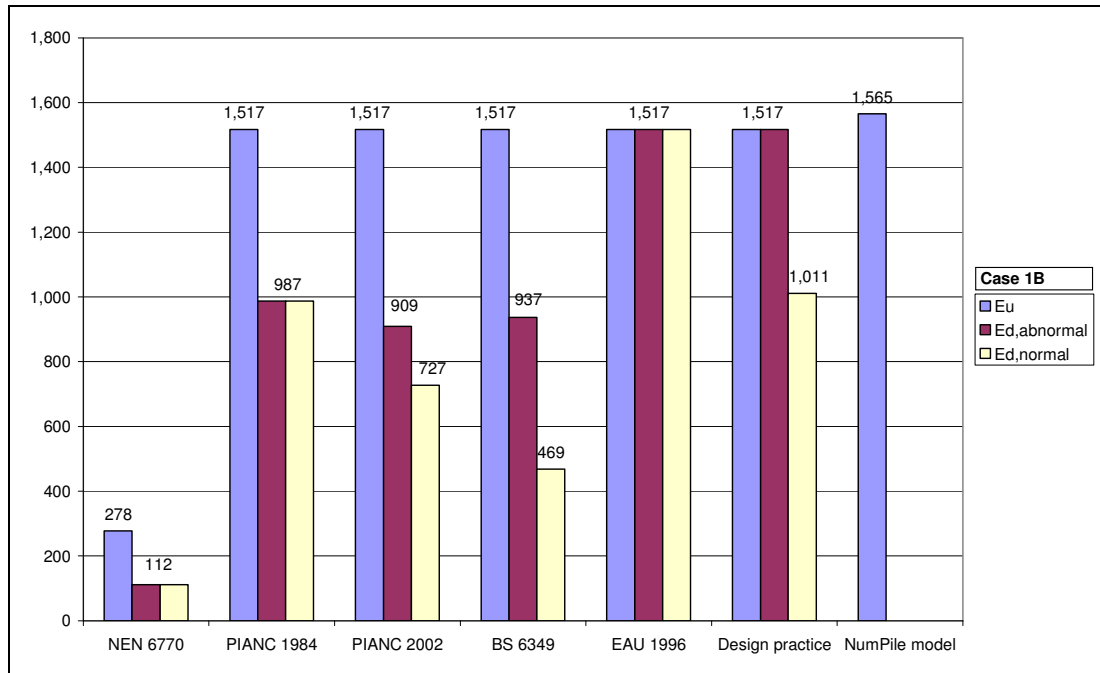


Figure 5-4 Graph of energy absorption capacity and allowed impact energy, Case 1B

Calculation of case 1B with the Bruijn model leads to the load-deflection curves displayed in Figure 5-5, with failure mode limits as indicated. Also the load-deflection curve according to the Blum model is plotted.

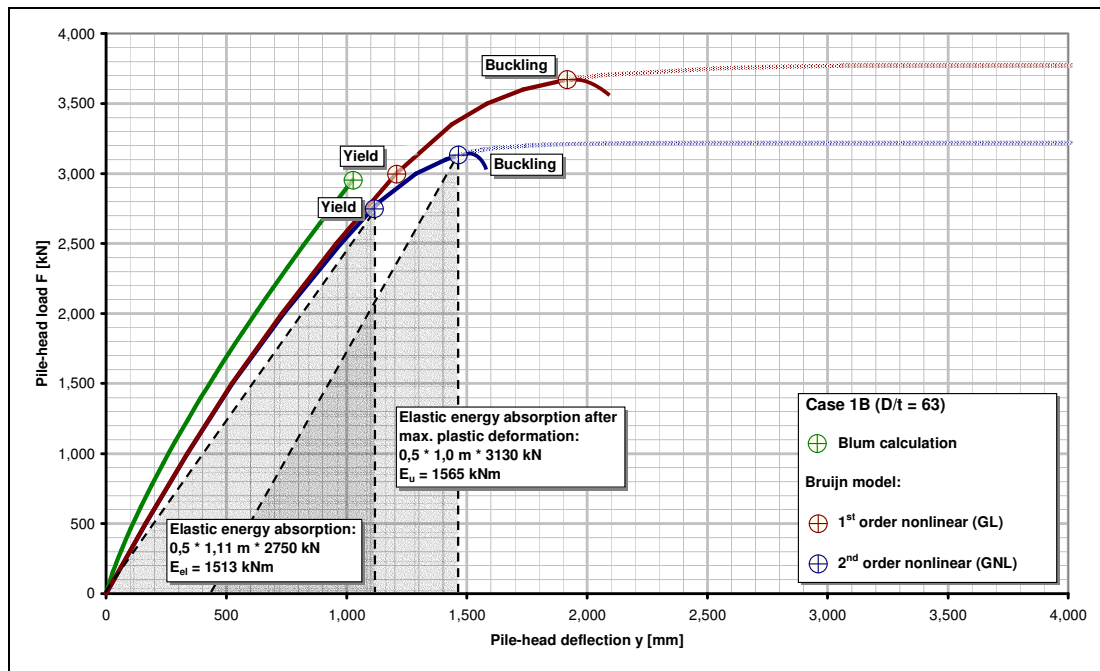


Figure 5-5 Load-deflection curves for Case 1B (Blum and Bruijn model)

Comments on Case 1B comparison:

- For this D/t ratio (63) the Bruijn model results are close to the Blum results. Because D/t ratio's of 50-70 are frequently applied, this means that the safety of most dolphins currently in use is confirmed by the Bruijn model

- According to NEN 6770 classification the cross-section is a Class 4 section (D/t ratio $\gg 45$), so the limit value for the bending moment is limited to a value well below the yield moment due to buckling sensitivity

Case 1C

In Table 5-5 the results of the calculation for Case 1C are presented. The resulting values for the energy absorption capacity and the allowed impact energy are presented in a column graph in Figure 5-6.

Case 1C									
Parameter	Unit	NEN 6770	PIANC 1984	PIANC 2002	BS 6349	EAU 1996	Design practice	Bruijn model	
<i>Limit values</i>									
M_u	kNm	129,056	129,056	129,056	129,056	129,056	129,056	129,056	150,850
F_u	kN	4,255	4,255	4,255	4,255	4,255	4,255	4,255	5,000
y_u	mm	1,132	1,132	1,132	1,132	1,132	1,132	1,132	2,411
E_u	kNm	2,409	2,409	2,409	2,409	2,409	2,409	2,409	4,250
Mechanism		Yield	Yield	Yield	Yield	Yield	Yield	Yield	Buckling
<i>Design values</i>									
M_d	kNm	129,056	105,783	129,056	103,245	129,056	129,056		
F_d	kN	2,837	3,533	3,404	3,454	4,255	4,255		
y_d	mm	665	886	843	860	1,132	1,132		
$E_{d,abnormal}$	kNm	943	1,565	1,436	1,485	2,409	2,409		
$E_{d,normal}$	kNm	943	1,565	1,149	743	2,409	1,606		
Mechanism		Yield	Yield	Yield	Yield	Yield	Yield		

Table 5-5 Case 1C comparison of standards and guidelines

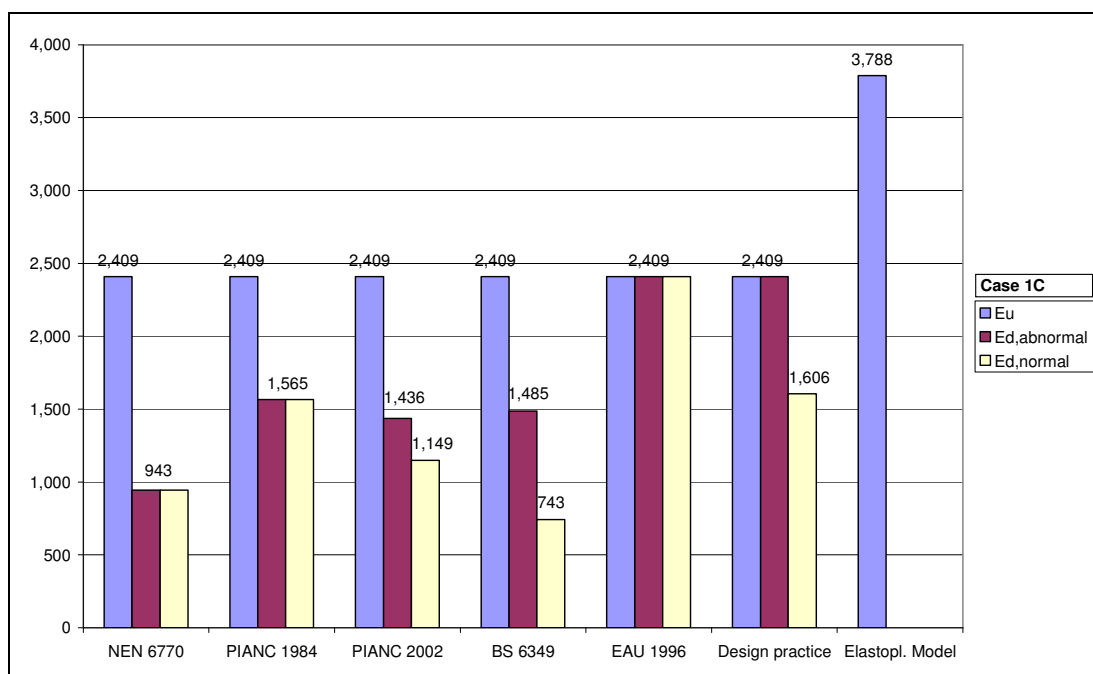


Figure 5-6 Graph of energy absorption capacity and allowed impact energy, Case 1C

Calculation of case 1C with the Bruijn model leads to the load-deflection curves displayed in Figure 5-7, with failure mode limits as indicated. Also the load-deflection curve according to the Blum model is plotted.

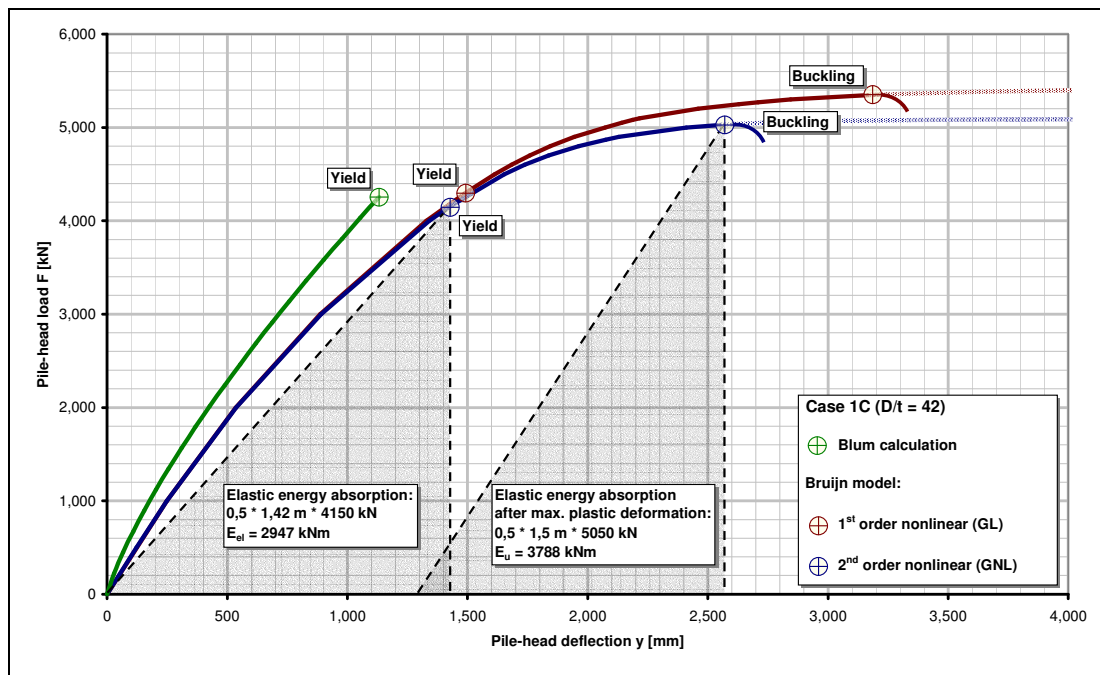


Figure 5-7 Load-deflection curves for Case 1C (Blum and Bruijn model)

Comments on Case 1C comparison:

- According to the Bruijn model plastic reserve capacity is available up to a deflection of almost 2 times the elastic deflection. This is almost sufficient for application of a lower safety factor (1,25 → 1,0) on the yield stress according to PIANC 2002
- If some plastic deformation has occurred, the elastic energy absorption capacity will increase to a maximum of $3788 / 2847 = 1,33$ times the original elastic energy absorption capacity; this confirms PIANC 2002 method of lowering the safety factor on the yield stress to 1,0 in this case
- The energy absorption capacity according to the Bruijn model (3788 kNm) is much larger than the energy absorption capacity according to all effective standards and guidelines (2409 kNm)
- NEN 6770 classification results in a Class 3 section ($35 < D/t < 45$) so the yield moment is the maximum allowable moment
- According to all guidelines yielding is normative for the limit state values, so the design is not assessed to be buckling-sensitive; this is confirmed by the Bruijn model, which shows significant yielding of the section until buckling occurs in the plastic range

Conclusions

The following conclusions can be drawn from the comparison:

- NEN 6770 is not applicable to dolphins because of very conservative buckling criteria, which are established for steel structures in e.g. buildings
- The lack of buckling and ovalisation criteria in all standards and guidelines except NEN 6770 leads to unsafe designs with high diameter-wall thickness ratio's (Case 1A, D/t 83)
- Dolphins with D/t ratio 50-70, designed according to the current standards and guidelines except EAU 1996, are safe according to the Bruijn model (Case 1B, D/t 63)

- EAU 1996 applies a safety factor of 1,0 on loads and strength, therewith assuming that the safety against failure is realised in the plastic range; however, for D/t ratio's of 50-70 the chance is significant that buckling occurs just after the yield stress is reached, resulting in a lack of safety in the plastic range
- Plastic yielding capacity according to EAU 1996 and PIANC 2002: confirmed by the Bruijn model (Case 1C, D/t 42); the calculated increase in elastic energy absorption capacity is 1,33
- Second order effects have an influence on the energy absorption capacity of the structure; this influence is proportional with the D/t ratio: With higher D/t ratio (e.g. 80) the strength reduction and buckling sensitivity due to increasing curvature and ovalisation is significantly larger than with lower D/t ratio (e.g. 40)

5.4. What are the consequences of these conclusions for the safety of the system?

From the comparison the following consequences for the safety of the system can be observed:

- the fault tree is expanded with new failure modes
- the existing failure mode yielding must be evaluated and possibly redefined
- the safety of the new system must be assessed using probabilistic calculations

Fault tree expanded

The safety of the system can be assessed by considering all possible failure modes. These failure modes can be acquired using a fault tree. In Figure 5-8 the fault tree is drawn up for a berthing system consisting of a berthing ship and a dolphin equipped with a fender.

The fault tree used in the current standards and guidelines ignores the failure modes in the shaded area. From the comparison it is concluded that these failure modes are significant, so the fault tree should be expanded to incorporate these failure modes.

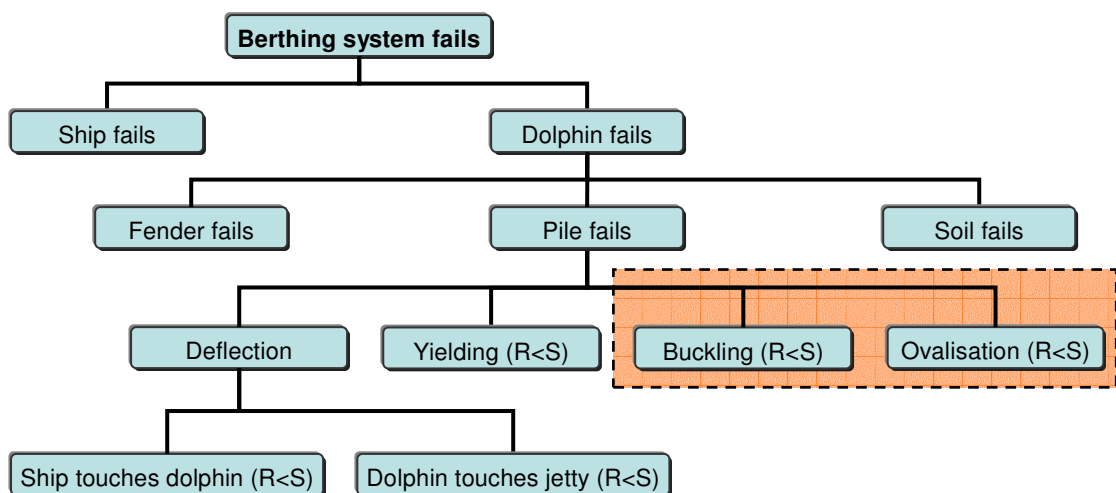


Figure 5-8 Fault tree for a berthing system

The following criterion for the critical buckling strain is applied in the Bruijn model:

$$\boxed{\varepsilon_{cr} = 0,25 \cdot \frac{t}{r'} - 0,0025} \quad \text{for} \quad \frac{r'}{t} \leq 60 \quad <5.1>$$

with

r' = local radius of curvature in the most compressed part of the circumference

For the ovalisation the following limit value is applied in the Bruijn model:

$$\boxed{a_{\max} = 0,05 \cdot D_e} \quad <5.2>$$

Evaluation failure mode yielding

Limit state yielding in current standards and guidelines: the pile fails if at any point of the pile the yield stress is exceeded.

This means that only linear-elastic pile behaviour is taken into account, and plastic deformation is not allowed to occur. An adequate safety margin should in this case be applied to prevent exceedance of the yield stress under abnormal impact.

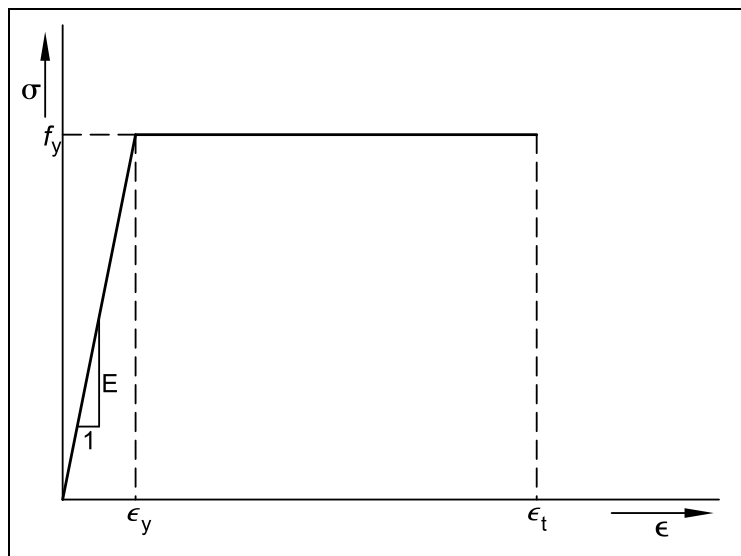


Figure 5-9 Stress-strain diagram

If the plastic branch of the stress-strain relation is taken into account (Figure 5-9), the following formulation of limit state yielding should be adopted:

- Limit state yielding is split up in limit state stresses and limit state strains
 - For limit state stresses the criterion should be: arithmetical exceedance of the yield stress f_y
 - For limit state strains the criterion should be: exceedance of the tensile strain ε_t in the pile wall. In other words: the strain capacity must be sufficient
- The following criterion can be set, in accordance with NEN 3650:
- strain $< 0,5\%$ → strain capacity is sufficient
 - strain $> 0,5\%$ → strain capacity must be proven

This way stress redistribution is allowed after the yield stress has been exceeded in one point in the pile, and the plastic deformation capacity can be included in the safety of the system.

Consequences of the choice for redefining the failure mode yielding:

- Calculation models which are more advanced than the currently recommended models (Blum / p-y) are required to assess the safety of the system in ultimate limit state conditions
- Deflections of the pile will generally increase leading to a larger probability of failure for limit state deformations (pile touches jetty / ship touches pile)

Safety of the new system

The recommended changes in the limit states require a complete new assessment of the safety of the system, because of:

- New limit states
- New limit state verifications
- Changed probabilities of failure: the failure modes are correlated and must be calculated in an assessment of the safety of the entire system

This new assessment should lead to appropriate partial factors of safety for all limit states to be checked in the design.

In Annex IV the results are presented of a further investigation of the safety of the new system. Because a quantitative analysis is not possible within the scope of this thesis project, a qualitative analysis is made by performing a FMECA (Failure Modes, Effects and Criticality Analysis) to give an overview of all foreseen unwanted events, the effects of these events and to assess the most critical events in terms of frequency of occurrence and seriousness of consequences.

The main conclusions which can be drawn from the qualitative analysis in Annex IV are:

- The most critical failure modes are: buckling of the pile, foundation instability, underwater ship-pile contact, because of a large probability of all follow-up effects occurring and because of a large seriousness of consequence
- It is preferable that abnormal impact is absorbed by progressive yielding instead of other failure modes. The reasons are:
 - Excessive berthing energy can best be absorbed by plastic yielding
 - Advance indication of failure is given by large deformations
 - Criteria can be established at what deformation repair or replacement should be executed
 - The safety against yielding can be assessed by structural analysis
- Partial safety factors should be established in accordance with this criticality and preferable failure mode

The in Annex IV identified problems with the quantitative analysis are:

- The establishment of a suitable probability distribution for design parameters like the approach velocity and the hydrodynamic coefficients is difficult due to a lack of physical data from measurements
- Explicit formulation of the reliability function $Z = R - S$ is difficult because of the mutual dependency of parameters making it necessary to iterate
- Calculation of the probabilities of failure with level II probabilistic methods is not possible because they require explicit reliability functions

- A Monte Carlo analysis can be performed to avoid having to formulate explicit reliability functions, but is not feasible in this project due to the limitations of the Bruijn model

These problems should be addressed in a future research project dealing with the safety of the system using probabilistic methods.

6. CONCLUSIONS AND RECOMMENDATIONS

6.1. Introduction

This chapter comprises the conclusions and recommendations resulting from the thesis study.

6.2. Conclusions

Plastic yielding capacity

Based on the current analysis it can be concluded that sufficient plastic yielding capacity is confirmed at a D/t ratio of about 40. An increase in elastic energy absorption capacity of up to 1,33 times the original elastic energy absorption capacity can be obtained after some plastic yielding.

This factor of 1,33 is lower than the safety factor of 1,7 assessed in the problem analysis. This difference can be attributed to 2nd order effects reducing the maximum strength of the pile

At larger diameter-wall thickness ratio's (60-80) this plastic yielding capacity is significantly smaller due to a much higher buckling sensitivity.

At a D/t ratio higher than 80 the critical buckling strain will be exceeded in the elastic range, thus reducing the ultimate energy absorption capacity to less than the full-elastic energy absorption capacity

Standards and guidelines

Although the presence of sufficient plastic yielding capacity is confirmed for some cases (low D/t ratio), EAU 1996 and PIANC 2002 still can be assessed to be unsafe in employing this plastic reserve.

The use of the plastic yielding capacity in the safety of the dolphin design should be accompanied by an assessment of the safety against failure according to the following failure modes:

- Limit state stresses: arithmetical exceedance of the yield stress f_y
- Limit state strains: exceedance of the tensile strain ε_t
- Limit state buckling: exceedance of the critical buckling strain ε_{cr}
- Limit state ovalisation: exceedance of the limit value for the ovalisation a_{max}

This means that limit state yielding as used in current design standards must be redefined and split up in above-mentioned limit state stresses and limit state strains. This is done to allow for stress redistribution according to plasticity theory.

Limit state criteria for these failure modes should be provided in the standards and guidelines. This will result in safe designs where the choice can be made to apply a low D/t ratio (below 40) and employ the plastic yielding capacity as safety margin or to apply a high D/t ratio (order 60-80) and realise the safety against failure in the elastic range.

Remaining conclusions:

- The Dutch steel standards (NEN 6770) can not be used for dolphin design because of very conservative buckling criteria limiting the allowable stresses to a fraction of the yield stress

- The energy absorption capacity according to the Blum model of dolphins with D/t ratio 50-70 is confirmed by the Bruijn model; this means that most of the dolphins currently used are designed with a correct safety assessment

Nonlinear calculation model

From the development of the Bruijn model for the prediction of the structural behaviour of a dolphin the following conclusions can be drawn:

- Application of the Beam on Elastic Foundation theory combined with the plasticity theory according to Gresnigt gives a good insight into the nonlinear structural behaviour of a flexible dolphin
- Deformation of the cross-section under influence of earth pressure, curvature and ovalisation (the so-called 2nd order effects) negatively affect the strength and stiffness of the berthing structure and consequently the energy absorption capacity. This influence increases with increasing D/t ratio
- The ability of the Bruijn model to predict the nonlinear structural behaviour of a dolphin is confirmed by comparison of the load-deflection curve generated by the Bruijn model with FEM calculations using TNO DIANA.
The prediction of the 2nd order effects by the Bruijn model differs somewhat from the DIANA calculation. The Bruijn model gives a conservative estimate of the 2nd order effects, leading to more strength and stiffness reduction than indicated by DIANA calculations. This can be attributed to:
 - Stress redistribution in DIANA, reducing the 2nd order effects compared to the Bruijn model
 - The modelling of the soil pressures against the pile, which is schematised rather simplified in the Bruijn model
- Buckling is a significant failure mechanism for dolphins. At large D/t ratio's (80 and higher) buckling in the elastic range can be expected according to the Bruijn model. According to DIANA calculations buckling in the elastic range can be expected starting at higher D/t ratio's than 80.
For D/t ratio's lower than 80 buckling after some yielding can be expected to occur
- Progressive ovalisation causing collapse of the cross-section is not assessed to be a significant failure mechanism, because with increasing ovalisation the buckling sensitivity decreases, so buckling is expected to occur before progressive ovalisation occurs

Literature investigation and problem analysis

From the literature investigation and the problem analysis the following conclusions can be drawn:

- The accuracy and functionality of hydrodynamic models to predict the berthing energy to be absorbed by the berthing structure is doubted:
 - The Kinetic Energy approach seems to be a too simplified representation of reality
 - The Long Wave approach and Impulse Response Function technique are complex models which are not easily comprehensible and applicable in a design environment
- The proposed approach velocities are not based on a thorough statistical analysis of sufficient amounts of real-time measurements
- If damage occurs the failure mode, extent of damage and responsibility for the damage are not known

6.3. Recommendations

Probabilistic analysis of the safety of the system

The following topics could be addressed in further research:

- Research for suitable and accurate probability distributions for the approach velocity and hydrodynamic influences
- Development of a model for the entire system (ship – dolphin – soil) or a part of the system (pile – soil) to perform a Monte Carlo analysis, resulting in probabilities of failure for all failure modes
- Establish partial factors of safety for all limit states

Nonlinear calculation model

The following topics could be addressed in further research:

- Research to resolve current limitations or inaccuracies in the calculation model:
 - Investigation of the effect of the soil in the pile on the structural behaviour; this could lead to a conclusion that the buckling sensitivity is reduced by the soil in the pile, so the buckling sensitivity is assessed conservatively if the influence of soil in the pile is neglected
 - Investigation of the relaxation and reloading behaviour to be incorporated in the load-deflection curve
 - Effect of layered soil, ranging wall thickness, cohesive soils on the structural behaviour
- Field tests to check the accuracy of the nonlinear calculation model
- Development of a program for the nonlinear calculation of a laterally loaded pile to be released to the design environment: such a program is easier to work with and more dedicated to the specific design situation than the complex FEM programs
- Make large amounts of case calculations to:
 - Further explore the magnitude of the plastic yielding capacity
 - Establish criteria in terms of D/t ratio when the incorporation of plastic reserve in the design safety is allowed

Research of hydrodynamics

Further research hydrodynamic models:

- Comparison of hydrodynamic models with each other and with model tests
- Establishment of criteria when to use which model:
 - Kinetic Energy approach: simplified model, e.g. use in situations of sheltered berthing conditions (no significant influence of waves, wind, currents)
 - Long Wave approach or Impulse Response Function technique: complex models, to be used in situations where the Kinetic Energy approach is not accurate anymore, e.g. exposed berthing conditions

Further research approach velocity:

- Set up measurement facilities for real-time measurements of approach velocities, perhaps in cooperation with terminal operators. This way more data is available for an assessment of allowable approach velocities in different conditions for different sizes of ships based on thorough statistical analysis

Damage analysis

An investigation of the occurrence of damage can be performed resulting in methods how to assess the causes of damage and responsibility for damage, remaining strength and course of action to be followed (repair / replacement / continued operation).

Annex I

Literature investigation

I.1 Introduction

This Annex comprises a literature investigation of berthing, dolphins, loads, strength, calculation models and design standards and guidelines.

I.2 An overview of berthing facilities

Firstly an overview of the different types of berthing facility is presented, providing the main characteristics and field of application for the berthing facilities available. Secondly a more detailed description of breasting dolphins and fender systems is provided.

Berthing facilities

Three basic types of berthing facility are distinguished:

- Quay wall
- Jetty
- Single Point Mooring (SPM) facility

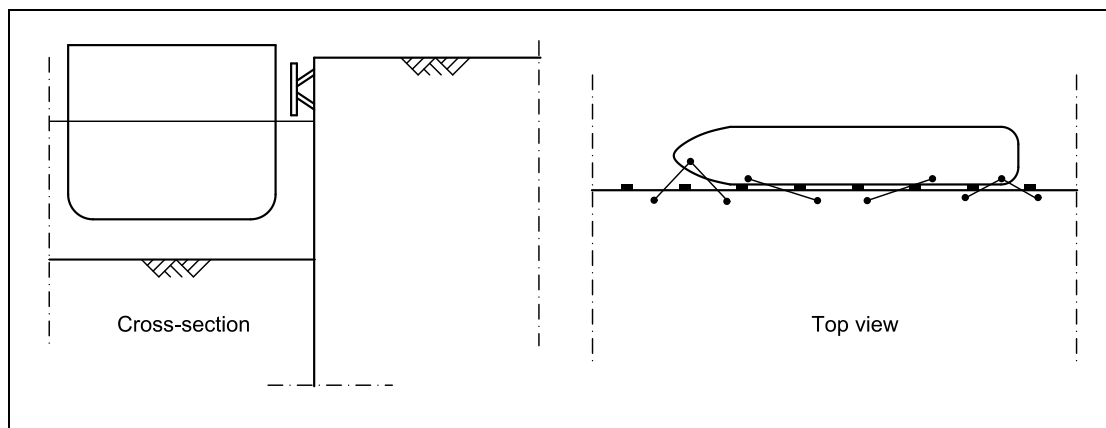


Figure I-1 Schematic view of a quay wall

The quay wall, schematically presented in Figure I-1, is the traditional berthing facility, consisting of an earth-retaining wall and fenders to ensure soft berthing. Because of the high stiffness of the structure, it is important to design a good fendering system to absorb the energy of the berthing ship without causing damage to the ship or the structure.

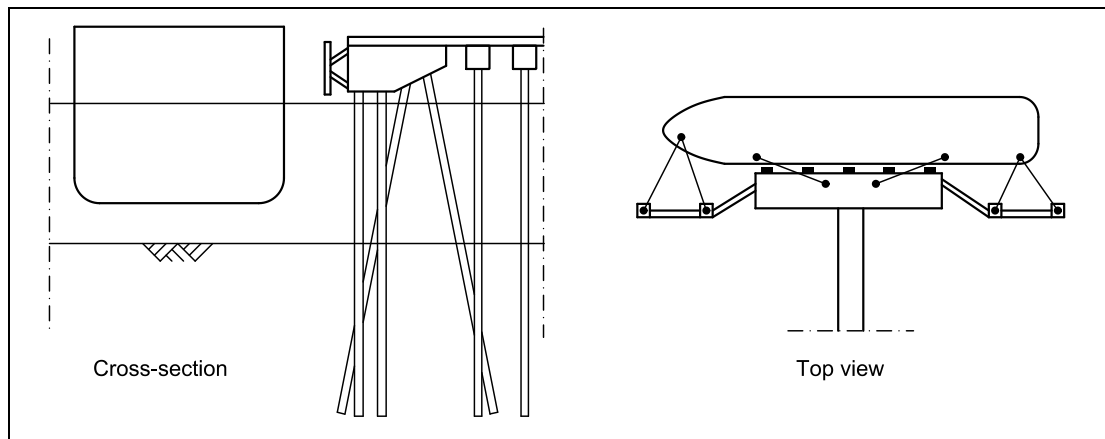


Figure I-2 Jetty structure

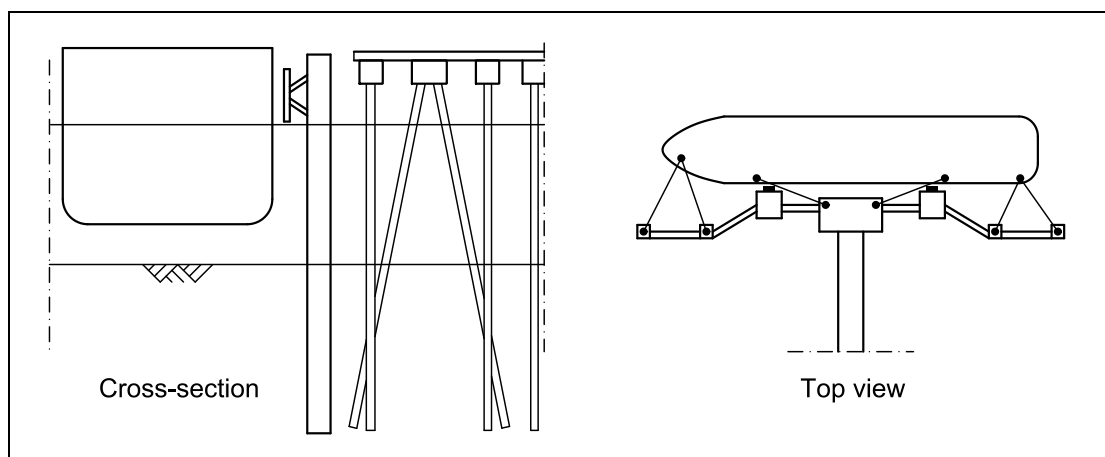


Figure I-3 Jetty with separate berthing structure

The jetty is an open pier structure. Generally less expensive than a quay wall, the jetty is applied in situations where loading- and unloading equipment allows for a lighter berthing structure. Liquid bulk terminals are generally equipped with jetties.

In some cases the ships berth directly to the jetty, refer to Figure I-2. But in most cases the functions of berthing and (un)loading are separated by application of a detached berthing structure like a dolphin, refer to Figure I-3. The advantage of this separation of functions is that the jetty and the berthing structure can be designed for the specific requirements of berthing and (un)loading respectively.

The detached berthing structure consists of breasting dolphins for handling the berthing impact and mooring dolphins for handling mooring lines. Breasting dolphins are discussed in more detail in the next section.

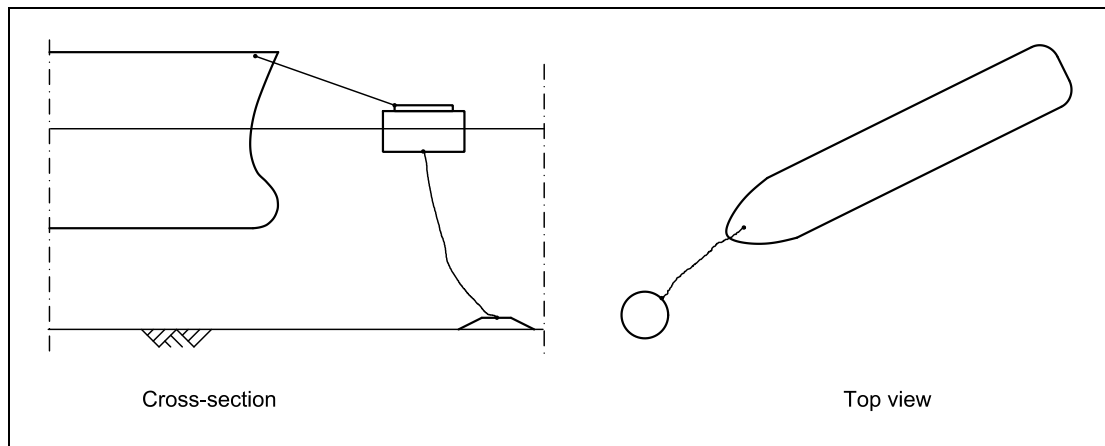


Figure I-4 Single point mooring facility

Single point mooring (SPM) facilities consist of a buoy or a turret or tower structure elevated from the sea bed, refer to Figure I-4. The basic principle is that only the bow of the ship is moored to the structure. The moored ship can freely weathervane around the structure to a stable position where the loads on the structure are minimal. SPM facilities are mostly applied in areas where no sheltered harbour area can be realised.

Breasting dolphins

Two principal types of breasting dolphin can be distinguished in respect to the way of handling the impact loads (refer to Figure I-5):

- Rigid dolphin with fender: the impact energy of the ship is absorbed by the fender; the dolphin is designed to be rigid, and may be a battered pile or a group of piles
- Flexible dolphin: the impact energy of the ship is absorbed by deflection of the pile; often a fender is added to increase the energy absorption capacity

Both types of dolphin can be applied in a berthing beam, a row of dolphins covered by a horizontal girder.

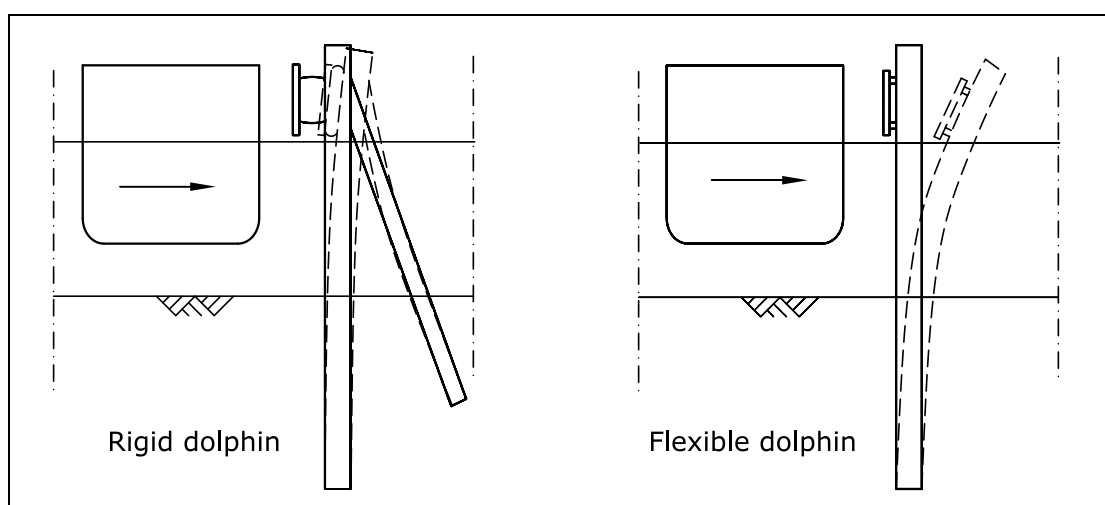


Figure I-5 Schematic view of rigid and flexible breasting dolphins

Where soil conditions are suitable the flexible dolphin is often attractive because it combines the functions of fender and breasting structure. The flexible dolphin can be a

cost-effective solution because of this. As the energy absorption capacity of a pile is a function of its length, this type of breasting dolphin is particularly attractive in “deep-water applications”. Since the pile is designed to absorb the impact energy of the ship by lateral deflection, this means that the capacity of the pile to withstand the loads depends on both the strength and stiffness of the pile. The pile stiffness should therefore be chosen with care:

- If the stiffness is chosen too low, the deflection of the pile will be too large and failure can occur if the pile touches the jetty or the ship touches the pile under water
- If the stiffness is chosen too high, the reaction force will be high and failure can occur due to yielding of the pile or yielding of the ship’s hull

The design of flexible dolphins is therefore different from the design of other structural applications.

In the case of rigid dolphins the fender is designed to absorb the impact energy of the ship. The pile or group of piles the fender is attached to is designed to transfer the reaction forces from the fender to the subsoil. The strength and stiffness of the pile or group of piles should therefore be high enough to withstand these reaction forces, making it a design as every other structural application.

NB. Since the flexible dolphin is the main investigation subject in this thesis study, most attention will go to the behaviour of the flexible dolphin without fender. The analysis however is valid for the rigid dolphin as well.

In Figure I-6 an example case of a flexible dolphin is presented, which gives some insight into the parameters playing a role and the order of magnitude of parameter values.

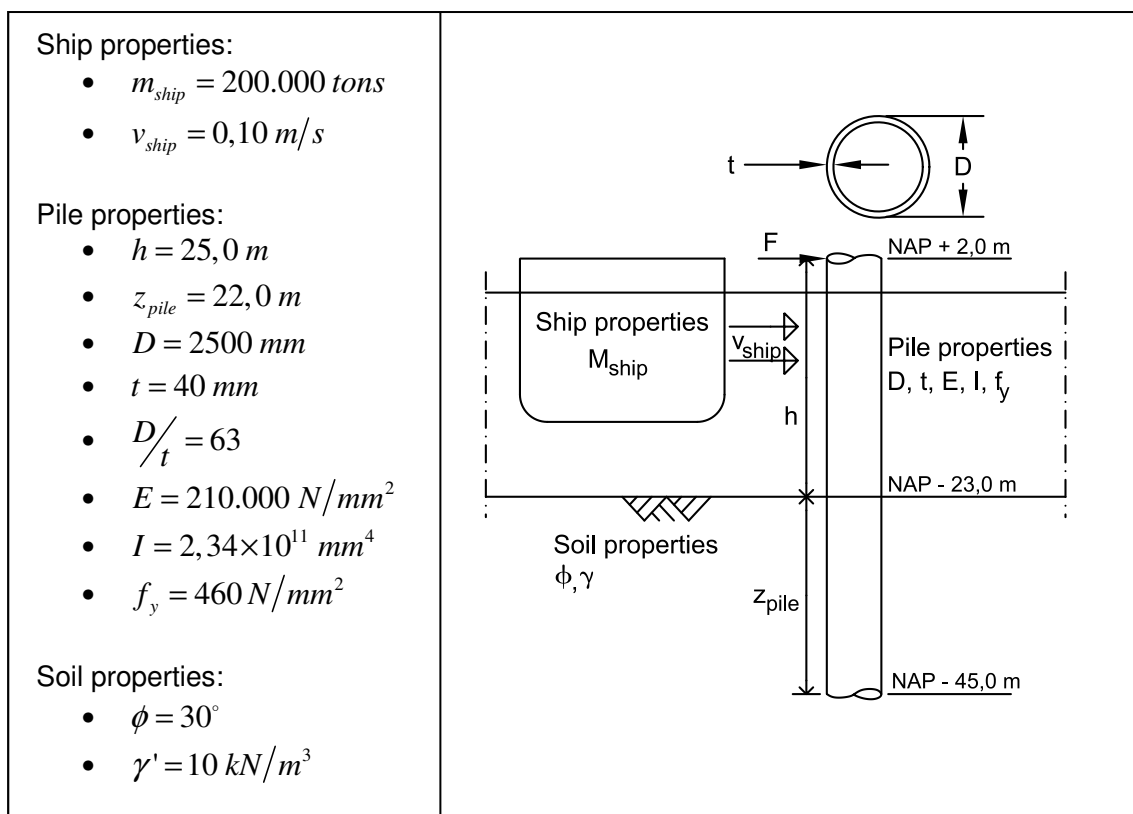


Figure I-6 Example case flexible dolphin


A jetty with detached berthing dolphins suitable for handling 80.000 tons oil tankers is Pier A of the BP Amsterdam Terminal, refer to Figure I-7.



Figure I-7 Berthing at Pier A, BP Amsterdam Terminal

Fenders

The principal function of fenders is to transform ships' berthing energies into reactions which both the ships and the berthing structures can safely sustain. The kinetic energy is then converted into potential energy of the fender, and subsequently back into kinetic energy of the ship. The energy is only temporarily stored by the fender, not dissipated. Fenders are mostly made of rubber which can be compressed up to 70-80% without damage.

In Table I-1 the fender systems most widely used in new installations are presented . The performance is expressed as a curve where the fender reaction force R is plotted against fender deflection (compression) δ . The area under the curve represents the energy absorption.



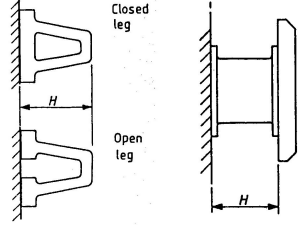
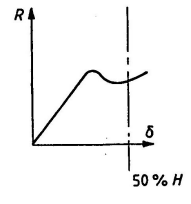
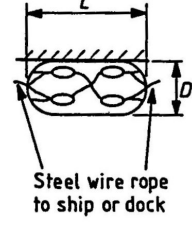
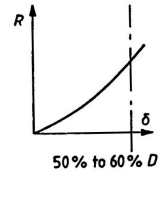
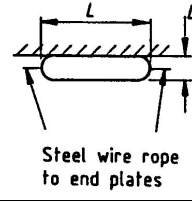
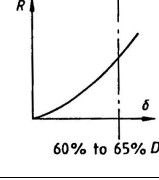
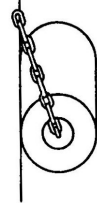
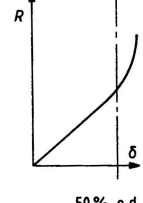
Type	Shape	Performance
Buckling fenders: + low reaction & high energy absorption – max reaction occurs almost every berthing – fender panel is required		
Pneumatic fenders: + full tidal range can be covered + low reaction force – large diameter keeps vessel further from wharf requiring larger reach for (un)loading equipment		
Foam-filled fenders: + full tidal range can be covered + low reaction force – large diameter keeps vessel further from wharf requiring larger reach for (un)loading equipment		
Side-loaded fenders: + economical – relatively low energy absorption – susceptible to damage by surging motion ship		

Table I-1 Fender types and characteristics

Factors influencing the required fender characteristics:

- Design ship impact energy; a function of mass, berthing velocity and geometrical factors
- Maximum hull pressure of the ship, bringing on requirements for the maximum allowed fender reaction force
- The range of ships using the berth (sizes, berthing velocities): this makes it difficult to design one fender system which suits the requirements of every incoming ship
- Use of the fender as primary or auxiliary structure to absorb impact energy; for a flexible dolphin equipped with a fender, the requirements for the fender are quite different from a fender system on a quay-wall
- Angular impact: reduction of the energy absorption capacity is expected under angular impact, which occurs every normal berthing
- Mooring requirements; in the mooring stage, the fender must allow safe loading and unloading operations, damping the motions of the moored ship under influence of surge, currents, wind and human operations

I.3 What happens when ships berth?

Firstly a general description is presented of the berthing process, outlining the mechanisms governing the behaviour of berthing structures under ship impact. Next the loads acting on the berthing structure, and the main principles of strength and failure of the structure are discussed successively.

Berthing process

The berthing process (with large vessels) generally takes place as follows, refer to Figure I-8:

1. With the assistance of tugs the vessel is positioned parallel to the berthing structure
2. Two tugs push the vessel sideways to the berthing structure and keep pushing during all following steps; two tugs pull the vessel to control the motions of the vessel
3. The vessel makes contact with a breasting dolphin (with bow or stern) and the kinetic energy of the vessel is converted into potential energy via deflection of the dolphin
4. The breasting dolphin swings back, converting the potential energy into kinetic energy of the vessel, in the form of translation and rotation
5. The vessel rotates around the first breasting dolphin and makes contact with the second breasting dolphin
6. At the second breasting dolphin the kinetic energy of the vessel (as a result of translation and rotation) is converted into potential energy of the construction
7. The breasting dolphin swings back, converting the potential energy back into kinetic energy of the vessel
8. The vessel rotates around the second breasting dolphin toward the first breasting dolphin
9. This movement repeats itself until all kinetic energy of the vessel is dissipated and the vessel has stopped moving

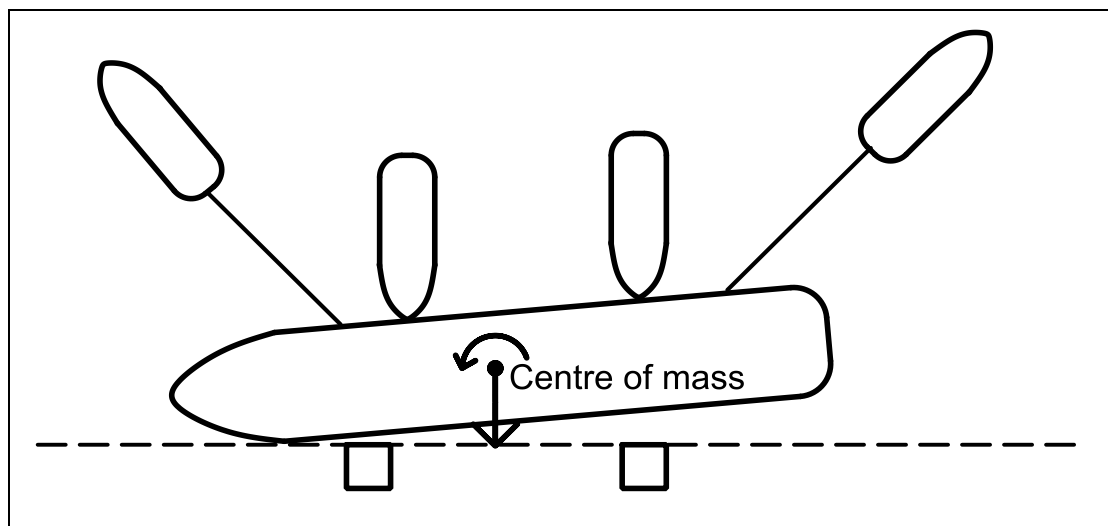


Figure I-8 Berthing model

Loads

The loads on the berthing structure are:

- Berthing impact
- Loads induced by the moored ship
- Hawser forces

Berthing impact: Energy

The berthing loads acting on the berthing structure are not simply a matter of static forces. The moving ship possesses kinetic energy, which is converted mostly into potential energy of the structure and back into kinetic energy of the ship for the duration of the impact. So the loads on the structure are time-dependent and are reduced to zero after a short period of time.



Vasco Costa, F., 1964

According to Vasco Costa ⁽¹⁾, graphs can be drawn of the histories of the impact of a ship on a structure, presenting the variation of force, approach velocity and deflection of the structure as a function of time, refer to Figure I-9:

- The most left series of graphs represent a perfectly elastic impact with no loss of kinetic energy and a rebound velocity equal to the approach velocity
- The most right series of graphs represent a perfectly inelastic impact with maximum loss of kinetic energy and a rebound velocity of zero; this is only a hypothetical situation which is physically not possible
- The series of graphs in the middle represent the more real situation of an imperfectly elastic impact where some loss of energy will occur and the rebound velocity will be smaller than the approach velocity.

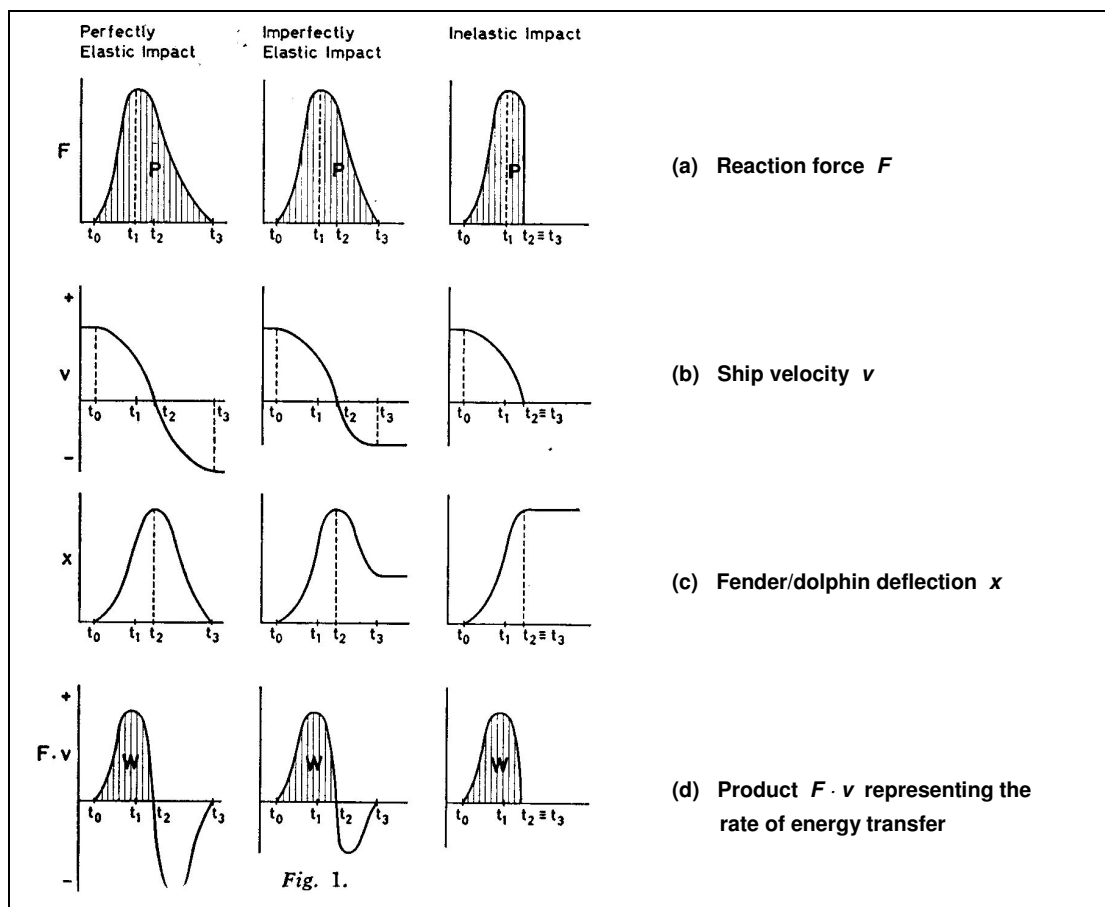


Figure I-9 Force, approach velocity and structural deflection as function of time

The shaded areas in Figure I-9d represent the kinetic energy transferred from the ship to the structure (in the diagram expressed by the symbol W for Work, in this report by the symbol E for Energy):

$$E = \int_{t_0}^{t_2} F \cdot v \cdot dt = \int_{y_0}^{y_2} F \cdot dy \quad <I.1>$$

with

F = reaction force of the structure [kN]

v = approach velocity of the ship [m/s]

y = deflection of the dolphin/fender [m]

Berthing impact: Force

According to the most right expression in <I.1> the energy absorption depends on the reaction force between ship and structure and the deflection of the structure. The energy absorption capacity of the berthing structure can therefore be expressed by a load-deflection curve. In Figure I-10 the assumed load-deflection curves for two structures A and B are drawn, where B is a structure with a larger stiffness and higher strength than A. For a certain energy absorption E ($= E_a = E_b$) the corresponding reaction force F and deflection y is pointed out for both structures.

Notice that the energy absorption apparently depends on both strength and stiffness of the structure.

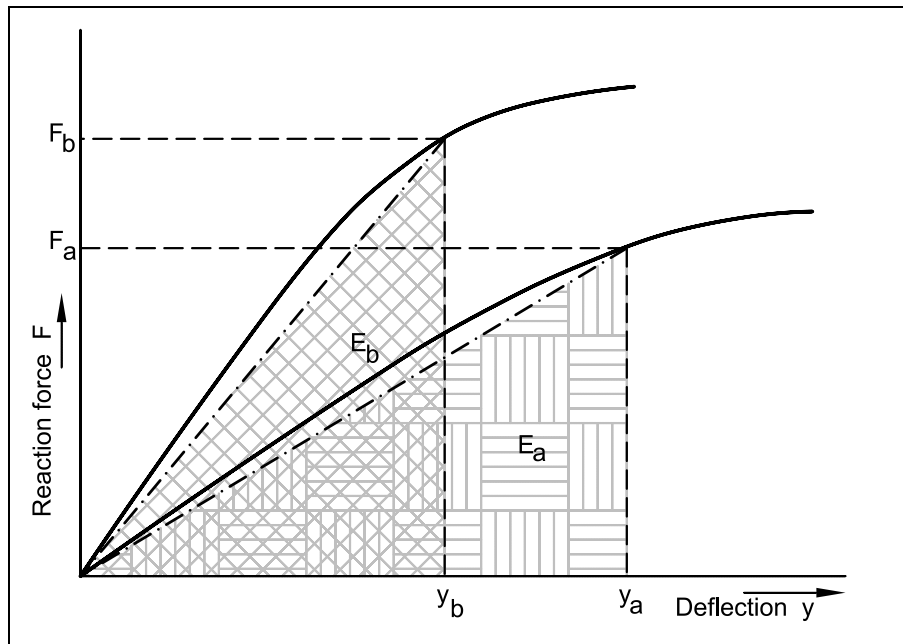


Figure I-10 Load-deflection curves for two berthing structures A and B

If the load-deflection curve is assumed linear, as shown in Figure I-10, equation <I.1> reduces to:

$$E = \frac{1}{2} \cdot F \cdot y \quad <I.2>$$

Mooring stage

When the ship is moored, the movements of the ship due to waves, currents, wind, and human operations such as loading and unloading induce loads to the berthing structure on a much smaller scale than the loads due to ship berthing.

That is why the technical requirements for berthing and mooring can be conflicting. When the berthing stage requires a fender system with most deflection around 2000 kN, in the mooring stage the fender will not act soft and consequently there is no damping of the small movements in the mooring stage. This can affect the efficiency of cargo loading and unloading.

Hawser forces

Most breasting dolphins are also equipped with bollards. The mooring lines are already fastened in the berthing stage, but they are not used to tow the ship to the berth. So the loads on the dolphin due to hawser forces are only effective in the mooring stage and must therefore be checked in combination with the other loads in the mooring stage.

Strength and stiffness

Regarding berthing impact, the strength and stiffness of the berthing structure can be expressed in a load-deflection curve, refer to Figure I-10.

This load-deflection curve is a function of the strength and stiffness of the different components of the berthing structure:

- Fender
- Pile
- Soil

Also the ship's strength and stiffness should be considered in the design.

In Figure I-11 the berthing system and its components are shown. These components of the berthing system are treated successively, outlining the key aspects in the strength and stiffness of the system.

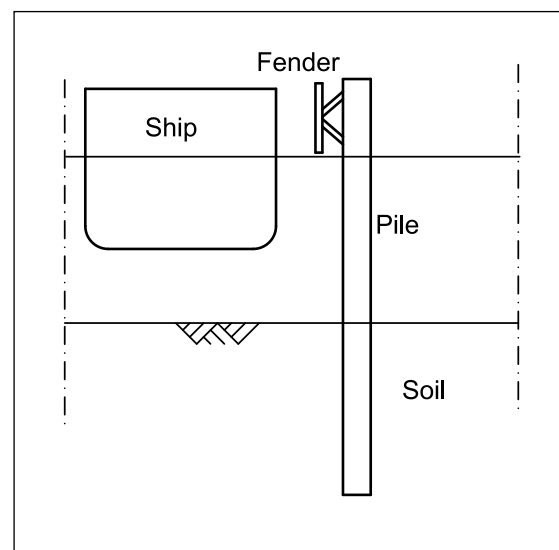


Figure I-11 Components of the berthing system

Strength and stiffness of the ship

While absorbing the berthing energy of a ship the berthing structure will give a reaction force to the ship. The hull of the ship should not incur plastic deformation due to this load. Since the development of ships has been leading to lighter hull construction, the permissible hull pressures given by ship-owners are decreasing. The reaction force can be distributed into the hull by using large fender panels.

Strength and stiffness of the fender

The performance of the fender is provided by the fender manufacturer in the form of a load-deflection curve (refer to Table I-1), with deflection meaning compression for most types of fenders. From this performance curve the energy absorption, the reaction force and the compression can be read. For angular compression correction factors are provided, because the energy absorption capacity of the fender is less under angular compression.

Strength and stiffness of the pile

The flexible dolphin absorbs energy by lateral deflection of the steel pile. From the typical load-deflection characteristics of the pile the energy absorption capacity can be determined, as treated in the section about force on page 77.

Because both reaction force and deflection of the pile influence the energy absorption capacity, an economic optimum has to be found between the strength and stiffness of the structure (determined among other things by the diameter, wall thickness and steel grade) and the safety of the structure (the risk of failure due to yield/buckling).

In order to activate as much deformation capacity as possible, the dolphin is normally assembled of sections with the same outside diameter but with varying wall thickness and steel grade, refer to Figure I-12.

At the location of the largest bending moments the strongest cross-section is applied, and at positions of smaller bending moments cross-sections with less strength and stiffness. This way the strength and stiffness of every pile section is used more optimal.

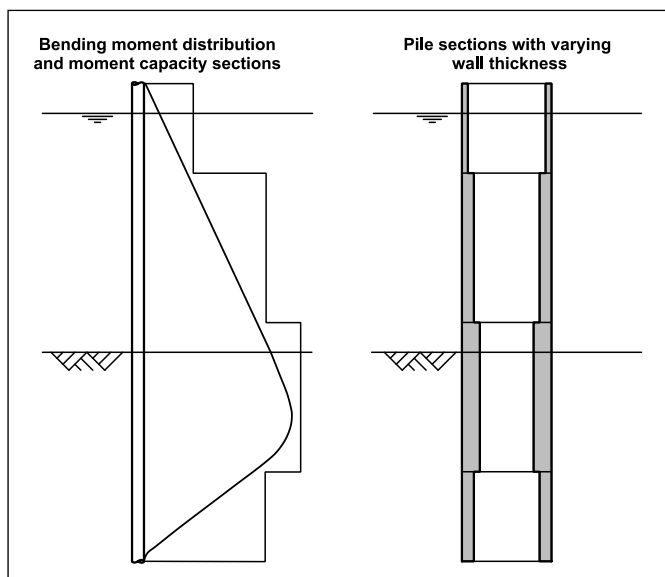


Figure I-12 Pile sections and bending moments

Application of high grade steel is usually recommended, due to high strength and energy absorption characteristics.

Strength and stiffness of the subsoil

The subsoil surrounding the dolphin will be activated by the deflection of the pile. Based on the characteristics of the soil (angle of internal friction, cohesion) the part of the soil that is activated by the movement of the pile will generate a reaction force due to internal friction to withstand the movement of the pile.

Division can be made into two types of soil behaviour:

- Drained deformation
- Undrained deformation.

Drained deformation occurs when the loads act on a timescale long enough to push away the water in the soil, so the strength of the soil is determined by the angle of internal friction. This is typically the case in sandy subsoil.

Undrained deformation occurs when the loads are acting so short that the water has no time to be pushed away, or when the permeability of the soil is so low that it takes a long time for the water to be pushed away. The strength of the soil is then determined by a combination of cohesion and friction. This is typically the case in clayey subsoil.

Failure

As stated already in the introduction: failure occurs when the loads exceed the strength. The way the structure fails as a result of the load exceeding the strength is called a failure mechanism. Usually a number of failure mechanisms have to be considered.

Failure mechanisms for the berthing system are, refer to Figure I-13:

- a. Yielding of the vessel's hull due to excessive hull pressures induced by the fender reaction
- b. Failure of the fender due to abnormal high impact energy or exceedance of the shear resistance
- c. Large deformations of the dolphin causing the ship to touch the dolphin under water
- d. Large deformations of the dolphin causing the dolphin to touch the jetty
- e. Failure of the pile:
 - Yielding
 - Buckling of the pile wall
 - Collapse of the cross-section due to significant unroundness (ovalisation)
 - Rupture in plate material or welding material
- f. Wedge-type failure of the soil due to insufficient driving depth, causing the dolphin to be pushed over completely, refer to Figure I-14a
- g. Soil failure due to exceedance of maximum soil resistance causing the soil to flow around the pile, refer to Figure I-14b
- h. Other mechanisms:
 - Damage to the jetty due to the vessel's large angle of approach causing the vessel to touch the jetty in between the dolphins
 - Low tide causing the ship to touch the fender panel too low or hit the dolphin below the fender panel

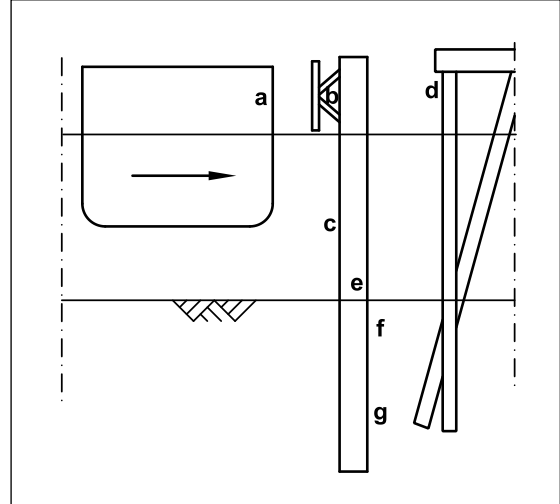


Figure I-13 Locations of failure mechanisms

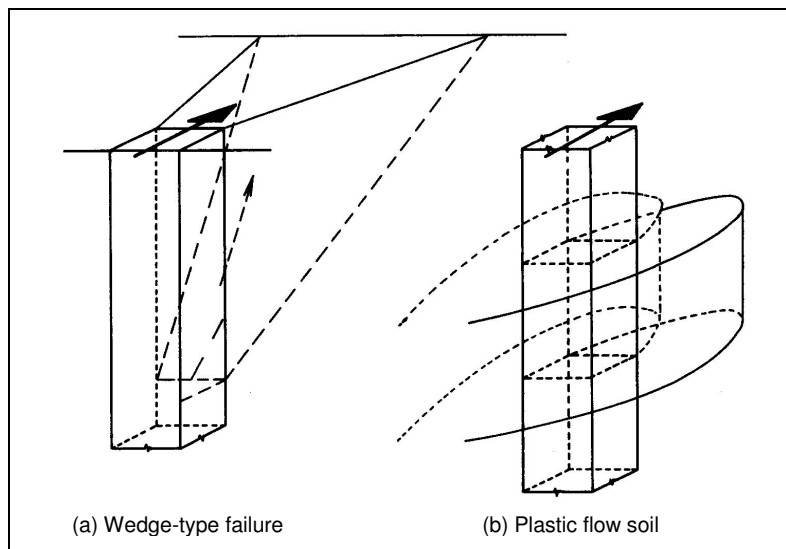


Figure I-14 Two types of soil failure

I.4 Design philosophy

Target of the structural design should be to employ a structure which is fit for purpose, with the following characteristics:

- Fulfil the functional requirements throughout the designated working life
- Withstand design actions throughout the designated working life
- Cost-effective in construction and maintenance
- Safe against failure in normal operation
- Failure in abnormal loading conditions does not lead to progressive failure of the entire structural system

For the design of a berthing structure the following topics must be dealt with:

1. Design parameters
2. Loads
3. Safety requirements
4. Calculation
5. Dimensioning
6. Costs

Ad 1. Design parameters

Knowledge of the site and soil conditions should be available to determine the following parameters:

- Soil parameters: soil layers, angle of internal friction, unit weight soil, cohesion
- Geometrical parameters: water level, bed level, sea bed slope
- Environmental conditions: wind, waves, currents, tide
- Ship parameters: design ship or range of ships using the berth, draught, mass, approach velocity

Ad 2. Loads

The loading conditions should be defined, determining all possible loads and load combinations to be checked. The loads on a berthing structure are treated already in the previous section

Ad 3. Safety requirements

A safe and reliable structural design must meet requirements regarding the desired safety level. For this reason design standards and guidelines are available which give guidance to the designer about:

- Schematisation of the structure
- Calculation models to be used
- Safety factors for loads and for strength parameters
- Failure mechanisms to be checked

In Section I.6 the standards and guidelines for berthing structures are discussed

Ad 4. Calculation

Calculation of the structural behaviour requires the following steps to be taken:

- Schematisation: the structure to be designed must be schematised in a structural model for the calculation
- Calculation model: a suitable calculation model must be chosen which is able to describe the structural behaviour using the available design parameters with a reasonable accuracy

- Interpretation of results: the outcome of the calculation must be interpreted considering the assumptions and limitations of the calculation model in relation to the structural behaviour in reality

In Section I.5 the calculation models for berthing structure design are discussed

Ad 5. Dimensioning

Using the interpreted results from the calculation a structural layout can be chosen which meets the functional requirements and withstands the loads with a safety margin corresponding to the desired safety level.

The resulting structural layout is expressed in dimensions like diameter, wall thickness, pile length and embedment and material properties like steel grade and yield stress.

Ad 6. Costs

Costs play a role in the whole process, because cost-effectiveness is an important criterion for a good structural design. Costs must be specified for design, construction and maintenance. In most cases alternative solutions are compared on cost-effectiveness and safety

I.5

Calculation models

Based on a subdivision in two main system approaches, the various calculation models are treated, describing the background of the model, field of application, and basic assumptions and restrictions when working with the model.

System approaches

In the literature on berthing structures and related subjects, two main system approaches can be distinguished:

- The hydrodynamic approach
- The pile-soil interaction approach

In Figure I-15 the two approaches are visualised in a schematic view of the berthing system.

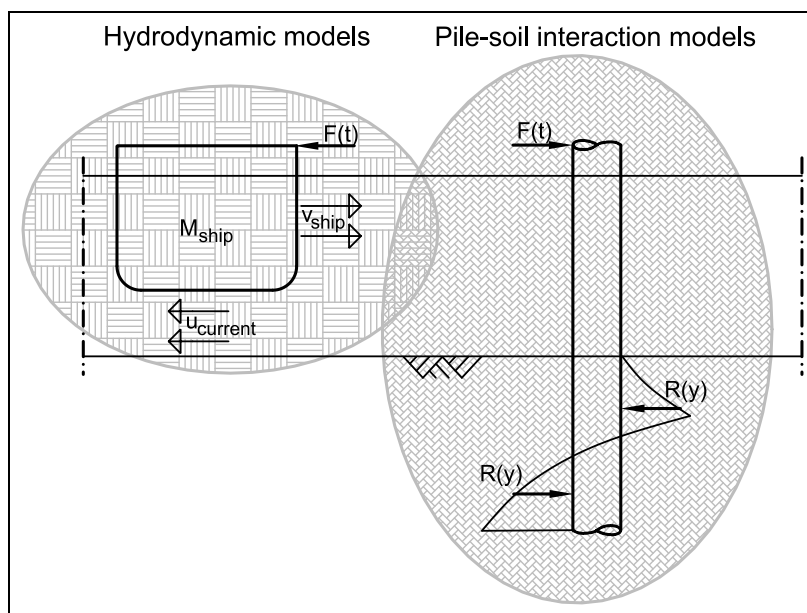


Figure I-15 Visualisation of the system approaches

Hydrodynamic models

The core of the hydrodynamic approach is the interaction between the ship and the surrounding fluid. Because the design of ships is based mostly on the behaviour of a sailing ship, extensive research is done into the behaviour of the sailing ship in waves, currents, storms etc. Mathematical representations of this behaviour are based on Newton's second law

$$m \cdot \ddot{y} = f(t) \quad <I.3>$$

describing the motion(s) $y(t)$ of a ship with mass m in response to some external force or moment $f(t)$.

Research into the behaviour of the berthing ship is the working field of the berthing structure designer rather than that of the ship designer. In other words, ships are not designed for berthing but for sailing, and the poor manoeuvring capabilities of the ship with low speeds especially become apparent in the berthing process. This is why berthing aids like tugs, guidance systems and berthing structures are necessary. Describing the berthing process of a ship assisted by several tugs with mathematical models is therefore a complicated matter.



When describing the ship-fluid system of a berthing ship, the following phenomena are relevant:

- Determination of the time-dependent loads on the ship caused by tug action, waves, currents, wind and berthing structure
- The influence of decreasing depth or keel clearance on the fluid motions and consequently on the ship motions
- The behaviour of the fluid around the ship, especially at the time of impact; i.e. the contribution of the fluid movement to the loads on the structure
- The representation of the berthing structure's behaviour under the influence of ship impact loads

The following models are based on the hydrodynamic approach and will be treated successively:

- Kinetic Energy approach (Saurin)
- Applied Long Wave theory (Kolkman/Middendorp)
- Impulse response function technique (Fontijn)

Kinetic Energy approach

The Kinetic Energy (KE) approach is based on work by Saurin . This approach has been adopted by several standards and guidelines, like the British Standards, the German EAU, and PIANC .

The basic assumption in the Kinetic Energy approach is that the kinetic energy of the ship at the moment of first contact with the berthing structure is to be absorbed by the berthing structure. In this way, the loads on the structure are separated from the reaction of the structure.

The basic equation for the kinetic energy of a moving ship is:

$$E_k = \frac{1}{2} \cdot m_s \cdot v_s^2 \quad <I.4>$$



Saurin, B.F., 1963



BS6349-4:1994
EAU 1996
PIANC, 1984
PIANC WG 33, 2002

Saurin assumed that the ship is positioned parallel to the berthing structure, and approaches the fender eccentrically from the centre of gravity, refer to Figure I-16.

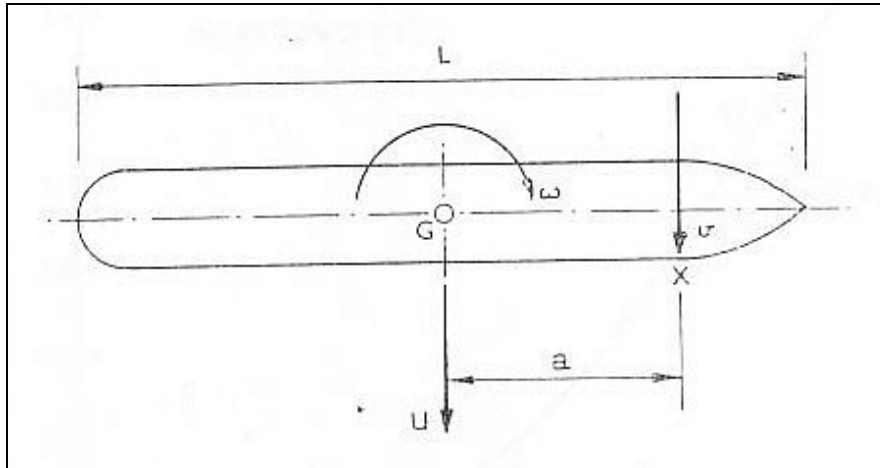


Figure I-16 Berthing configuration in Saurin's approach

The portion of the kinetic energy transferred to the fender is:

$$E_d = \frac{1}{2} \cdot m_s \cdot v_s^2 \cdot C_e \cdot C_m \cdot C_s \cdot C_c \quad <1.5>$$

with

E_d = design energy to be absorbed by the structure [kJNm]

m_s = mass of design vessel [tonnes]

v_s = approach velocity of the ship [m/s]


C_e = eccentricity factor (geometry of the impact) [0,55...0,85]

C_m = hydrodynamic mass factor [1,5...2]

C_s = softness factor [0,9...1]

C_c = berth configuration factor [0,9...1]

With this formula effort is made to estimate the influence of the motions of the ship and the surrounding water on the loads acting on the berthing structure using a few factors which can be applied to the berthing energy. That makes this a clear and easy to use method, but care should be taken whether the conditions in the specific situation agree with the assumptions and simplifications made in the KE approach.

v_s : The approach velocity is the variable with the most influence on the magnitude of the design energy. It is also a variable for which measurement data is scarcely available. According to several sources, the proposed design velocities by standards and guidelines are not based on sufficient data from real-time measurements .

This can partly be attributed to the fact that the approach velocity is significantly influenced by human operations (competence of ship master, communication between tugs) during the berthing process.



Horst, C.S. van der,
2000, § 9.2
Koopmans, M., 1998,
Ch. 8
PIANC WG 33, 2002,
§ 4.2.3

C_e : The eccentricity factor is a correction factor to account for the ship berthing eccentrically to a fender structure. According to Saurin, the eccentricity factor can be calculated with the following formula:

$$C_e = \frac{K^2}{K^2 + R^2} \quad <1.6>$$

with


K = radius of gyration of the ship [m]

R = distance of point of contact to the centre of the mass (measured parallel to the wharf [m])

From the nature of this correction factor it can be clearly seen that berthing eccentrically means a reduction in the energy to be absorbed by the structure, because the more eccentricity, the more kinetic energy will be transformed into rotational energy rather than energy to be absorbed by the structure. Therefore it can be used as a design tool to try to make the eccentricity of the fender structure as large as possible, though care should be taken whether the second impact will become heavier than the first impact as a result of this.

C_m : The hydrodynamic mass factor, also named virtual mass factor, accounts for the mass of the water moving with the ship. This hydrodynamic mass only becomes important when inertia plays a role, i.e. with changing velocities. Because a berthing manoeuvre occurs at low velocity but with rapid changes of velocity, this inertia effect is very large. Important parameters for the magnitude of this effect are:

- hull shape
- berthing velocity
- ship deceleration
- water depth / underkeel clearance

Much research work has been done in formulating an accurate expression for the hydrodynamic mass factor, among others by Grim, Saurin, Vasco Costa, Giraudet, Rupert, and Ueda. In PIANC  several formulae are mentioned. Because of its simplicity, being only dependent on the breadth and draught of the ship, mostly the formula of Vasco Costa is used:

$$C_m = 1 + 2 \cdot \frac{D}{B} \quad <1.7>$$

PIANC proposes values dependent only on the underkeel clearance, with linear interpolation in-between:

Large keel clearances ($0,5 \cdot D$): $C_m = 1,5$

Small keel clearances ($0,1 \cdot D$): $C_m = 1,8$

As yet, discussions about an accurate expression for the hydrodynamic mass factor are still going on, after decades of research trying to establish appropriate values for application in the Kinetic Energy approach. Considering the amount of research that has been conducted, it seems unlikely that fundamental progress can be made to improve the Kinetic Energy method. It can rather be observed, that effort is made to gain better results in describing the berthing process with the aid of numerical models.



PIANC WG 33, 2002,
§ 4.2.5



Middendorp, P., 1983

Long Wave theory

The Long Wave (LW) theory, as applied by Middendorp ⁱ, is based on research conducted by Kolkman. It is based on the classical Long Wave theory for the propagation of waves in relatively shallow water. Characteristic for this theory is the assumption that on both sides of the (sideways) moving ship, a surface wave is generated. The resulting pressure distribution on the ship accounts for the hydrodynamic forces on the ship. Refer to Figure I-17 for a schematic view.

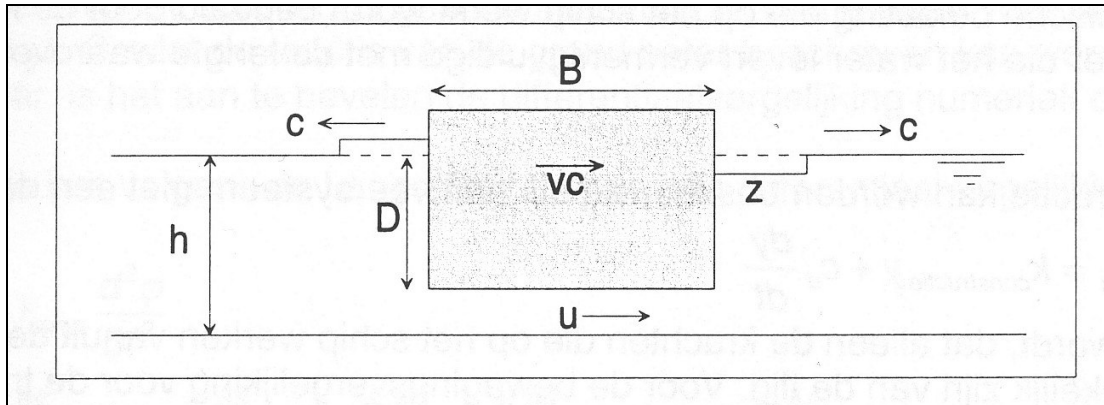


Figure I-17 Schematic view Long Wave approach

The applied Long Wave theory presents a formulation for the behaviour of the moving ship during contact with the fender structure. When applying this theory in design, the result will be a ship displacement-time history, with which the berthing energy and the reaction force of the fender structure is determined.

Basic assumptions in the Long Wave theory are:

- Shallow water
- Infinite long ship: flow only in direction perpendicular to ship axis
- Vertical fluid motion negligible in proportion to horizontal fluid motion
- Only flow forces in the form of friction under the keel of the ship are taken into account



Fontijn, H.L., 1988b,
Appendix J
Koopmans, M., 1998,
§ 4.3
Horst, C.S. van der,
2000, § 4.5

Several literature sources describe the Long Wave theory, making use of different symbols, parameters etc. ⁱ

The general formula, drawn up by evaluating the equations of motion, continuity and momentum, is:

$$\ddot{y} + A \cdot \ddot{y} + B \cdot \dot{y} + C \cdot y = 0 \quad <I.8>$$

The coefficients A , B and C are composed of parameters related to ship mass, inertia, wave propagation, construction stiffness, impact eccentricity, ship-fluid friction, water depth, and keel clearance.

This is a linear ordinary homogeneous differential equation of the third order with constant coefficients. In the case of linear spring characteristics for the reaction of the structure, an analytical solution can be obtained of the form:

$$y(t) = \sum_{m=1}^3 C_m \cdot e^{w_m \cdot t} \quad <I.9>$$

In the case of nonlinear spring characteristics a solution can be obtained using numerical procedures.

Impulse response function technique

In the classical theory of ship motions it is common practice to formulate the equation of motion as follows:

$$(m + a) \cdot \ddot{y} + b \cdot \dot{y} + c \cdot y = f(t) \quad <I.10>$$


with

a = added mass coefficient

b = hydrodynamic coefficient of the damping force

c = hydrostatic restoring coefficient

Above-mentioned equation has the form of a linear differential equation of the second order with constant coefficients. The equation can be solved analytically, only when the hydrodynamic phenomena are linearised, and a , b and c are constants. This is the case in absence of a free water-surface. When considering ship motions however a free water-surface is present. In this case the parameters a and b are dependent on the frequency of the ship motions. This complicates finding a solution for the differential equation.

Fontijn approaches this differential equation using the impulse response function (IRF) technique , stating that a unit pulse yields a response which can be described by an impulse response function, which can be deduced from the above-mentioned differential equation by means of inverse Fourier transformation. The response of the ship to arbitrary motions is fully characterised by the impulse response function.

In this way, the exciting forces and the resulting motions of the ship are connected by means of a convolution integral over the entire time history of the forcing function(s) according to:

$$y(t) = \int_{-\infty}^t f(\tau) \cdot k(t - \tau) \cdot d\tau \quad <I.11>$$

The fender reaction forces are represented in the external force function $f(\tau)$. The impulse response function holds the properties of the ship, the surrounding fluid and the geometry of the impact.

Input for the model is: design ship characteristics (mass, length, breadth, draught), berthing structure characteristics (load-deflection curves), geometry of the impact (water depth, keel clearance, eccentricity).

The solution can be found using numerical integration. The results are ship displacement-time histories and fender force-time histories, with which the berthing energy and fender structure reaction can be evaluated for different fender structure designs.

Basic assumptions and restrictions:

- Only horizontal motion of the ship-fluid system
- Ship-fluid system is linear
- Ship motions remain small, so viscous effects can be taken into account without violating the linearity-concept
- Vessel is considered rigid, prismatic, rectangular cross-section, symmetrical mass distribution



Fontijn, H.L., 1988a
§ 1.3.3

Pile-soil interaction models

The pile and the surrounding subsoil are treated as an integrated system in most models for the calculation of the structural behaviour of the breasting dolphin. This is done because the deformation of the pile and the reaction of the subsoil are directly coupled. The aim is to generate an accurate load-deflection graph, with which the energy absorption capacity and the reaction force as function of the berthing energy are known.

The following models can be counted as pile-soil interaction models and are treated successively:

- Classical calculation models (Blum)
- Subgrade reaction model (spring model)
- P-y curve method
- Finite Elements Method (FEM)
- Plastic pipeline design method (Gresnigt)

Classical calculation models (Blum)

In the classical calculation models effort is made to simplify a statically indeterminate system into a statically determined system. Methods are developed by:

- Blum
- Brinch Hansen
- Tschebotarioff
- Ohde

Of these models only the Blum model will be treated.

The original Blum model was set up for sheet piling, but with some modifications the model is applied to laterally loaded piles. The basic scheme for the Blum model is presented in Figure I-18.

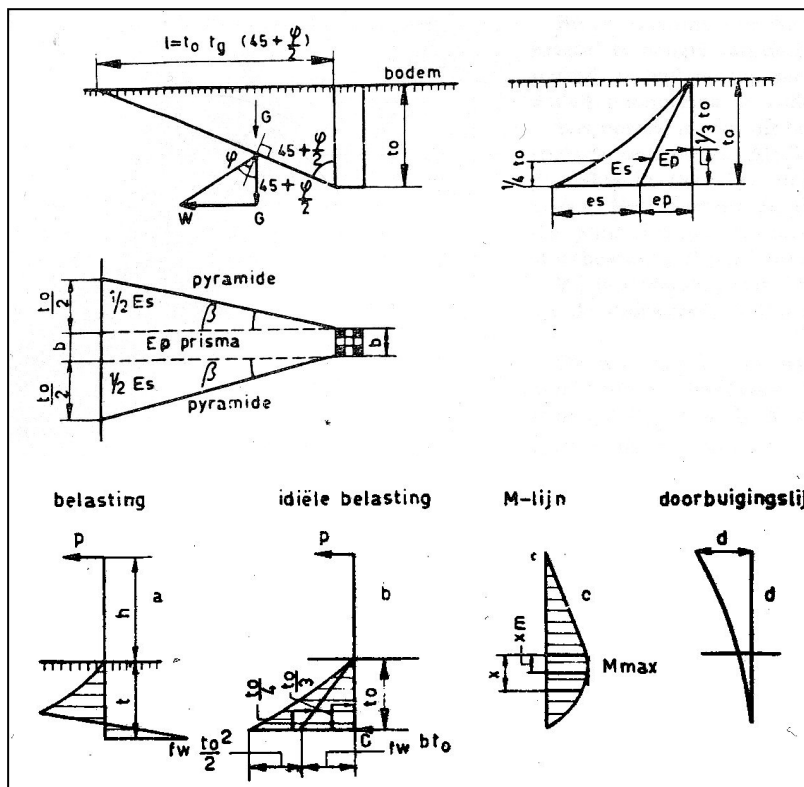


Figure I-18 Basic scheme of Blum model

The soil pressure distribution is determined using the theory of Coulomb (straight sliding faces), but also other methods, such as those with curved sliding faces can be applied. The limit state reaction of the mobilised passive soil wedge is determined by the passive horizontal soil pressure coefficient λ_p :

$$\lambda_p = \tan^2 \left(45^\circ + \frac{\phi}{2} \right) \quad <I.12>$$

with ϕ = angle of internal friction [degrees]

For the calculation of the pile deflection, Blum assumed a virtual restraining point. The deflection of the pile is then calculated using the Euler formula for bending:

$$y = \frac{F \cdot l'^3}{3 \cdot EI} \quad <I.13>$$

with

y = deflection of the pile head [m]

F = horizontal load on the pile head [kN]


l' = pile length from point of load application to estimated point of restraint [m]

This is a rather crude approximation of the deflection in reality.

With <I.13> the load-deflection curve is determined. The energy absorption can then be calculated using the linearised formula for the energy absorption (<I.2>):

$$E = \frac{1}{2} \cdot F \cdot y \quad <I.14>$$

Subgrade reaction model (spring model)

The subgrade reaction model is also known as the Beams on Elastic Foundation (BEF) theory or 'spring model'. The soil is modelled as uncoupled springs with a certain linear or nonlinear spring characteristic. It was originally developed by Winkler and Zimmerman for the calculation of rails in railway construction .



Hetenyi, M., 1974

The basic formula of this theory is:

$$EI \cdot \frac{d^4 y}{dx^4} + k_h \cdot y = f(x) \quad <I.15>$$

with k_h = modulus of subgrade reaction

This is basically the equation for bending of beams, only with the soil reaction apart from the external loads.

Refer to Figure I-19 for a layout scheme of the spring model. The pile is divided into a number of elements with length Δx , for which the differential equation can be worked out in the form of constitutive relations, equations of equilibrium and kinematical equations.

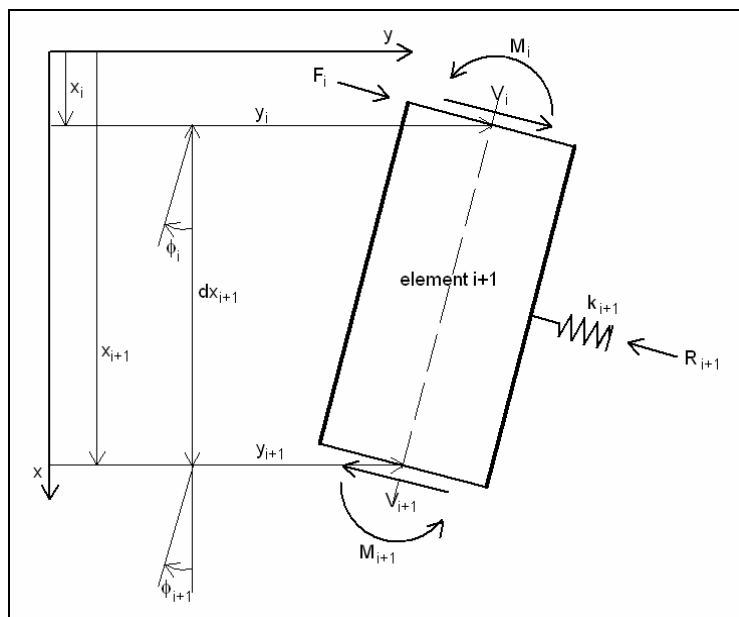


Figure I-19 Scheme of spring model

The reaction of the soil as a function of the deflection of the pile can be modelled:

- linear elastic; only the modulus of subgrade reaction is required as input parameter (e.g. according to Ménard [\[1\]](#)). In this case an analytical solution to the differential equation can be obtained.
- full plastic; in this case the limit soil reaction, e.g. according to Brinch Hansen [\[2\]](#), is required as input parameter
- elastoplastic; in this case a nonlinear spring characteristic is required, the most basic being a bilinear spring characteristic, refer to Figure I-20.



Ménard, L. et al, 1971



Brinch Hansen, J. and
Christensen, N.H.,
1961

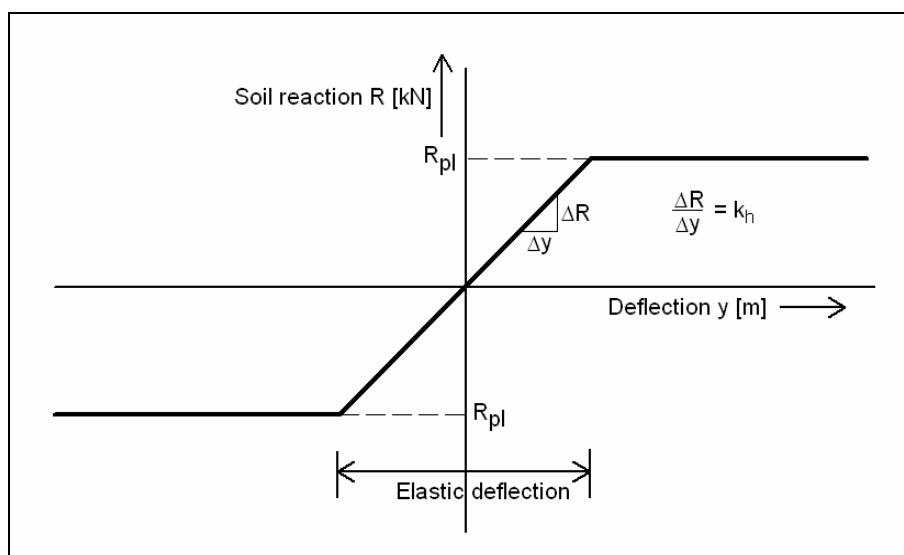


Figure I-20 Bilinear spring characteristic

In the case of a nonlinear spring characteristic, a numerical model is required to solve the differential equation and obtain the member forces, curvatures and displacements due to lateral loading. In several literature sources detailed instructions can be found how to produce a numerical model for the laterally loaded pile case [\[3\]](#).



CUR 166, § 4.2.4
Jones, G., 1997
Verruijt, A., 2003, Ch. 8



Reese, L.C., H.
Matlock, 1956



Matlock, H., 1970
Reese, L.C., M.W.
O'Neill and N.
Radhakrishnan, 1970

P-y curve method

The p-y curve method is based on research by Matlock and Reese and was first presented in the form of non-dimensional curves for rapid manual analysis of laterally loaded piles. When computers became more and more available to perform numerical model calculations, the p-y curve method in its current form was proposed by Matlock and Reese.

The purpose of the model is to produce non-linear load-deflection curves for a laterally loaded pile which can be used as non-linear spring characteristic in a numerical model based on the Beams on Elastic Foundation theory.

A typical set of p-y curves for a laterally loaded pile are shown in Figure I-21. Notice that the stiffness and plastic limit increase with increasing depth.

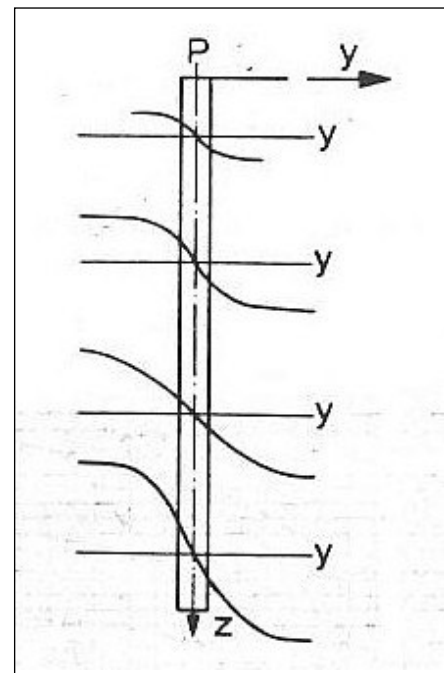


Figure I-21 Typical set of p-y curves

The p-y curves are based on field testing, and describe the combined pile-soil interaction. Care should be taken when applying these p-y curves, that the target conditions are comparable to the testing conditions, as for the pile properties (wall thickness, diameter, steel parameters) and the soil properties (type of soil, strength and stiffness parameters).

Finite Elements Method (FEM)

A general description of the Finite Elements Method (in several literature sources also referred to as FEA or Finite Element Analysis): a numerical method in which the structural elements and/or soil are divided into finite elements for which a coupled system of partial or ordinary differential equations is solved.

In this way, the Beams on Elastic Foundation theory is also part of the Finite Elements Method family. But mostly only the models in which the structural elements or soil are/is divided into small 4, 6, 8, or n node solid elements are called FEM models. Refer to Figure I-22 for the representation of a bar modelled in a FEM program.

For every node in the mesh the stresses, strains and deformations are calculated, making it a suitable model for performing advanced nonlinear structural analysis.

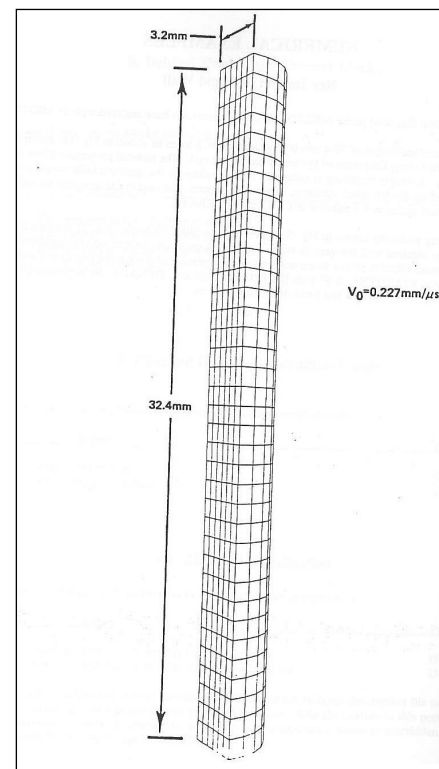



Figure I-22 Bar modelled in FEM program

Two types of FEM model can be distinguished in relation to pile-soil interaction:

- Structural analysis programs: designed to calculate stresses and deformations for complex structures under static and dynamic loading such as offshore platforms, production machines or space shuttles. Example programs are DIANA, ANSYS, and Stardyne.
- Soil and rock analysis programs: designed to accurately predict stresses and deformations of soil and rock under all kinds of loading conditions such as in the vicinity of foundation structures, ground water flow and soil works. An example program is Plaxis.

Often these programs are specifically accurate in predicting structural or soil behaviour, but when it comes to soil-structure interaction both types of programs lack the capabilities to perform analysis of the nonlinear behaviour of both structure and soil. Future development of computer and model capabilities will probably result in more and more accurate algorithms for soil-structure interaction analysis.


Plastic pipeline design method (Gresnigt)

A pile-soil interaction method for an application different from the laterally loaded pile is produced by Gresnigt .



Gresnigt, A.M., 1986

In the past, the analysis of buried steel pipelines had been based on elastic theory. In several cases, especially at dyke crossings, the pipelines were judged to be deficient in safety according to the elastic design criteria. But by applying plastic theory, the actual load-bearing and deformation capacity was expected to be substantially larger than calculated with elastic analysis.

Extensive testing and theoretical analysis provided the basis for plastic design criteria for buried steel pipelines, incorporated in the Dutch standards .



NEN 3650-2: 2003

In this case, as opposed to the other pile-soil interaction methods, the core of the research was the behaviour of the steel pipe rather than the behaviour of the soil. The aim of the research was to establish a reliable expression for the ultimate load-bearing and deformation capacity, represented by a moment-curvature diagram, due to internal pressure and external loads, refer to Figure I-23.

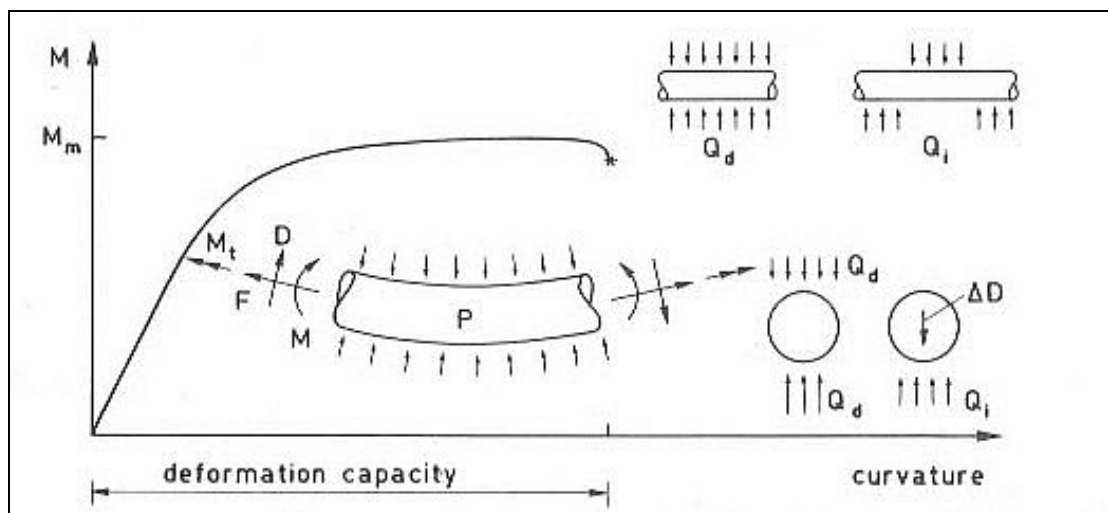


Figure I-23 Moment-curvature diagram with loads acting on the pipe

Due to the highly theoretical approach, the resulting expressions seem to be applicable to the behaviour of steel tubular sections in all kinds of applications, such as pile foundations and flexible dolphins.

The case of the buried steel pipeline shows good resemblance to the case of the flexible dolphin:

- In both cases, steel hollow tubular sections under lateral loading conditions (i.e. loads due to soil action and reaction) are considered. Internal pressure has a large influence on the structural behaviour of pipelines, but in the extensive test setup also bending without internal pressure is investigated
- Important issue in both cases is the prediction of the occurrence of buckling and providing design criteria to prevent the occurrence of buckling

Conclusions calculation models

Hydrodynamic models

The following conclusions can be drawn:

- The Kinetic Energy approach seems to be a good and easy to use model for designing a berthing structure under sheltered conditions with little influence of currents, waves and wind
- For more exposed conditions, the Kinetic Energy approach fails to accurately predict the hydrodynamic influences on the energy to be absorbed by the berthing structure; in this case, more advanced hydrodynamic models like the Long Wave approach or the Impulse Response Function technique seem to be more appropriate
- One of the parameters with a significant influence on the loads, the approach velocity, is influenced significantly by human operations during the berthing process. The currently proposed values for the allowed approach velocities seem to be based on a very limited amount of data from real-time measurements.
- In general it is expected that the loads on the berthing structure will still be significantly deviating as a result of the variances in approach velocities, whatever theoretical model is used to accurately predict the motions of the ship in the water.

Pile-soil interaction models

The following conclusions can be drawn:

- The Blum method, as an easy to use method, seems to be a good model for determining the required embedment and for a first estimate of the deflections
- The p-y curve method is a more accurate model based on large-scale field testing, and can therefore be used if the target conditions are not significantly different from the testing conditions. This way an easy to use, accurate model is generated within certain limits
- More advanced FEM models, having a sound theoretical foundation and simulation capabilities which are close to reality, are suitable in complex applications, and in future also for more simple applications, provided that the ease of use of these FEM models becomes better
- Most pile-soil interaction models assume elastic pile behaviour, so in most models it is not possible to evaluate elastoplastic pile behaviour. Apart from the FEM models, only the theory of Gresnigt provides a possibility to perform elastoplastic calculations based on the subgrade reaction theory

I.6 Standards and guidelines

In general, standards and guidelines dictate the design method to be followed, the safety factors to be applied and the mechanisms to be checked in the structural design.

In different countries different standards and guidelines are effective providing varying instructions to the designer which models to use and which mechanisms to check. First the appropriate standards and guidelines are evaluated, pointing out the relevant issues when dealing with berthing structures. Next some conclusions are presented.

Standards and guidelines assessment

NEN 6770: Steel structures

Source: The Netherlands

General description: General standards for design and construction of steel structures in the Netherlands

Relevant parts:

- In the Dutch standards no specific guidelines are available for the design of berthing structures. The sections in NEN 6770 dealing with steel tubular sections are mainly intended for the application of steel tubes in bridges and buildings. Design of tubular sections for significant lateral loading is not dealt with.
- Formulas for the serviceable and ultimate load-bearing capacity of beams subjected to pure bending are based on elastic and plastic section moduli.
- Buckling is incorporated in the form of classification of cross-sections based on the D/t ratio, for which the maximum allowable bending moment is full-plastic (M_p), full-elastic (M_e) or reduced elastic (M_{ef}). Refer to Figure I-24 for the characteristic moment-curvature diagrams for the different categories.

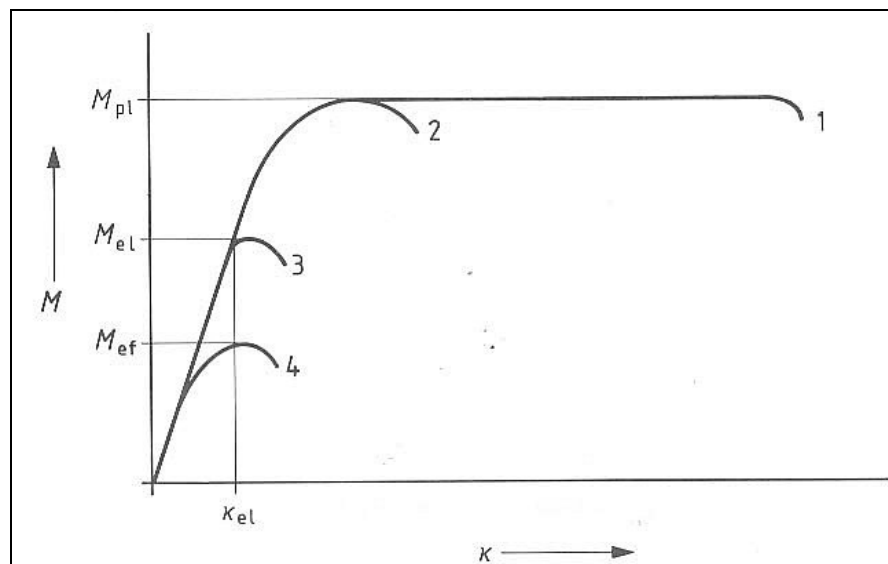


Figure I-24 Moment-curvature graphs for cross-section categories 1 to 4

According to this classification, most dolphins belong to category 4, because of a D/t ratio larger than about 50. This means that most dolphins are not allowed to be loaded to the yield limit, but somewhere below this limit. This criterion is considered to be conservative.



NEN 3650-2: 2003

NEN 3650: Requirements for pipeline systems – Part 2: Steel

Source: The Netherlands

General description: Standards for the design and construction of steel pipelines for the transport of oil or gas.

Relevant parts:

- In Quire 6 (Katern 6), the plasticity theory according to Gresnigt is treated, giving formulas for the calculation of the elastic and plastic load-bearing and deformation capacity of a tubular pipe section under influence of internal pressure, soil pressure, normal and shear forces, and bending moments. These formulas are used to determine the load-bearing and deformation capacity in serviceability and ultimate limit state.



Gresnigt, A.M., 1986



EAU 1996

EAU 1996: Recommendations of the Committee for Waterfront Structures, Harbours and Waterways

Source: Germany

General description: Guidelines for the design and construction of waterfront structures in harbours and waterways.

Relevant parts:

- In section 13, the design of berthing dolphins is treated, proposing the Blum method to calculate the energy absorption capacity of the dolphin
- The Kinetic Energy method is proposed for the calculation of the berthing energy
- Safety factor on the yield stress is 1,0 for berthing impact
- Safety factor on the yield stress is 1,5 for loads in the mooring stage
- This means, that for the berthing impact the safety against failure is assumed to be realised somewhere else, possibly in an assumed plastic deformation capacity



BS6349-2:1988

BS6349-4:1994

BS 6349: Maritime structures

Source: United Kingdom

General description: Standards for the design and construction of structures in the marine environment.

Relevant parts:

- The calculation method for the loads on the dolphin is the Kinetic Energy method
- For the methods of pile analysis reference is made to the p-y curve method of Matlock and Reese
- Safety factor for the berthing energy is 2
- Safety factor on the yield stress is 1,25



PIANC, 1984

PIANC 1984

Source: International Navigation Congress

General description: Recommendations for the design and construction of fender systems.

Relevant parts:

- The Kinetic Energy approach (recommended in design) is treated extensively, giving alternative values for the different coefficients, particularly the hydrodynamic mass coefficient
- Two mathematical models, the Long Wave approach and the Impulse Response Function approach are treated

- Safety factor on the yield stress of the pile is 1,25
- Methods for the calculation of soil-structure interaction are treated, such as Blum, Beams on Elastic Foundation, p-y curve method
- Recommended method is: make design using Blum, then check the results with the p-y curve method



PIANC WG 33, 2002

PIANC 2002

Source: International Navigation Congress

General description: Recommendations for the design and construction of fender systems.

PIANC 2002 is an update of PIANC 1984. Effort was made to make an updated overview of fender systems including performance and test details. Also some other subjects of the 1984 report were further investigated:

- C_m values (hydrodynamic mass factor)
- Parameters and coefficients for design of fender systems
- Hull pressure
- Approach velocity
- Guidelines for future fender design

Relevant parts:

- Within given limitations (suitability must be checked for the specific situation), the Kinetic Energy approach is still recommended and outlined in detail, elaborating on C_m values and approach velocity.
- Some basic information on more advanced hydrodynamic models is given, stating that exposed terminals should be designed using computer simulations with these models. Only models with frequency-dependent coefficients can reproduce the correct motion and damping behaviour in these cases.
- No specific criteria are given for the decision which hydrodynamic model to use
- For the design of flexible dolphins, load factors are recommended as follows, depending on the pile capacity to resist overloads by plastic yielding:
 - no yielding possible: load factor 1,25
 - yielding possible until a displacement of at least two times the maximum elastic displacement: load factor 1,0
- For the geotechnical design of dolphins, the methods of Blum, Matlock & Reese (p-y curve method) and FEM analysis are mentioned, of which the FEM method is considered to be the best method to describe the pile-soil interaction

Conclusions standards and guidelines

Conclusions that can be drawn from the standards and guidelines assessment:

- The standards mostly rely on generally accepted and used methods for the design of berthing structures
- The standards EAU 1996 and BS6349, giving specific guidelines on the subject of berthing structures, seem to be the most appropriate standards for the design of berthing structures
- The Kinetic Energy approach still is recommended by all standards and guidelines treated, although reasonable doubt exists about the theoretical background and the accuracy of the calculation results of this approach, especially in more exposed hydrodynamic conditions
- Other, theoretically more accurate hydrodynamic methods are mentioned (Long Wave approach, Impulse Response Function approach), but with reservations as to whether the models are sufficiently tested and confirmed in practice

- The same conclusions can be drawn for the pile-soil interaction models: although the Blum model is generally believed to yield conservative results for the deflection of the pile, still this model is the most used method for the design of dolphins
- The p-y curve method is also mentioned frequently as an accurate model for the prediction of the soil-structure interaction (especially in the US). Because of the empirical basis of the model, care should be taken whether the model is suitable for the specific situation
- Plastic design is generally not dealt with in the standards and guidelines, but there is reason to believe that the plastic yielding capacity is considered to provide a significant safety against failure, especially for EAU 1996 which proposes a safety factor of 1,0 on the yield stress
- Only PIANC 2002 gives specific guidelines for the use of plastic yielding capacity in the design of safety against abnormal impacts, although no guidelines are presented how to assess this plastic yielding capacity

Annex II

Setting up a calculation model

II.1 Introduction

The model must meet the following criteria:

- Sound theoretical foundation: correct interpretation of reality in the model formulations
- Ability to perform nonlinear calculations: avoid simplifications and assumptions conflicting the nonlinearities involved in the structural behaviour
- Transparent model structure: verifiable and interpretable calculations and results
- Adjustability: possibility to adapt formulas, change parameters, in general develop the model

II.2 Type of model

Options for the type of model are:

- Analytical model (manual calculations)
- Numerical model
- Finite Elements Method (FEM) model

Because of the complexity of the theory of nonlinear structural behaviour an analytical solution is not possible. Therefore a complete manual calculation will not be performed. Manual calculation can however be performed to verify model steps.

A FEM model, being based on the calculation of stresses and strains at many points in the model, gives a relatively good representation of reality and has a sound theoretical foundation. However, the calculation algorithms are very complex making FEM not a transparent model structure, so interpretation of the results is rather difficult. Furthermore the FEM model is hardly adjustable in order to set up a clear and limited testing environment. A FEM model can however be used to verify the developed model.

A numerical model is transparent, adjustable and is suitable for the incorporation of nonlinearities. A numerical model can be developed from a simple linear model to a complex nonlinear model. Another advantage is that by developing a numerical model insight is gained in the calculation method, and the influence of parameters on the results is traceable. That is why the concept of the numerical model is chosen for the nonlinear structural analysis.

II.3 Basic formulation model

For the numerical model the basic formulation is presented in this section, based on the theory of subgrade reaction. The pile is divided into elements for which constitutive relations, equations of equilibrium and kinematical equations can be drawn up.

Analysis of a pile element subjected to a distributed lateral load $f(z)$, refer to Figure II-1, leads to the following basic equations:

Equilibrium of forces:

$$\frac{dV}{dz} = -f(z) \quad <II.1>$$

Equilibrium of moments:

$$\frac{dM}{dz} = V \quad <II.2>$$

From these two equations it follows that

$$\frac{d^2 M}{dz^2} = -f(z) \quad <II.3>$$

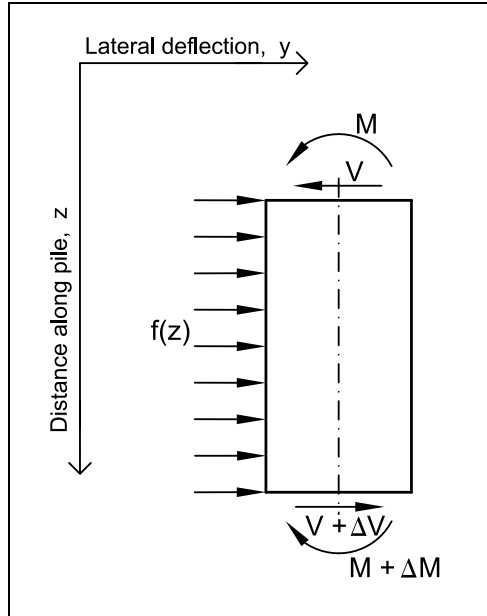


Figure II-1 Element of a laterally loaded pile

The second basic equation is the well known bending equation:

$$\frac{d^2 y}{dz^2} = -\frac{M}{EI} \quad <II.4>$$

Eliminating the bending moment M from these equations yields the partial differential equation:

$$EI \cdot \frac{d^4 y}{dz^4} = f(z) \quad <II.5>$$

If the forces due to soil reaction are separated from the expression $f(z)$ and expressed according to the subgrade reaction theory, the partial differential equation becomes:

$$EI \cdot \frac{d^4 y}{dz^4} + k_h \cdot y = f(z) \quad <II.6>$$

An analytical solution can be obtained in the case of linear elastic behaviour of both pile and soil. The general solution takes the following form:

$$y(z) = e^{\frac{z}{\lambda}} \cdot \left(C_1 \cdot \cos\left(\frac{z}{\lambda}\right) + C_2 \cdot \sin\left(\frac{z}{\lambda}\right) \right) + e^{-\frac{z}{\lambda}} \cdot \left(C_3 \cdot \cos\left(\frac{z}{\lambda}\right) + C_4 \cdot \sin\left(\frac{z}{\lambda}\right) \right) \quad <II.7>$$

with

$$\lambda = \frac{4 \cdot EI}{k_h}$$


The constants C_1 , C_2 , C_3 and C_4 must be determined from the boundary conditions. In general two boundary conditions can be formulated for both ends of the pile, so the four constants can indeed be determined.

If nonlinear behaviour is taken into account an analytical solution can not be obtained, the equation must then be solved using numerical methods.

II.4 Modelling of the pile

In this section the partial differential equation is worked out for the pile in three steps (in line with the analysis of the pile in section 4.5):

- Linear model: $M - \kappa$ relation linear, constant EI
- First order nonlinear model: $M - \kappa$ relation nonlinear, introduction of λ
- Second order nonlinear model: $M - \kappa$ relation reduced nonlinear, introduction of M'_m , E' , f'_y , E' and a

The theory used for this section is borrowed from the design rules for the plastic design of buried steel pipelines by Gresnigt . This was the only theory for plastic design found in the literature investigation (Annex I, pages 88 and further).



Gresnigt, A.M., 1986

Linear model (FL: physical linear; GL: geometrical linear)

In order to derive the equations for the linear numerical model, the pile element in Figure II-2 is considered, defining the variables as shown.

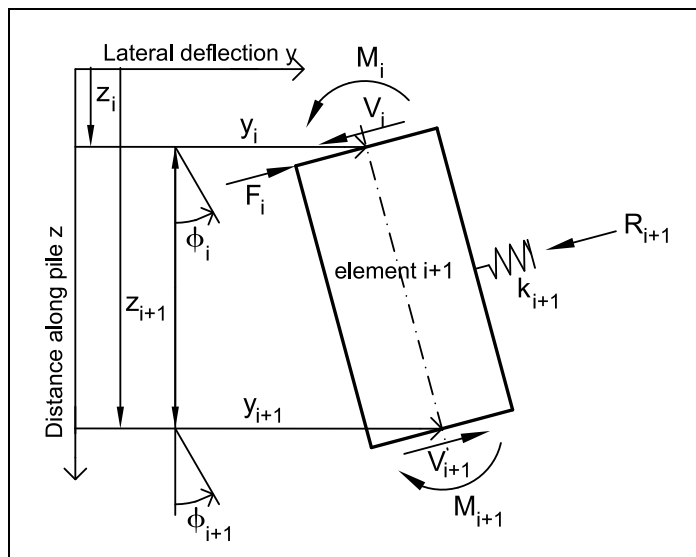


Figure II-2 Element of pile, numerical representation

Similar to the previous section, equations of equilibrium can be drawn up for the pile element.

From an evaluation of the equilibrium of forces and moments the following equation is obtained for element $i+1$:

$$M_{i+1} - 2 \cdot M_i + M_{i-1} = 0,5 \cdot (R_i + R_{i+1}) \cdot dz_{i+1} - F_i \cdot dz_{i+1} \quad \text{<II.8>}$$

This formula relates the bending moments to the forces acting on the pile, and is the numerical equivalent of the basic differential equation <II.3>.

The numerical equivalent of the bending equation <11.4>, relating the lateral deflection of the pile to the bending moment using the flexural stiffness, is

$$\frac{y_{i+1}}{d_{i+1}} - \frac{y_i}{d_{i+1}} - \frac{y_i}{d_i} + \frac{y_{i-1}}{d_i} = -\frac{dz_{i+1} \cdot M_{i+1}}{4 \cdot EI_{i+1}} - \frac{dz_{i+1} \cdot M_i}{4 \cdot EI_{i+1}} - \frac{dz_i \cdot M_i}{4 \cdot EI_i} - \frac{dz_i \cdot M_{i-1}}{4 \cdot EI_i} \quad <11.9>$$

These two numerical equations are the basic equations for the numerical model. The variables in the model are the lateral deflection y_i and the moments M_i for $i = 0, 1, \dots, n$. That means there are $2 \cdot (n+1)$ variables, for which the model gives $2 \cdot (n-1)$ equations. The 4 remaining equations must be derived from the boundary conditions. The model can then calculate a unique solution.

From these equations the other parameters can be derived:

- Shear force V
- Curvature κ
- Rotation ϕ

This linear model is limited to the yield moment M_e , because only in the elastic range the bending stiffness EI is constant.

First order nonlinear model (FNL: physical nonlinear; GL: geometrical linear)

If plastic yielding of the pile is taken into account, the model must be adapted to incorporate the nonlinear $M - \kappa$ relation as presented in equation <4.10>.

In order to do this equation <11.9> must be rewritten. Because the new relations can not be gathered in one equation like <11.9>, a series of equations is formulated. The deflection y must be calculated as function of bending moment M , so the calculation sequence is as follows:

$$M \Rightarrow \lambda(M) \Rightarrow \kappa \Rightarrow \phi \Rightarrow y$$

NB.

Notice that for this purpose the intermediate $\lambda(M)$ function is derived in section 4.5 on page 26.

$$\lambda: \quad \lambda_{i+1} = -1506,601 \cdot \beta^6 + 15304,715 \cdot \beta^5 - 64514,38 \cdot \beta^4 + 144383,76 \cdot \beta^3 - 180849,1 \cdot \beta^2 + 120130,99 \cdot \beta - 33034 \quad <11.10>$$

with

$$\beta = \frac{M}{0,5 \cdot M_p} = -\frac{\left(\frac{M_i + M_{i+1}}{2}\right)}{0,5 \cdot M_p}$$

$$\kappa: \quad \kappa_{i+1} = -\frac{\left(\frac{M_i + M_{i+1}}{2}\right)}{EI} \quad \text{for } M < M_e \quad (\text{elastic range}) \quad <11.11>$$

$$= \frac{f_y}{E \cdot r \cdot \sin(\lambda_{i+1})} \quad \text{for } M > M_e \quad (\text{plastic range})$$

$$\varphi: \quad \varphi_{i+1} = \varphi_i - \kappa_{i+1} \cdot dz_{i+1} \quad <\text{II.12}>$$

$$y: \quad y_{i+1} = y_i - \varphi_{i+1} \cdot dz_{i+1} \quad <\text{II.13}>$$

Second order nonlinear model (FNL: physical nonlinear; GNL: geometrical nonlinear)

When second order effects are taken into account, which means the reduction of the strength and flexural stiffness under influence of bending and earth pressure, the reduced $M - \kappa$ relation as derived in section 4.5 page 28 can be used.

This requires the introduction of the following variables:

- Reduced full-plastic moment M'_m
- Reduced yield stress f'_y
- Reduced Young's modulus E'
- Ovalisation a

$$\mathbf{M}'_m: \quad M'_{m,i+1} = \left(\frac{c_1}{6} + \frac{c_2}{3} \right) \cdot \left(1 - \frac{2}{3} \cdot \frac{a'_{i+1}}{r_g} \right) \cdot M_{pl} \quad <\text{II.14}>$$

with

$$c_1 = \sqrt{4 - 3 \cdot \left(\frac{n_y}{n_p} \right)^2}$$

$$c_2 = \sqrt{4 - 3 \cdot \left(\frac{n_y}{n_p} \right)^2 - 2 \cdot \sqrt{3} \cdot \left| \frac{m_y}{m_p} \right|}$$

$$n_y = -0,125 \cdot \frac{R_{i+1}}{dz_{i+1}} - 0,2 \cdot \frac{M'_{m,i+1} \cdot \kappa'_e}{r_g}$$

$$n_p = t \cdot f'_{y,i+1}$$

$$m_y = \left(\frac{1}{16} \cdot \frac{R_{i+1}}{dz_{i+1}} \cdot r_g + 0,071 \cdot M'_{m,i+1} \cdot \kappa'_e \right) \cdot \left(1 + \frac{a'_{i+1}}{r_g} \right)$$

$$m_p = 0,25 \cdot t^2 \cdot f'_{y,i+1}$$

$$\kappa'_e = \frac{f'_{y,i+1}}{E'_{i+1} \cdot r_g}$$

$$\mathbf{f}'_y: \quad f'_{y,i+1} = \left(\frac{M'_{m,i+1}}{M_{pl}} \right) \cdot f_y \quad <\text{II.15}>$$

$$\mathbf{E}': \quad E'_{i+1} = E \cdot \left(1 - 1,5 \cdot \frac{a'_{i+1}}{r_g} \right) \quad <\text{II.16}>$$

$$\mathbf{a}': \quad a'_{i+1} = \left(0,5 \cdot k_{y,i} \cdot \frac{R_{i+1}}{dz_{i+1}} \cdot \frac{r_g^3}{EI_w} + (\kappa'_e)^2 \cdot \frac{r_g^5}{t^2} \right) \cdot \left(1 + 3 \cdot \frac{a'_{i+1}}{r_g} \right) \quad <\text{II.17}>$$

with

$$k_{y,i} = 0,042$$

$$EI_w = \frac{E \cdot t^3}{12 \cdot (1 - \nu^2)}$$

Because of the reduced $M - \kappa$ relation the formulas for λ and κ should be altered to employ the reduced values of the full-plastic moment and the yield stress and Young's modulus respectively:

$$\lambda: \quad \lambda_{i+1} = -1506,601 \cdot \beta^6 + 15304,715 \cdot \beta^5 - 64514,38 \cdot \beta^4 + 144383,76 \cdot \beta^3 - 180849,1 \cdot \beta^2 + 120130,99 \cdot \beta - 33034 \quad <\text{II.18}>$$

with

$$\beta = \frac{-\left(\frac{M_i + M_{i+1}}{2} \right)}{0,5 \cdot M'_{m,i+1}}$$

$$\kappa: \quad \kappa'_{i+1} = -\frac{\left(\frac{M_i + M_{i+1}}{2} \right)}{E'_{i+1} I} \quad \text{for } M < M'_{el,i+1} \quad <\text{II.19}>$$

$$= \frac{f'_{y,i+1}}{E'_{i+1} \cdot r \cdot \sin(\lambda_{i+1})} \quad \text{for } M > M'_{el,i+1}$$

with

$$M'_{el,i+1} = \pi \cdot r^2 \cdot t \cdot f'_{y,i+1}$$

With these equations, the numerical model contains sufficient information to simulate the second order nonlinear pile behaviour. Next step is to work out equations for the simulation of the nonlinear soil behaviour.

II.5 Modelling of the soil

The soil behaviour can be simulated using different models. Firstly the different models are presented based on an evaluation of the soil behaviour. Secondly a choice is made for the soil model to be used in the numerical model.

Thirdly the chosen soil model will be treated in more detail, demonstrating the theoretical background of the model and the formulas to be used in the numerical model.

Soil models

The soil reaction depends on the lateral deflection of the pile. In Figure II-3 the horizontal soil stress distribution around the pile is given for 3 stages: before lateral loading and with 2 steps of increasing lateral loading. The soil stress characteristic in the right part of the figure reflects this soil behaviour.

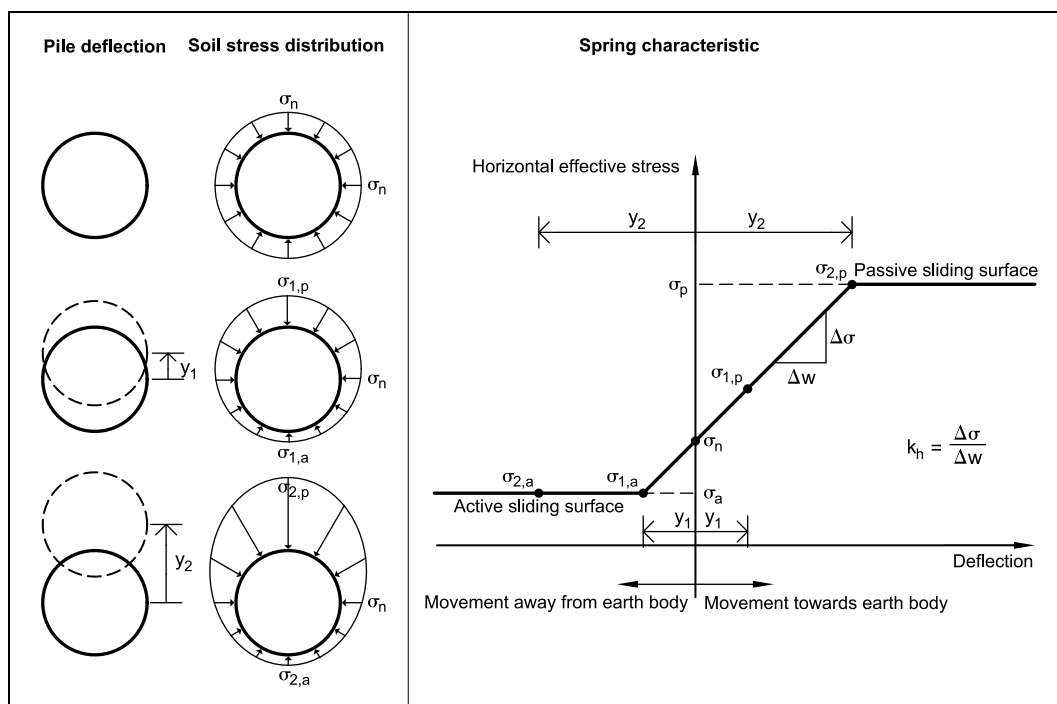


Figure II-3 Soil reaction depending on the lateral deflection of the pile

In a two-dimensional view of the pile-soil system (Figure II-4a) distinction is made between the soil reaction on the right side and the soil reaction on the left side. The side where the pile movement is towards the earth body is the passive side; the side where the pile movement is away from the earth body is the active side.

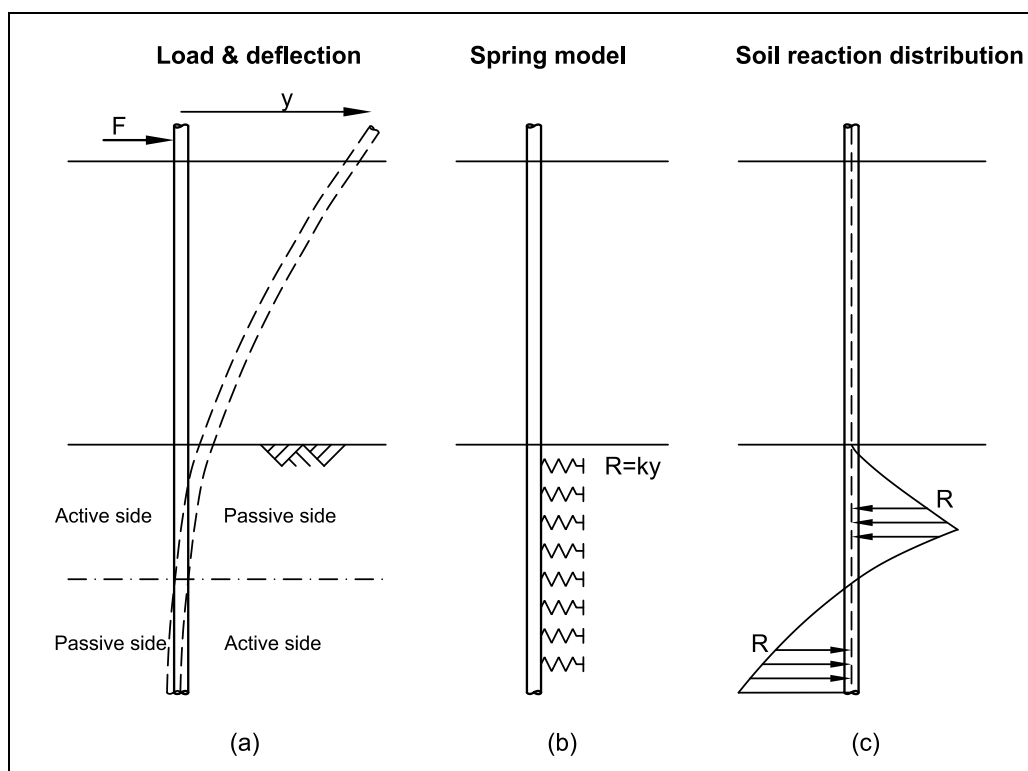


Figure II-4 Pile deflection, definition active and passive side, and resulting soil reaction

Classical soil models like Blum and Brinch Hansen (based on Blum, added theory for cohesive soils) use an assumed soil stress distribution based on full-plastic soil behaviour to assess the limit state reaction of the soil. This means that only passive and active sliding surfaces are considered, depending on the direction of the pile movement. Refer to Figure II-5 for the resulting soil stress characteristic. No elastic range is taken into account, resulting in a conservative estimate of the soil reaction (larger soil reactions) and consequently an underestimation of the pile deflection.

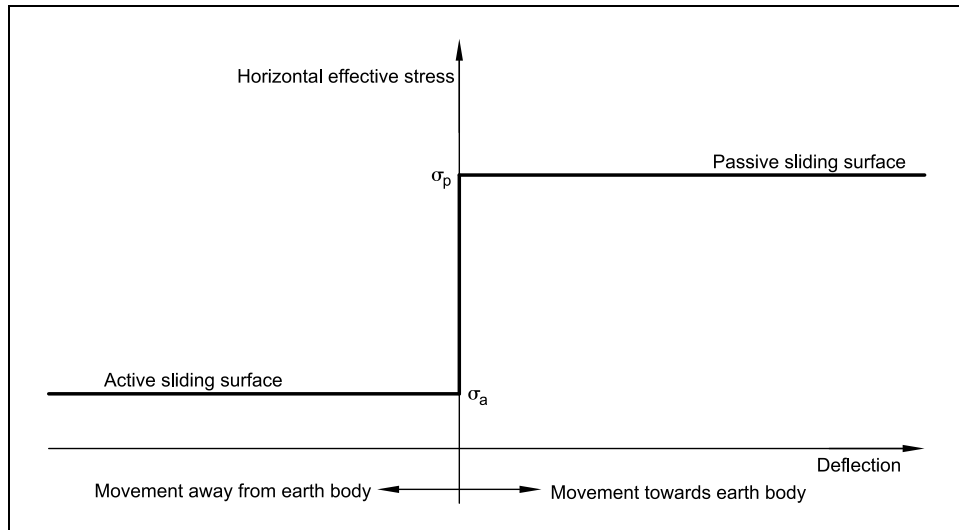


Figure II-5 Soil stress characteristic used in Blum model

Models like the subgrade reaction model, also known as the beam on elastic foundation theory or the 'spring model', simulate the soil behaviour using springs. The soil reaction on both sides is merged into one spring (Figure II-4b) with a nonlinear spring characteristic as presented in Figure II-6. Notice that in this figure the resultant soil reaction (= resultant soil stress integrated over the width of the pile) is plotted against the pile deflection, while in the graph on the right side of Figure II-3 the soil stress is plotted against deflection.

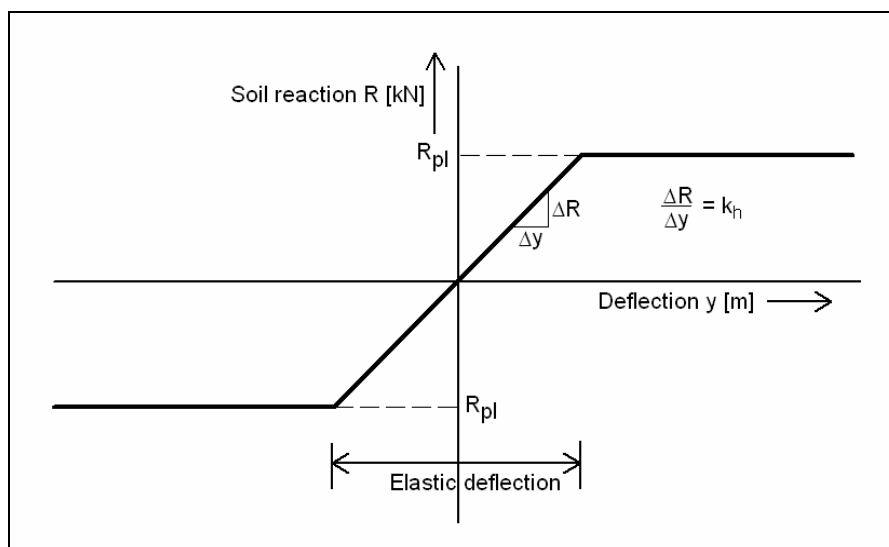


Figure II-6 Bilinear spring characteristic for soil reaction

In the elastic range the relation between soil reaction and deflection is determined by the modulus of subgrade reaction (k_h). The modulus of subgrade reaction depends on the soil type and is a function of depth. For sandy soils the value of k_h increases approximately linear with depth.

Based on experimental data from field tests with laterally loaded piles, the p-y curve method is intended to give realistic values for the soil reaction in all layers of the soil. A typical set of p-y curves is displayed in Figure II-7.

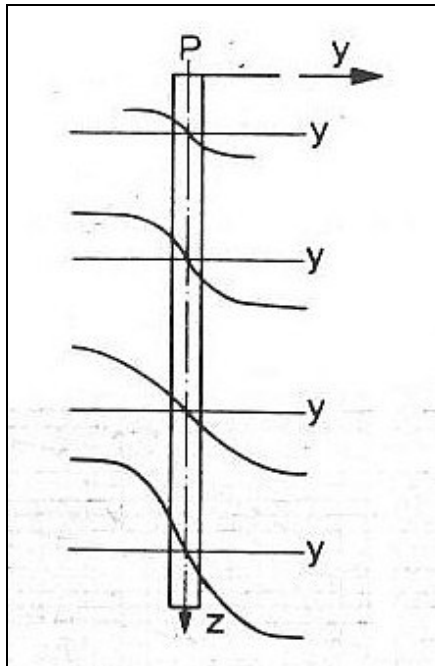


Figure II-7 Typical set of p-y curves

As can be seen from Figure II-7, the p-y curves show a good resemblance with the spring characteristic used in the beam on elastic foundation method (Figure II-6).

Choice of most suitable model

The following soil models are available:

- a. Blum / Brinch Hansen
 - Poor mathematical representation of reality
 - Model layout doesn't allow for nonlinear analysis
- b. Subgrade reaction model (spring model)
 - Appropriate model for analysis because of clear separation soil and pile
 - Suitable for numerical modelling
 - Nonlinear behaviour can be taken into account
- c. P-y curve method
 - Good approximation of reality
 - Based on empirical data, not very suitable for a theoretical structural analysis
 - Integrated pile-soil interaction behaviour: difficult to analyse
 - Target conditions should correspond to the field testing conditions
- d. Finite Elements Method (FEM)
 - Too complex
 - Difficult for analysis

Choice:

The subgrade reaction model is clearly the most suitable model to be used in the numerical model. While the p-y curve method is estimated to give more reliable results for the soil reaction, the model is semi-empirical and based on integrated soil-pile interaction behaviour that makes the p-y curve method not suitable for use in this analysis.

More detailed treatment of subgrade reaction model

The subgrade reaction model simulates the soil behaviour using uncoupled springs. The spring characteristic for these springs is given in Figure II-8. In this figure the elastic deflection is determined by the modulus of subgrade reaction (k_h) and the plastic limit by the limit soil reaction (R_{pl}).

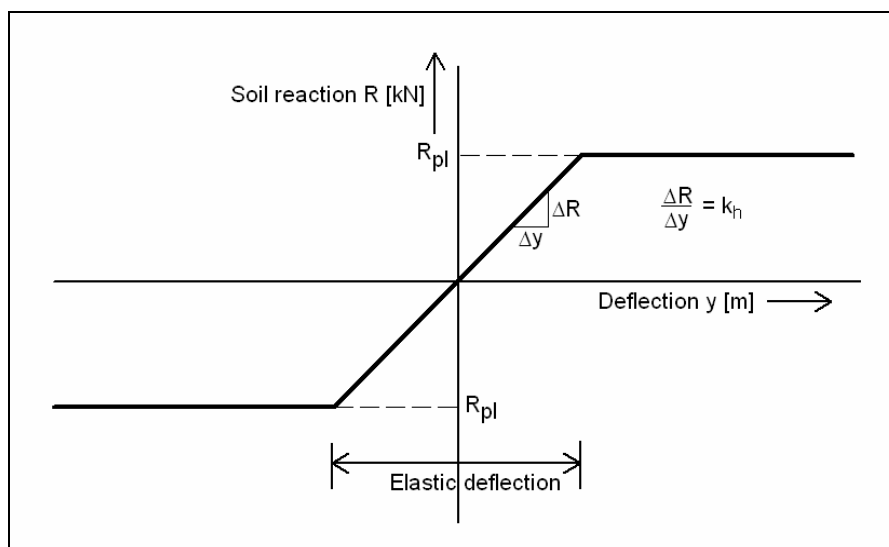



Figure II-8 Nonlinear spring characteristic for soil reaction

For the modulus of subgrade reaction the theory of Ménard is used, for the plastic limit the theory of Brinch Hansen is applied. These theories are suitable for Dutch soil conditions, and are also used in MHORPILE, a commercial program from GeoDelft for the calculation of laterally loaded piles.

Ménard

The Ménard theory  establishes a relation between the modulus of subgrade reaction, the stiffness of the soil, and the pressiometric modulus (E_p), which can be measured in a soil investigation. The relation has an empirical nature and is based on field tests.

The Ménard formula is:

$$\frac{1}{k_h} = \frac{1}{3 \cdot E_p} \cdot \left(1,3 \cdot r_0 \cdot \left(2,65 \cdot \frac{r}{r_0} \right)^\alpha + \alpha \cdot r \right) \quad <II.20>$$

with

E_p = pressiometric modulus $\approx \beta \cdot q_c$ [kN/m²]

r_0 = 0,3 m (reference radius)

r = radius = $D/2$ [m]



Ménard, L. et al, 1971

α = soil-dependent coefficient [-]
 β = soil-dependent coefficient [-]
 q_c = cone resistance [kN/m²]


For the soil-dependent coefficients α and β the following values are used:

Soil type	α	β
Peat	1	3,0
Clay	$\frac{2}{3}$	2,0
Loam	$\frac{1}{2}$	1,0
Sand	$\frac{1}{3}$	0,7
Gravel	$\frac{1}{4}$	0,5

Table II-1 Soil-dependent coefficients α and β used in Ménard theory

If the pressiometric modulus is not known from the soil investigation, the cone resistance can also be used, as shown in the formula.

Brinch Hansen

The Brinch Hansen theory  is based upon a further development of the theory of Blum.


 Brinch Hansen, J. and
 Christensen, N.H.,
 1961

Blum developed his theory for the full-plastic soil reaction in non-cohesive soils for sheet piling applications. Brinch Hansen further developed this theory for laterally loaded piles and for cohesive soils.

Brinch Hansen provided graphs for the soil pressure coefficient as a function of depth, pile diameter and soil friction angle, refer to Figure II-9.

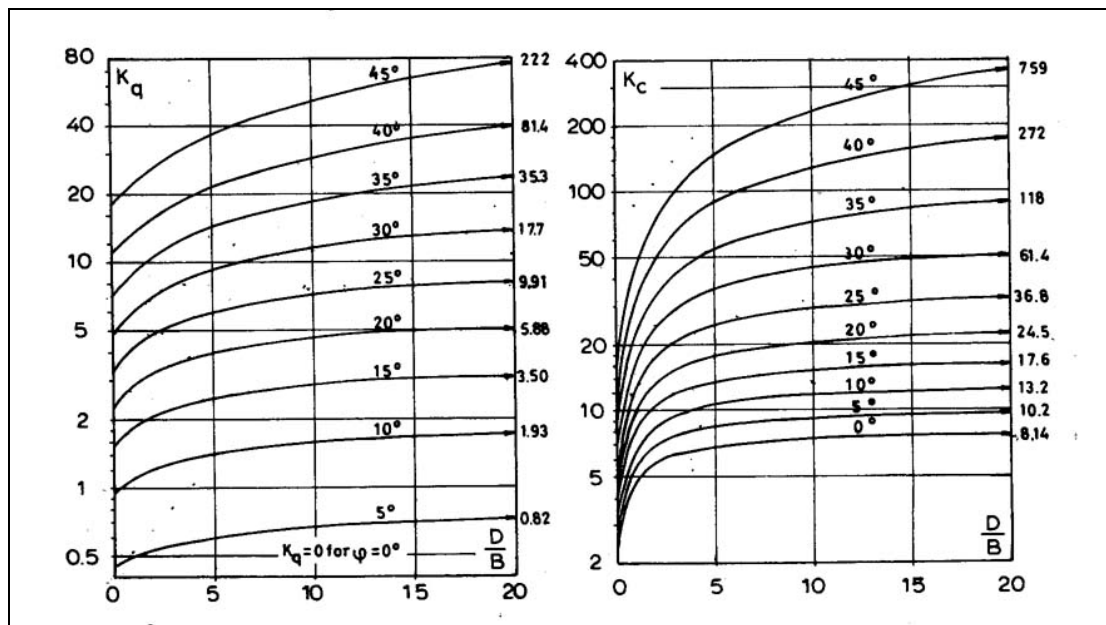


Figure II-9 Brinch Hansen graphs for earth pressure coefficients

The full-plastic soil reaction as a function of depth according to Brinch Hansen is shown in Figure II-10.

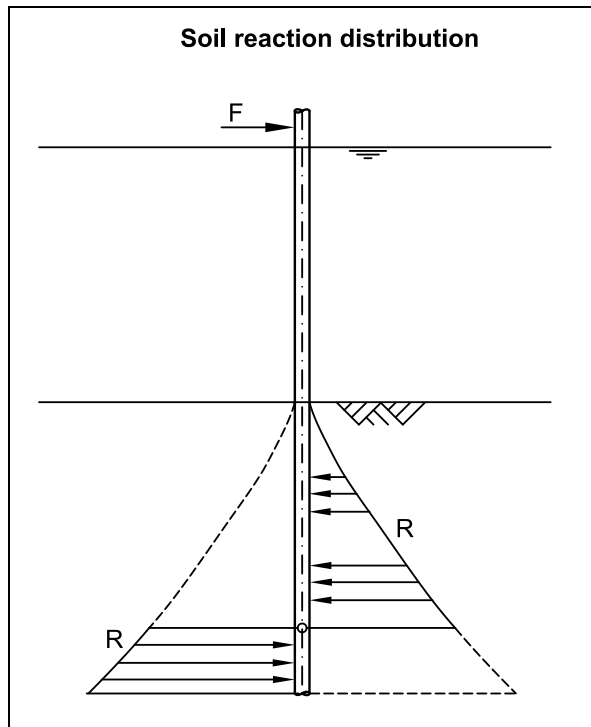


Figure II-10 Plastic limit according to Brinch Hansen

Brinch Hansen uses the following formula to calculate the horizontal stress:

$$\sigma_p = K_q^{\frac{z}{D}} \cdot \sigma_v' + K_c^{\frac{z}{D}} \cdot C \quad <II.21>$$

with

$K_q^{\frac{z}{D}}$ = lateral earth pressure coefficient [-]

σ_v' = vertical effective stress = $\gamma' \cdot z$ [kN/m²]

$K_c^{\frac{z}{D}}$ = cohesion coefficient [-]

C = cohesion [kN/m²]

γ' = effective unit weight soil [kN/m³]

z = depth below bed level [m]

In this analysis only non-cohesive soils are considered, so the cohesion term is further neglected.

The soil reaction (R_{pl}) for one spring can then be calculated with:

$$R_{pl} = \sigma_p \cdot D \cdot dz = K_q^{\frac{z}{D}} \cdot \gamma' \cdot z \cdot D \cdot dz \quad <II.22>$$

The following procedure is followed for the calculation of $K_q^{z/D}$:

$$K_q^{z/D} = \frac{K_q^0 + K_q^\infty \cdot a_q \cdot \left(\frac{z}{D}\right)}{1 + a_q \cdot \left(\frac{z}{D}\right)} \quad <II.23>$$

with

$$K_q^0 = e^{\left(0,5 \cdot \pi + \left(\frac{\pi}{180}\right) \cdot \phi\right) \cdot \tan \phi} \cdot \cos \phi \cdot \tan \left(45^\circ + \frac{\phi}{2}\right) - e^{-\left(0,5 \cdot \pi - \left(\frac{\pi}{180}\right) \cdot \phi\right) \cdot \tan \phi} \cdot \cos \phi \cdot \tan \left(45^\circ - \frac{\phi}{2}\right)$$

$$K_q^\infty = \left(1,58 + 4,09 \cdot \tan^4 \phi\right) \cdot \left(e^{\pi \cdot \tan \phi} \cdot \tan^2 \left(45^\circ + \frac{\phi}{2}\right) - 1\right) \cdot \cot \phi \cdot K_0 \cdot \tan \phi$$

$$a_q = \frac{K_q^0}{K_q^\infty - K_q^0} \cdot \frac{K_0 \cdot \sin \phi}{\sin \left(45^\circ + \frac{\phi}{2}\right)}$$

$$K_0 = 1 - \sin \phi$$

ϕ = angle of internal friction [degrees]

II.6 Actions

The action caused by the berthing ship is represented by a static lateral load applied at the pile-head.

II.7 Boundary conditions

The boundary conditions to be satisfied in the calculation are:

- $M(z=0) = 0$ (bending moment at pile head)
- $V(z=0) = -F$ (shear at pile head)
- $M(z=l) = 0$ (bending moment at pile foot)
- $V(z=l) = 0$ (shear at pile foot)

II.8 Solve technique

The following equations are valid for each pile element:

z : $z_{i+1} = z_i + dz_{i+1}$

k_h :
$$k_{h,i+1} = \frac{3 \cdot \beta_{i+1} \cdot q_{c,i+1}}{1,3 \cdot 0,3 \cdot \left(2,65 \cdot \frac{0,5 \cdot D}{0,3}\right)^{\alpha_{i+1}} + \alpha_{i+1} \cdot 0,5 \cdot D} \cdot D \cdot dz_{i+1}$$

with

α_{i+1} = soiltype coefficient (1/3 for sand)

β_{i+1} = soiltype coefficient (0,7 for sand)

$q_{c,i+1}$ = cone resistance $\left(\frac{kN}{m^3}\right)$

$$\mathbf{q}_c : \quad q_{c,i+1} = \begin{cases} z_{i+1} - h & \text{for } z_{i+1} > h \\ \text{value from CPT} & \end{cases} \Rightarrow \text{Theoretical distribution for sand} \\ \Rightarrow \text{Input from soil investigation}$$

$$\mathbf{EI}' : \quad EI'_{i+1} = E'_{i+1} \cdot \pi \cdot r_g^3 \cdot t$$

with

$$r_g = \frac{(D-t)}{2}$$

$$\mathbf{M} : \quad M_{i+1} = 2 \cdot M_i - M_{i-1} + 0,5 \cdot (R_i + R_{i+1}) \cdot dz_{i+1} - F_i \cdot dz_{i+1}$$

$$\mathbf{V} : \quad V_{i+1} = V_i - F_{i+1} + R_{i+1}$$

$$\mathbf{R} : \quad R_{i+1} = \text{smallest value of : } \begin{bmatrix} k_{i+1} \cdot \left(\frac{y_i + y_{i+1}}{2} \right) \\ K_q^{H/D} \cdot \gamma' \cdot \left(\left(z_{i+1} - \frac{dz_{i+1}}{2} \right) - h \right) \cdot D \cdot dz_{i+1} \end{bmatrix} \quad \text{for } z_{i+1} > h$$

$$\mathbf{M}'_m : \quad M'_{m,i+1} = \left(\frac{c_1}{6} + \frac{c_2}{3} \right) \cdot \left(1 - \frac{2}{3} \cdot \frac{a'_{i+1}}{r_g} \right) \cdot M_{pl}$$

with

$$c_1 = \sqrt{4 - 3 \cdot \left(\frac{n_y}{n_p} \right)^2}$$

$$c_2 = \sqrt{4 - 3 \cdot \left(\frac{n_y}{n_p} \right)^2 - 2 \cdot \sqrt{3} \cdot \left| \frac{m_y}{m_p} \right|}$$

$$n_y = -0,125 \cdot \frac{R_{i+1}}{dz_{i+1}} - 0,2 \cdot M'_{m,i+1} \cdot \kappa'_e$$

$$n_p = t \cdot f'_{y,i+1}$$

$$m_y = \left(0,0625 \cdot \frac{R_{i+1}}{dz_{i+1}} \cdot r_g + 0,071 \cdot M'_{m,i+1} \cdot \kappa'_e \right) \cdot \left(1 + \frac{a'_{i+1}}{r_g} \right)$$

$$m_p = 0,25 \cdot t^2 \cdot f'_{y,i+1}$$

$$\kappa'_e = \frac{f'_{y,i+1}}{E'_{i+1} \cdot r_g^2}$$

$$\mathbf{f}'_y : \quad f'_{y,i+1} = \left(\frac{M'_{m,i+1}}{M_{pl}} \right) \cdot f_y$$

$$\mathbf{E}' : \quad E'_{i+1} = E \cdot \left(1 - 1,5 \cdot \frac{a'_{i+1}}{r_g} \right)$$

$$\mathbf{a}' : a'_{i+1} = \left(0,5 \cdot k_{y,i} \cdot \frac{R_{i+1}}{dz_{i+1}} \cdot \frac{r_g^3}{EI_w} + (\kappa'_e)^2 \cdot \frac{r_g^5}{t^2} \right) \cdot \left(1 + 3 \cdot \frac{a'_{i+1}}{r_g} \right)$$

with

$$k_{y,i} = 0,042$$

$$EI_w = \frac{E \cdot t^3}{12 \cdot (1 - \nu^2)}$$

$$\lambda : \lambda_{i+1} = -1506,601 \cdot \beta^6 + 15304,715 \cdot \beta^5 - 64514,38 \cdot \beta^4 + 144383,76 \cdot \beta^3 - 180849,1 \cdot \beta^2 + 120130,99 \cdot \beta - 33034$$

with

$$\beta = \frac{-\left(\frac{M_i + M_{i+1}}{2} \right)}{0,5 \cdot M'_{m,i+1}}$$

$$\kappa : \kappa'_{i+1} = -\frac{\left(\frac{M_i + M_{i+1}}{2} \right)}{EI'_{i+1}} \quad \text{for } M < M'_{el,i+1}$$

$$= \frac{f'_{y,i+1}}{E'_{i+1} \cdot r \cdot \sin(\lambda_{i+1})} \quad \text{for } M > M'_{el,i+1}$$

$$\varphi : \varphi_{i+1} = \varphi_i - \kappa'_{i+1} \cdot dz_{i+1}$$

$$\mathbf{y} : y_{i+1} = y_i - \varphi_{i+1} \cdot dz_{i+1}$$

Run sequence

All calculations are run from top to bottom, starting with the element at the pile head where the loads are applied, and working down towards the last element at the bottom of the pile.

The sequence for calculation of the different variables is as follows:

1. A first estimate of the begin conditions φ_0 and y_0 is made using 'forget-me-not's
2. Using the theory of Blum a first approximation of the development of the bending moments (M) along the pile axis is given
3. The reduced moment-curvature relation is calculated for every cross-section based on these bending moments, resulting in values for the reduced full-plastic moment (M'_m), reduced yield stress (f'_y), reduced Young's modulus (E') and ovalisation (a')
4. The curvature (κ), rotations (φ) and displacements (y) are calculated from these bending moments with the reduced moment-curvature relation
5. The soil reactions (R) and the shear forces (V) are calculated from the displacements
6. Because the bending moments are dependent on the soil reactions and shear forces, a new calculation is performed for the bending moments (M)
7. If the boundary conditions are not satisfied after step 6, the begin conditions φ_0 and y_0 are adjusted and the model will go to step 2.
8. Steps 2-7 are executed repeatedly until the boundary conditions are satisfied

9. The resulting values of ϕ_0 and y_0 are the resulting pile head rotation and pile head displacement.
10. Graphs of the different variables as function of z can be plotted.

The result is a pile head displacement caused by the input force F . If the calculation is repeated for a range of values of F , a load-deflection diagram can be drawn.

Begin conditions

The following begin conditions at the pile head are required:

- Initial pile head deflection y_0 [m]
- Initial pile head rotation ϕ_0 [m/m]

A first approximation of these begin conditions can be made using the method of Blum, which applies the 'forget-me-not's $y_0 = \frac{F \cdot l^3}{3 \cdot EI}$ and $\phi_0 = \frac{F \cdot l^2}{2 \cdot EI}$, with the pile length based on an estimated point of restraint

Begin conditions for the forces, bending moments and curvatures are:

- Shear force $V_0 = -F$ [kN]
- Bending moment $M_0 = 0$ [kNm]
- Soil reaction force $R_0 = 0$ [kN]
- Curvature $\kappa_0 = 0$ [1/m]

Iteration

An obstacle in performing the iteration is that it is difficult to find an algorithm for changing the begin conditions based on the calculated bending moments and shear forces, in order to iterate towards satisfying the boundary conditions. The calculation is very sensitive for changes in the begin conditions, so these values have to be chosen carefully, otherwise the calculation will not converge to a solution.

That is why the calculation cannot be run automatically. The begin conditions have to be adapted manually based on the calculated bending moments and shear forces.

II.9 Input

The following parameters are used in the calculation:

- Loads:
 - Horizontal pile head load F [kN]
- Pile:
 - Location of load application h [m] (level above bed)
 - Embedment pile z_{pile} [m] (level below bed)
 - Diameter D [mm]
 - Wall thickness t [mm]
 - Flexural rigidity in elastic range EI [kNm²]
 - Yield stress f_y [N/mm²]
- Soil:
 - Friction angle ϕ [degrees]

- Effective weight γ' [kN/m²]
- Cone resistance from CPT q_c [MPa]
- Soil type coefficients α, β [-]
- Calculation
- Step size dz [m]

The calculation starts with a first approximation of the bending moments using the method of Blum. For this calculation the following parameters are required:

- Passive earth pressure coefficient λ_p [-]
- Minimum pile driving depth t_0 [m] (level below bed)

II.10 Output

The numerical output is written to an output sheet. Using this output sheet, graphs can be drawn up for the different variables.

In Figure II-11 and Figure II-12, graphs are presented for the bending moments, shear forces, soil reaction forces, curvature, rotations and displacements, in the following case:

- Pile length = 47 m
- Embedment in the soil = 22 m
- Diameter = 2500 mm
- Wall thickness = 40 mm
- D/t ratio = 63
- Soil = sand
- Angle of internal friction = 30°
- Horizontal pile head load = 3000 kN

In this case, the stresses at the location of the maximum moment have just crossed the yield limit. This can be seen in the curvature diagram, where just below the bed level the curvatures are significantly higher due to plastic yielding.

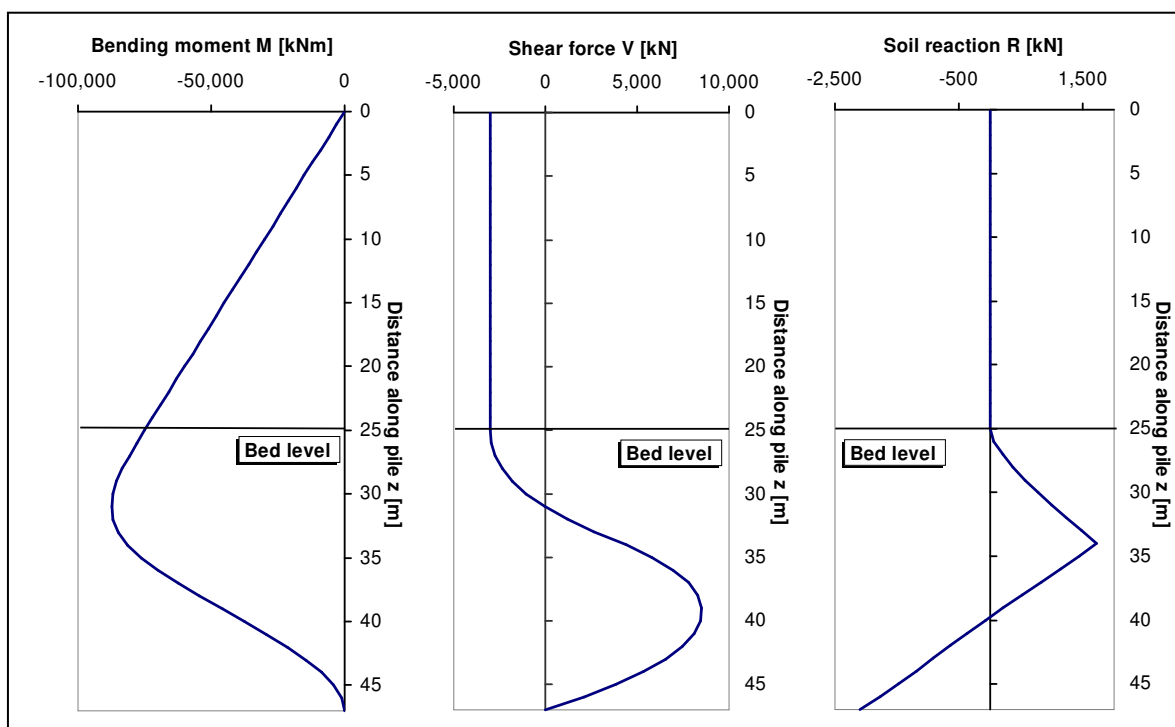


Figure II-11 Graphs of bending moment, shear force and soil reaction

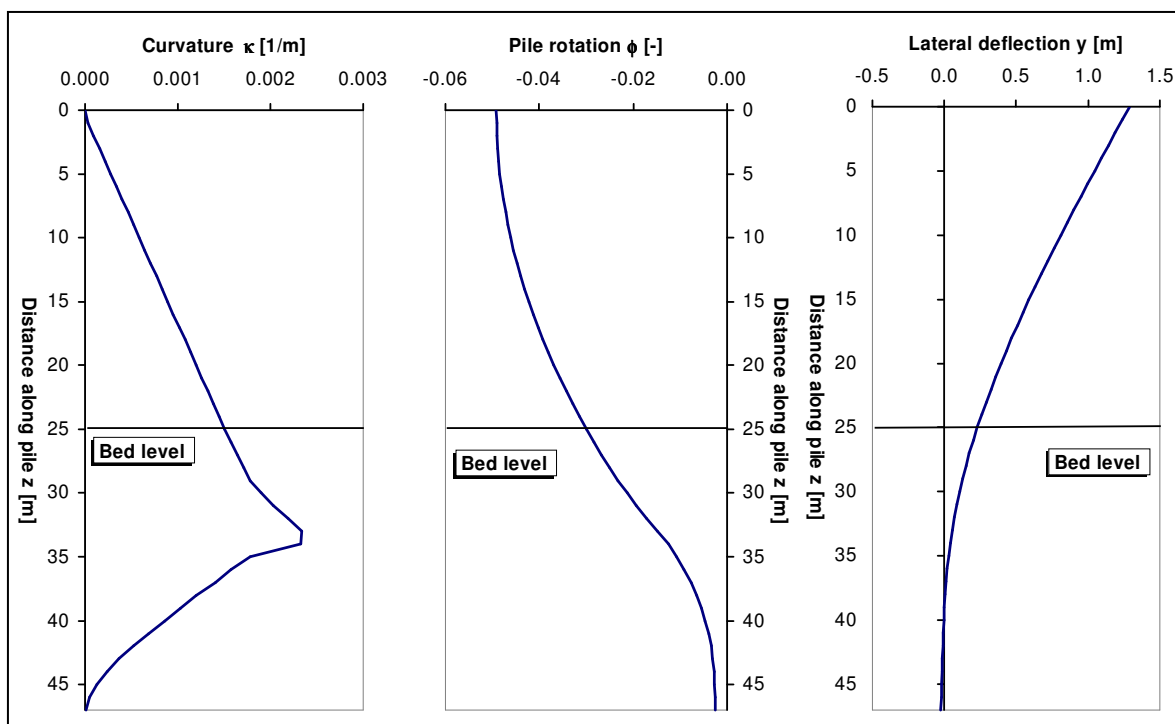


Figure II-12 Graphs of curvature, pile rotation and lateral deflection

When the calculation is repeated for several values of the horizontal load F , a load-deflection diagram can be drawn up, refer to Figure II-13.

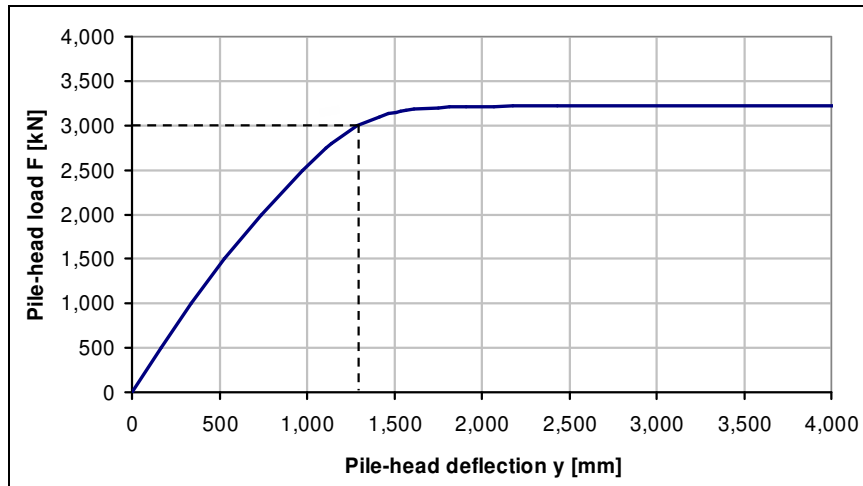
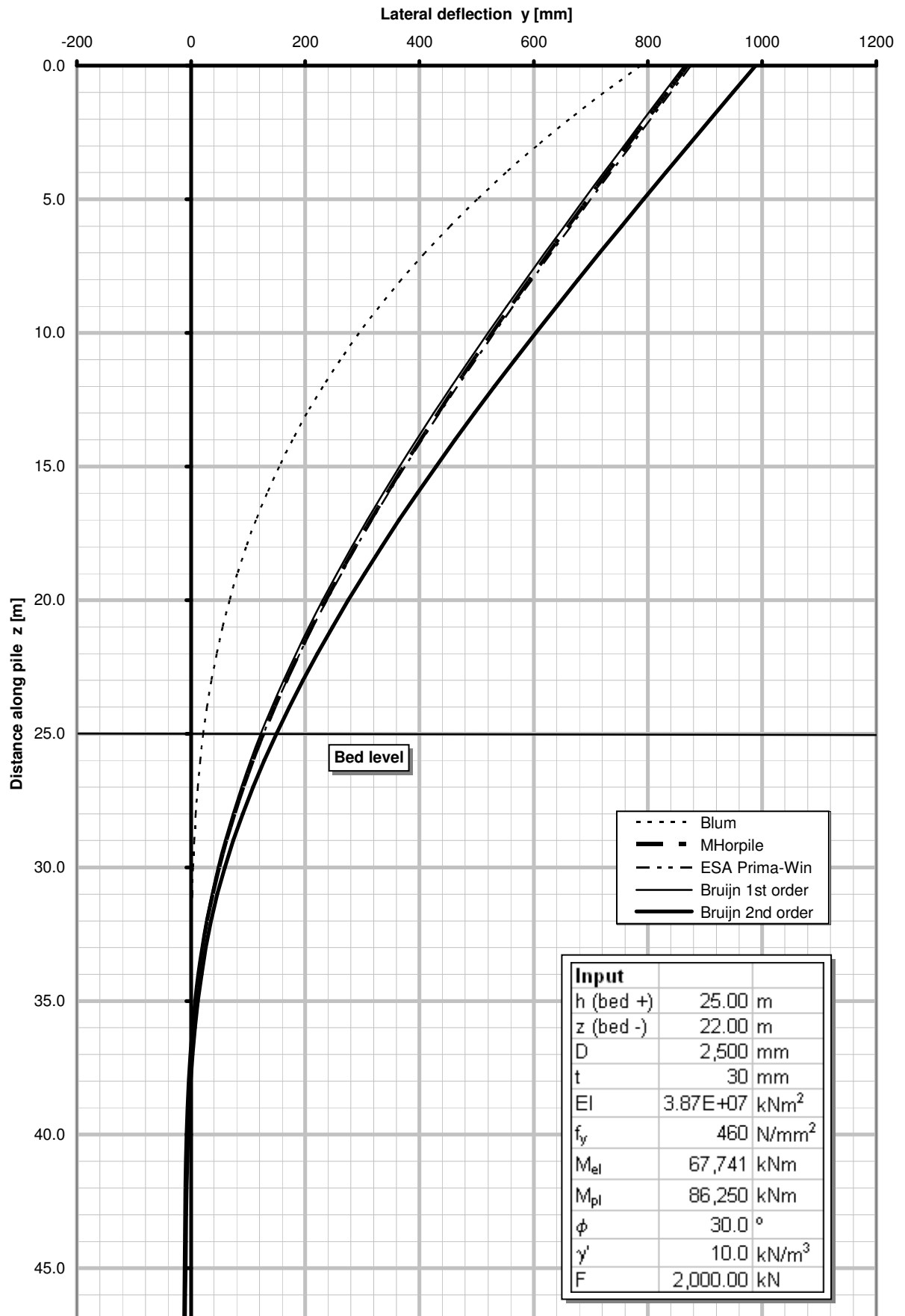


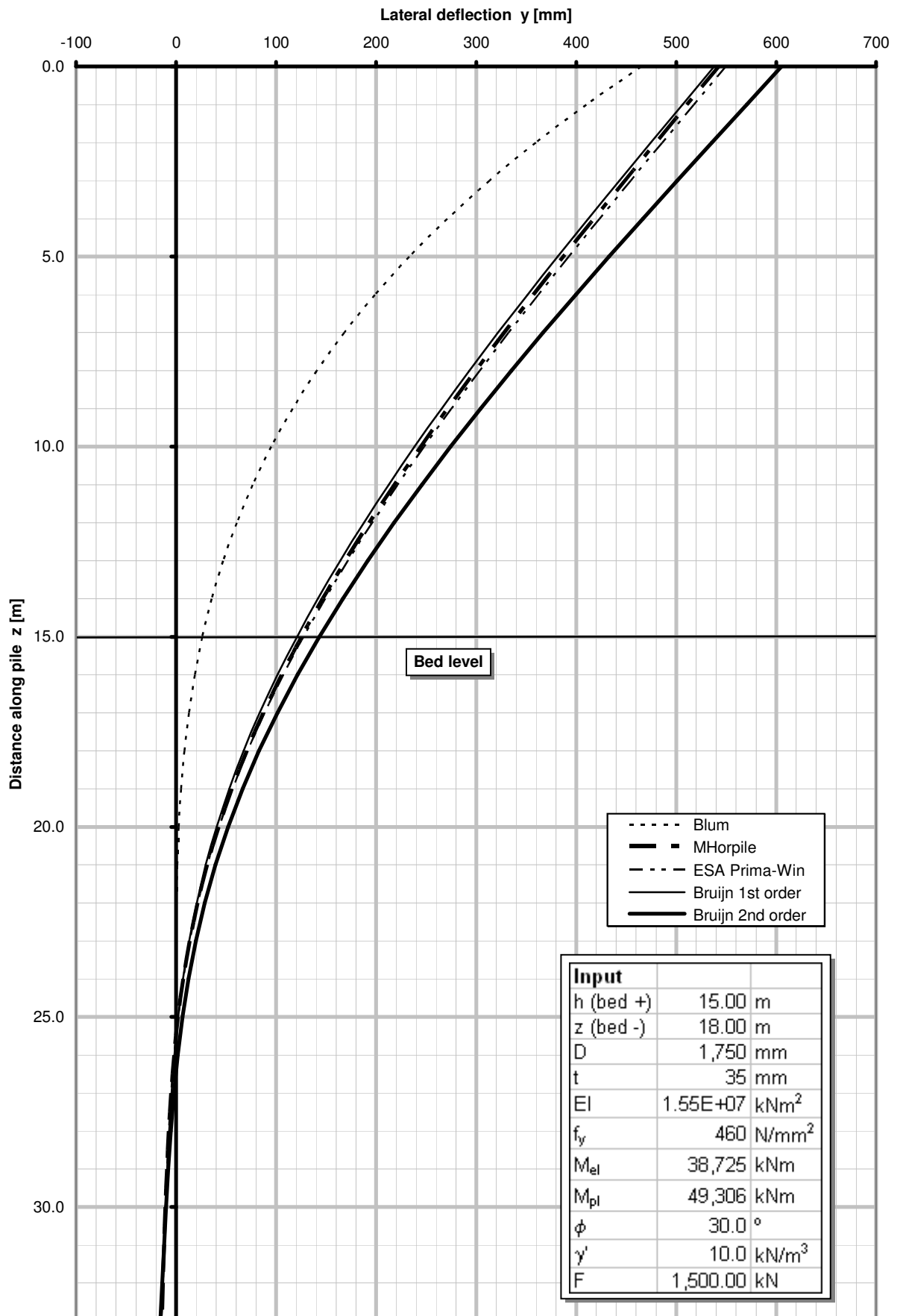
Figure II-13 Load-deflection diagram

The point indicated in Figure II-13 corresponds to the loading situation for which the graphs in Figure II-11 and Figure II-12 are plotted.

Annex III

Comparison Bruijn model with linear models





Annex IV

Assessment of the safety of the system

IV.1 Introduction

It is concluded from the evaluation of design standards and guidelines (section 5.4, page 63 and further), that a new assessment of the safety of the system is required. A quantitative assessment is preferable because it can result in partial factors of safety to be applied in the design.

Firstly the method of quantitative analysis is treated, and the problems are identified which make quantitative analysis not feasible in this thesis project.

Secondly a qualitative analysis is presented which gives some insight in the safety of the system.

IV.2 How can I assess the safety of the system in a quantifiable way?

Procedure

The following procedure can be followed:

1. Represent the relevant load and strength parameters by probability distributions or exceedance frequency curves to account for:
 - natural variations in parameter values
 - uncertainties in the design values used
2. Establish limit states and limit state criteria
3. Formulate a reliability function ($Z = R - S$) for each limit state
4. Calculate the probability of failure for each limit state and for the entire system using level II or level III probabilistic calculation method e.g. Monte Carlo simulation

Application to dolphin design

The above-mentioned method gives good insight into the safety of the system. However, when trying to follow this method in the case of dolphin design, the following issues arise:

- ad 1. Probability distributions for the parameters
Due to a lack of physical data e.g. from measurements the choice of a suitable distribution and associated parameters for the approach velocity and the hydrodynamic coefficients is rather difficult and probably inaccurate.
- ad 3. Formulation of the reliability function ($Z = R - S$)
When dealing with nonlinear material behaviour, explicit formulation of the reliability function is not possible. This is caused by the mutual dependency of several variables making it necessary to iterate. See example below.

Formulation of the reliability function for limit state yielding

Strength

$$R = f_y' = \frac{M_m'}{M_{pl} \cdot f_y}$$

with

$$M_{pl} = \pi \cdot r^2 \cdot t \cdot f_y$$

$$M'_m = f(M'_m, R_{soil}, a', f'_y, E')$$

The formula for M'_m contains an internal iteration and can therefore not be expressed explicitly in the reliability function.

Actions

$$S = \sigma = \frac{M}{W}$$

with

$$M = f(F, R_{soil})$$

$$R_{soil} = f(\gamma, \phi, y)$$

$$y = f(M, EI)$$

The bending moment M , soil reaction R_{soil} and pile deflection y must be determined by iteration over all elements along the pile axis using boundary conditions to establish the equilibrium state. The actions can therefore not be expressed explicitly in the reliability function.

Reliability function

$$Z = R - S = f'_y - \sigma = \frac{M'_m}{M_{pl} \cdot f_y} - \frac{M}{W} = ??$$

ad 4. Calculation of probabilities of failure

A possible method to avoid explicit formulation of the reliability function is to perform a Monte Carlo analysis, which is basically a repeated running of the Bruijn model with randomly chosen parameter values based on the probabilistic distributions attached to the parameters. This calculation is repeated a large number of times (e.g. 10.000 times), then the probability of failure for each failure mode can be estimated with:

$$P_f \approx \frac{n_f}{n} \quad <IV.1>$$

with

n = total number of simulations

n_f = number of simulations for which $Z < 0$

This method is not applied in this stage of the project, because the Bruijn model is not suitable to run 10.000 times with differing parameters, for two reasons:

- The Bruijn model is not automated
- It takes several minutes to reach a solution in one run; 10.000 runs would take weeks

The process can be accelerated by applying Importance Sampling, which is a method to increase the failure domain in proportion to the problem space.

However, applying Importance Sampling does not solve all problems with the probabilistic calculation, so this method is not feasible.

Conclusion: quantitative analysis not feasible

From the above remarks it can be concluded that the obstacles for running a quantitative analysis are too high for this thesis project.

Therefore the focus in the rest of this Annex will be on a qualitative analysis of the safety of the system.

IV.3 Qualitative analysis of the safety of the system

A qualitative analysis which can be used to systematically assess failure modes and the consequences for the functioning of the system is the so-called FMECA (Failure Modes, Effects and Criticality Analysis).

The general aim of an FMECA is to give an overview of all foreseen unwanted events and consequences in a system and to assess the most critical events in terms of frequency of occurrence and seriousness of consequences. This insight can help to identify events which must be prevented at all cost, events which are preferable to occur first if failure occurs, and measures which can be taken to prevent or suspend failure or to reduce the consequence of failure.

The following steps will be taken:

- Risk analysis: assessment of failure modes, consequence of failure, downtime, possible measures to enlarge safety
- Criticality analysis: assessment of criticality of failure modes by arranging them according to frequency of occurrence and seriousness of consequences
- How to take up excessive loading: assessment of the safety of the system from the loads side

Advantage of used method:

- The safety of the system is approached systematically, pointing out the failure modes with large consequences which should be prevented from occurring and the failure modes with minor consequences which are preferable to occur first

Disadvantages of used method:

- Limited insight in the safety against failure of the entire system compared to the probabilistic method mentioned earlier
- Optimal safety can not be assessed in a quantifiable way
- Limited insight into the correlations between parameters and failure modes and the influence of the different loads and strength parameters on the safety of the system

Risk analysis

On the following page the risk analysis is presented in a table, presenting:

- Failure events for the different system parts.
- Effects of occurrence of the event:
 - Main effects are mentioned first
 - Possible follow-up effects are mentioned next in order of occurrence
- A qualitative description of the consequence of failure, the damage cost
- Downtime of the berth
- Is advance indication of failure given, so that the occurrence of failure can be detected in an early stage?
- Measures which can be taken to enlarge safety

Component	Nr	Event	Main effect / Possible follow-up effects	Damage cost	Downtime	Advance indication of failure?	Measure
Ship	1	Yielding of ship's hull	Permanent deformation hull Cracks in hull	ship repair cost ship repair cost cleaning cost	moderate	no	Enlarge fender panel
	2	Fender failure	Loss of fender Overload of pile => pile failure Overload of hull => hull failure	replacement fender see pile failure see hull failure	low	no	Higher capacity fender
Pile	3	Progressive yielding / rupture pile	Cracking of pile wall, loss of strength Ship touches pile under water Leakage of cargo Pile touches jetty	replacement pile ship repair cost cleaning cost jetty + facilities repair cost	high very high	yes, large deformations	Higher yield strength pile Enlarge diameter Enlarge wall thickness
	4	Buckling pile	Local buckling pile wall, loss of strength Ship touches pile under water Leakage of cargo Pile touches jetty	replacement pile ship repair cost cleaning cost jetty + facilities repair cost	high very high	no	Enlarge D/t ratio
Ship-pile	5	Ovalisation pile	Collapse of pile section, loss of strength Ship touches pile under water Leakage of cargo Pile touches jetty	replacement pile ship repair cost cleaning cost jetty + facilities repair cost	high very high	no	Enlarge D/t ratio
	6	Ship touches pile under water	Yielding of ship's hull Cracks in hull Leakage of cargo Denting pile, buckling pile	ship repair cost ship repair cost cleaning cost replacement pile	moderate	no	Drive pile under an angle Enlarge distance pile-fenderface
Pile-jetty	7	Pile touches jetty	Damage to jetty Damage to loading / unloading equipment Pile loss	jetty repair cost facilities repair cost replacement pile	very high	yes, large deformations	Enlarge distance pile-jetty
Soil	8	Foundation instability	Pile is run over Ship touches jetty Ship damage	recover / replacement pile jetty repair cost ship repair cost	very high	no	Extend driving depth
	9	Soil rupture	Soil flow around pile, pile rotates in soil Pile is run over Ship touches jetty	reset pile recover / replacement pile ship + jetty repair cost	high	yes, slow deformations	Extend driving depth Enlarge pile diameter

Criticality analysis

In the criticality analysis the different failure modes are arranged by frequency of occurrence and consequence of failure. The factors in the criticality analysis are:

- λ_i = frequency of occurrence of failure mode i (a very rough estimate)
- t_i = uptime of the system (is equal for all failure modes, because failure of the berthing system is considered)
- P_{si} = probability of occurrence of all follow-up effects when the failure mode occurs; in the column "damage to:" the system parts are mentioned which are involved if all follow-up effects occur
- S_i = consequence of failure; the following values are assumed for damaged system parts:
 - fender: € 50.000,= (replacement fender)
 - pile: € 100.000,= (replacement pile)
 - jetty: € 1.000.000,= (repair of severe damage to jetty)
 - ship: € 100.000,= (repair of severe damage to ship)
 - cargo: € 5.000.000,= (loss of oil and cleaning cost)
- $C_i = \lambda_i \cdot t_i \cdot P_{si} \cdot S_i$ = criticality factor or risk

In Table IV-1 the criticality analysis is presented. The failure modes are arranged in order of decreasing 'criticality'. It must be emphasised that the values in Table IV-1 are only indicative for the frequency of failure and the consequence of failure.

Nr	Event	Damage to:	λ_i [1/yr]	t_i [yr]	P_{si}	S_i [€]	C_i [€]
1	Ship touches pile under water	ship, cargo, pile	0.05	50	0.05	5,200,000	650,000
2	Buckling pile	pile, ship, jetty	0.05	50	0.2	1,200,000	600,000
3	Foundation instability	pile, ship, jetty	0.02	50	0.5	1,200,000	600,000
4	Yielding of ship's hull	ship, cargo	0.05	50	0.01	5,100,000	127,500
5	Rupture pile	pile, ship, jetty	0.02	50	0.1	1,200,000	120,000
6	Ovalisation pile	pile, ship, jetty	0.01	50	0.2	1,200,000	120,000
7	Soil rupture	pile, ship, jetty	0.02	50	0.1	1,200,000	120,000
8	Pile touches jetty	pile, jetty	0.01	50	0.2	1,100,000	110,000
9	Fender failure	fender, pile, ship	0.1	50	0.05	250,000	62,500

Table IV-1 Criticality analysis

The following remarks can be made to explain the chosen values in the criticality analysis:

1. Ship touches pile under water
The consequences of severe damage to the ship with possible cargo leakage are very costly. Even though the probability of cargo leakage is very low, damage to the ship must be prevented at all cost
2. Buckling pile
Buckling as unknown failure mode is assessed to occur more frequently than other failure modes; probability of serious consequences is quite large because no advance indication of failure is given
3. Foundation instability
A large probability of all follow-up effects occurring is attached to foundation instability because in this case the pile is run over without significant energy absorption, so the chance of the ship hitting the jetty is quite large

4. Yielding of the ship's hull
Yielding of the hull by exceedance of the allowed hull pressures does in very few cases lead to serious damage of the ship and loss of cargo. Because of the large consequences in the case this actually happens, the criticality is still relatively high
5. Rupture pile
Failure of the pile by progressive yielding leading to rupture of the pile wall is assessed to have low probability of serious consequence because of the long process of deformation and energy absorption preceding actual failure. Also the deformation at which failure occurs can be estimated by structural analysis
6. Ovalisation pile
Collapse of the cross-section by progressive ovalisation is not expected to occur often. This is because ovalisation increases the buckling sensitivity, so buckling is expected to occur before progressive ovalisation of the cross-section occurs
7. Rupture soil
Failure of the soil by exceedance of the ultimate soil resistance is governed by the uncertainty in the values of the soil parameters in reality, so the calculated ultimate soil resistance can differ from the ultimate soil resistance in reality. On the other hand, advance indication of failure is given by large deformations combined with continuing energy absorption
8. Pile touches jetty
The probability of the pile touching the jetty by large deformations is considered small, because mostly other failure modes (buckling / ship touches pile under water) will have occurred with such large deformations
9. Fender failure
Fender failure is expected to occur most often of all failure modes, but the consequences are considered very small

How to take up excessive loading?

In the foregoing section only the strength side of the system is reviewed regarding the safety of the system. This is only part of the problem, as the subject of how to take up excessive loading is not assessed yet.

The following steps are taken to cover this subject:

1. Nature of excessive loading
2. Criteria for choice of preferred failure mode
3. Preferred failure mode

1. Nature of excessive loading

Abnormal impact can occur due to:

- Exceedance of the allowed approach velocity, e.g. due to misjudgement of the ship's master or due to tug failure
- Extreme climate conditions, e.g. high waves, wind and currents causing excessive loads on the ship and consequently on the berthing structure
- Berthing of a larger ship than allowed for the berthing structure
- Too small berthing eccentricity causing a larger portion of the ship's energy to be transferred to the berthing structure

A combination of these causes could also occur.

The main characteristic of abnormal impact is that an excessive amount of energy is transferred to the berthing structure and must be absorbed.

2. Criteria for choice of preferred failure mode:

- Absorption of excessive berthing energy
- Consequence of failure: repair and replacement costs
- Advance indication of failure
- Clear criteria when to repair/replace
- 'Designable': this means that in the design phase the safety against failure for the preferred failure mode can be assessed and adjusted with a reasonable accuracy (example: the safety against yielding of the pile can be assessed more accurately than the safety against soil failure, so yielding of the pile is better 'designable')

3. Preferred failure mode

Since the functional requirement of the dolphin is to receive the berthing ship, it is apparent that the dolphin is the designated part of the system to fail first due to abnormal impact. Also the consequence of failure and the downtime are larger for ship and jetty than for the dolphin.

Therefore the aim should be to let failure of the dolphin occur first, preferably with advance indication of failure so failure is detected in an early state and repairable with minimum costs.

If the failure modes of the dolphin are considered in more detail, the following conclusions can be taken:

- The fender is the cheapest and easiest replaceable part of the dolphin. However, the fender does not always absorb the full abnormal impact during failure, so overloading of other structural parts like the pile and the ship hull are still possible to occur in case of fender failure. Especially the ship hull can suffer from concentrated loads when the fender fails due to exceedance of the shear resistance so the fender panel can not perform the function of distributing the reaction force into the hull.
- Soil failure is not in all cases preceded by advance indication of failure. Also the absorption of the full abnormal impact is not guaranteed, and it is difficult to assess and adjust the safety against soil failure, so the 'designability' of soil failure is low
- Buckling and collapse of the pile lead to a rapid loss of strength with no significant advance indication of failure. Therefore these two failure modes have to be prevented from occurring
- Progressive yielding is preferable because of advance indication of failure by large deformations. Criteria can be established at what deformation repair or replacement should be executed in order to prevent other failure modes from occurring. The safety against yielding can be assessed by structural analysis.

The preferred failure mode when dealing with abnormal impact is therefore progressive yielding. Criteria should in this case be established to make sure progressive yielding occurs before other failure modes occur.

Conclusions qualitative analysis

- Failure modes which are assessed to be the most critical include buckling of the pile, foundation instability and underwater ship-pile contact
- Safety factors should be established in accordance with this criticality: safety factors should be high for the failure modes buckling, foundation instability, ship-pile contact and smaller for e.g. fender failure, yielding of ship's hull

- It should be considered that absorbing abnormal impact by progressive yielding is preferable due to advance indication of failure and the ability to set criteria how much deformation is allowed and when repair or replacement should be executed

SYMBOLS

A	Cross-sectional area	mm^2
a	Ovalisation	mm
a'	Ovalisation at the end of the elastic range	mm
D	Diameter	mm
E	Energy	kNm
$E_{d;normal}$	Design energy due to normal berthing impact (SLS)	kNm
$E_{d;abnormal}$	Design energy due to abnormal berthing impact (ULS)	kNm
E	Modulus of elasticity	N/mm^2
E'	Reduced modulus of elasticity (2 nd order)	N/mm^2
EI	Bending stiffness	kNm^2
EI_w	Bending stiffness of the pile wall per unit width	Nmm^2/mm
F	Force	kN
f_y	Yield stress	N/mm^2
f_y'	Reduced yield stress (2 nd order)	N/mm^2
h	Level above bed	m
I	Moment of inertia	mm^4
$K_q^{z/D}$	Lateral earth pressure coefficient	-
k_h	Modulus of subgrade reaction	kN/m^3
k_{yi}	Deformation coefficient depending on loading angle γ	-
M	Bending moment	kNm
M_e	Full-elastic moment	kNm
M_e'	Reduced full-elastic moment (2 nd order)	kNm
M_p	Full-plastic moment	kNm
M_m'	Reduced full-plastic moment (2 nd order)	kNm
m	plate moment per unit width	Nmm/mm
m_{ship}	ship mass (DWT)	ton
n	plate normal force per unit width	N/mm
q_c	Cone resistance	kN/m^2
Q	Earth pressure	N/mm
R	Soil reaction	kN
R_{pl}	Full-plastic soil reaction	kN
r, r_g	Average radius of the pile cross-section	mm
r'	Radius of plate curvature of an ovalised cross-section	mm
t	Wall thickness	mm
v, v_{ship}	(approach) Velocity of the ship	m/s
V	Shear force	kN
W	Section modulus	mm^3
y	Lateral deflection of the pile	mm
z	Level, distance along pile	m
z_{pile}	Embedment of the pile	m
dz	Step size in longitudinal direction of the pile	m

α, β	Soil-dependent coefficients	-
β	Nondimensional parameter indicating the magnitude of the bending moment in proportion of the full-plastic moment	-
γ	Loading angle for earth pressure Q	-
γ'	Effective unit weight soil	kN/m ³
ε	Strain	-
ε_y	Yield strain	-
ε_t	Tensile strain	-
κ	Curvature	1/m
κ_e	Full-elastic curvature	1/m
κ_e'	Reduced full-elastic curvature (2 nd order)	1/m
λ	Angular rotation indicating the transition between the elastic and the plastic part of the cross-section	rad
λ_p	Passive earth pressure coefficient	-
σ	Stress	N/mm ²
σ_v'	Vertical effective stress soil	kN/m ²
ϕ	Angle of internal friction	degrees
ϕ	Rotation	rad

Subscripts in so far as they are not already indicated above:

d	Design value
e, el	Full-elastic value
p, pl	Full-plastic value
u	Value in Ultimate Limit State (ULS)
0	Begin condition

REFERENCES

- Brinch Hansen, J. and Christensen, N.H., 1961, *The ultimate resistance of rigid piles against transversal forces*. Bulletin no. 12 of the Geoteknisk Institut
- BS6349-2:1988, *Maritime structures - Part 2: Code of practice for design of quay walls, jetties and dolphins*. London: British Standard Institution, January 1988. 108 p.
- BS6349-4:1994, *Maritime structures - Part 4: Code of practice for design of fendering and mooring systems*. 2nd edition. London: British Standards Institution, October 1994. 48 p.
- CUR 166, juli 2001, *Damwandconstructies*. Gouda: Civieltechnisch Centrum Uitvoering Research en Regelgeving. 544 p.
- EAU 1996, *Recommendations of the Committee for Waterfront Structures: Harbours and Waterways*. Committee for Waterfront Structures, 1996. 7th English Edition. Berlin: Ernst&Sohn. 599 p.
- Foeken, R.J. van, A.M. Gresnigt, 1998, *Buckling and Collapse of UOE manufactured steel pipes*. TNO-report 96-CON-R0500. Rijswijk: TNO Building and Construction Research. 160 p.
- Fontijn, H.L., 1988a, *Fender forces in ship berthing - Part I: Text*. Delft: TUDelft. 192 p.
- Fontijn, H.L., 1988b, *Fender forces in ship berthing - Part II: Figures & Appendices*. Delft: TUDelft. 96 p.
- Gresnigt, A.M., 1985, *Kritieke stuik en kritieke rotatie in verband met plooiën van stalen transportleidingen*. IBBC-TNO Report OPL 85-343. 40 p.
- Gresnigt, A.M., 1986, *Plastic design of buried steel pipelines in settlement areas*. Heron Vol. 31 nr. 4. 113 p.
- Hetenyi, M., 1974, *Beams on elastic foundation; theory with applications in the fields of civil and mechanical engineering*. Ann Arbor: University of Michigan Press. 255 p.
- Horst, C.S. van der, 2000, *Probabilistische beschouwing van het afmeerproces*. Afstudeerrapport. Delft: TUDelft. 248 p.
- Jones, G., 1997, *Analysis of Beams on Elastic Foundations*. London: Thomas Telford Publishing. 164 p.
- Koopmans, M., 1998, *Dynamische analyse van afmeerkrachten van schepen*. Afstudeerrapport. Delft: TUDelft. 135 p.
- Matlock, H., 1970, *Correlations for design of laterally loaded piles in soft clay*. Proc. of the Second Annual Offshore Technology Conference, Houston, April 1970. Vol. I, pp. 577-595
- Ménard, L. et al, 1971, *Méthode générale de calcul d'un rideau ou d'un pieu sollicité horizontalement en fonction des resultats pressiométriques*. Sols-soils 22-23 VI

Middendorp, P., 1983, *Onderzoek naar de optredende krachten en energieën t.g.v. het afmeren van een VLCC in ondiep water - Deel 2*. Afstudeerrapport. Delft: THDelft. 67 p.

NEN 3650-2: 2003, *Eisen voor buisleidingsystemen - Deel 2: Staal*, Delft: Nederlands Normalisatie-instituut, 2003.

NEN 6770, *Staalconstructies: TGB 1990*. 2e druk. Delft: Nederlands Normalisatie-instituut, mei 1997. 188 p.

PIANC, 1984, *Report of the international commission for improving the design of fender systems: supplement to bulletin no. 45*. Brussels: International Navigation Association. 158 p.

PIANC WG 33, 2002, *Guidelines for the Design of Fender Systems: 2002*. Brussels: International Navigation Association. 70 p.

Reese, L.C., H. Matlock, 1956, *Non-dimensional solutions for laterally loaded piles with soil modulus assumed proportional to depth*, Proc. of the Eighth Texas Conference on Soil Mechanics and Foundation Engineering. 41 p.

Reese, L.C., M.W. O'Neill and N. Radhakrishnan, 1970, *Rational design concept for breasting dolphins*. Journal of the Waterways and Harbors Division, May 1970. Vol. 96, No. 2, pp. 433-450

Saurin, B.F., 1963, *Berthing forces of large tankers*. Proc. of the 6th World Petroleum Congress, Frankfurt, June 1963. Section VII, pp. 63-73

Vasco Costa, F., 1964, *The berthing ship: The effect of impact on the design of fenders and berthing structures*. London: Foxlow publications. 48 p.

Verruijt, A., 2003, *Offshore Soil Mechanics: Lecture notes CT5341*. 9e druk. Delft: TUDelft. 180 p.